Dysfunction of the protein quality control system in neurodegeneration: A study of the co-chaperone and ubiquitin ligase CHIP in vitro and in zebrafish

Yasaman Pakdaman

Thesis for the degree of Philosophiae Doctor (PhD)
University of Bergen, Norway
2021

UNIVERSITY OF BERGEN

Dysfunction of the protein quality control system in neurodegeneration: A study of the co-chaperone and ubiquitin ligase CHIP in vitro and in zebrafish

Yasaman Pakdaman

Thesis for the degree of Philosophiae Doctor (PhD)
at the University of Bergen

Date of defense: 15.09.2021

Year: 2021

Title: Dysfunction of the protein quality control system in neurodegeneration: A study of the co-chaperone and ubiquitin ligase CHIP in vitro and in zebrafish

Name: Yasaman Pakdaman

Print: Skipnes Kommunikasjon / University of Bergen

Scientific environment

This PhD work was conducted during the period of 2017-2021 at the Department of Clinical Science (K2) and Department of Biological Sciences, University of Bergen, Bergen, Norway, under the supervision of Professor Stefan Johansson, Professor Ståle Ellingsen, researcher Ingvild Aukrust, and Professor Per Morten Knappskog. Financial grant was provided by a four-year PhD fellowship from the University of Bergen and the Western Norway Health Authorities (Helse Vest´s Open Research Grant #912250).

UNIVERSITY OF BERGEN

Acknowledgements

My sincere appreciation goes to my main supervisor Professor Stefan Johansson for his tremendous support and excellent supervision. I am very grateful for the opportunity to learn and complete this thesis in your group. Your great enthusiasm and incredible expertise have been helping me immensely during this journey. I also wish to deeply thank my co-supervisors Professor Ståle Ellingsen, Dr. Ingvild Aukrust, and Professor Per Morten Knappskog for their inspiring guidance and continuous motivation. Your insightful feedback and suggestions have been vital to the progress of this work. Thank you for your continued support and patience during scientific and technical challenges.

All my co-authors are acknowledged for their invaluable contributions. My particular appreciation goes to Dr. Will Norton, our great collaborator at the University of Leicester, UK, as well as Dr. Elsa Denker, Dr. Helene Bustad Johannessen and Sigrid Erdal for their significant contributions to the papers in this thesis. I am also thankful to Dr. Monica Sanchez-Guixe for her valuable guidance in the beginning of my career, and Eirik Austad for the great work he has done to the benefit of this thesis as a part of his master's degree project.

I would also like to thank all my colleagues for creating a fabulous working atmosphere both at the Department of Biological Sciences and at the Department of Clinical Science. Special thanks to my former office mates and current friends Anny Gravdal Svanbring and Dinka Smajlagic for always comforting me and giving me hope during the hardest, most disappointing moments in my PhD life. This thesis will always remind me of all the tears and laughter we have shared.

Completing a PhD is a big achievement, and so is finding true friends with whom you would genuinely share the joy and satisfaction of good days as much as the frustration of long, unsuccessful hours of work. For me, the most precious achievement was getting to know a beautiful soul in the beginning of this journey with whom I am now sharing every minute of my life. To my beloved husband, Ehsan: thank you for deciding to help a first-year student seven years ago and still not giving up on her! Thank you for all you have done, in particular, for your great help in preparing the figures of this thesis. I am forever blessed for having you by my side as my best friend and an

incredible mentor. I would not have been able to complete this work without your continuous support.

Finally, my deepest thanks goes to my amazing family for their infinite love and support. Big thanks to my brother, Amirhossein, for his kind visits which caused the sorrow of long distances less severe. To my beautiful mom, Esmat: thank you for teaching me to chase my dreams even though you knew it would take me miles away from you! I owe you all those seconds of the past few years, when you needed me the most, but I could not be there for you…

Yasaman Pakdaman

Bergen, May 2021

پیشکش به روح بلند پدرم،
To my father, Taqi,
May his beautiful soul rest in eternal peace...

و به مادر عزیزم
And to my beloved mother, Esmat.

Abstract

The C-terminus of Hsc70 interacting protein (CHIP) is a dimeric co-chaperone and E3 ubiquitin ligase encoded by the STIP1 homology and U-box containing protein 1 (*STUB1*) gene. As a major player in the protein quality control system, CHIP acts to regulate ubiquitination and elimination of chaperone-bound, misfolded and damaged proteins. The primary structure of CHIP consists of an N-terminal tetratricopeptide repeat (TPR) domain which mediates interaction of CHIP with molecular chaperones and a C-terminal U-box domain that functions as E3 ubiquitin ligase and facilitates ubiquitination of substrates. A central coiled coil region is responsible for dimerization and stability of CHIP structure.

Several bi-allelic mutations, scattered over all domains of the *STUB1* gene, are reported in patients with the autosomal recessive spinocerebellar ataxia type 16 (SCAR16) disease. SCAR16 is characterized by early-onset and progressive cerebellar atrophy, mainly resulting in gait disturbance and lack of coordination in muscles. We studied the pathogenic effect of six selected *STUB1* mutations in a heterologous system and reported profound impacts for some of these mutations on the ubiquitin ligase activity, structural stability and dimerization of CHIP.

Heterozygous mutations in the *STUB1* gene have been lately described in association with a dominantly inherited cerebellar ataxia disease called spinocerebellar ataxia type 48 (SCA48). SCA48 patients present adult-onset ataxia phenotypes often associated with cognitive-psychiatric features. We reported novel *STUB1* mutations in three families affected with SCA48. *In vitro* functional analyses of these variants revealed significant biochemical impacts on CHIP structure and function, similar to those previously reported for the recessive *STUB1* variants associated with SCAR16. However, the healthy status of SCAR16 carriers is not consistent with the reported pathogenicity of heterozygous *STUB1* variants in SCA48 patients, and should be further investigated.

Zebrafish animal models are being increasingly utilized in the genetic studies of neurodegeneration due to the strong similarity of their genome to that of mammalian orthologs, and a simple yet highly conserved structure of their nervous system. There is a high degree of conservation in the amino acid sequence of CHIP as well as its ubiquitin

ligase activity and expression pattern between zebrafish and human orthologs. We have generated zebrafish animals with mutated *STUB1* gene (*stub1*), causing a truncation in the U-box domain of Chip. Characterization of the mutant zebrafish indicated development of phenotypes overlapping with those of mammalian models with CHIP deficiency and SCAR16 patients. These phenotypes include significant reduction of body size, altered morphology of Purkinje cells of cerebellum and changes in anxiety-like behavior. Our findings provide the first evidence of zebrafish potential in modeling *STUB1*-mediated diseases, and may improve our knowledge regarding the pathogenic role of an impaired U-box domain in the development of SCAR16/SCA48 diseases.

List of publications

Paper I

Pakdaman Y., Sanchez-Guixe M., Kleppe R., Erdal S., Bustad HJ., Bjrkhaug L., Haugarvoll K., Tzoulis C., Heimdal K., Knappskog PM., Johansson S., Aukrust I. ***In vitro characterization of six STUB1 variants in spinocerebellar ataxia 16 reveals altered structural properties for the encoded CHIP proteins.*** Bioscience Reports. 2017; 37

Paper II

Pakdaman Y., Berland S., Bustad HJ., Erdal S., Thompson BA., James PA., Power KN., Ellingsen S., Krooni M., Berge LI., Sexton A., Bindoff LA., Knappskog PM., Johansson S., Aukrust I. ***Genetic dominant variants in STUB1, segregating in families with SCA48, display in vitro functional impairments indistinctive from recessive variants associated with SCAR16***. Manuscript in Review

Paper III

Pakdaman Y., Denker E., Austad E., Norton WHJ., Rolfsnes HO., Bindoff LA., Tzoulis C., Aukrust I, Knappskog PM., Johansson S., Ellingsen S. ***U-box domain truncation in the Chip protein affects Purkinje neuron morphology and leads to behavioral changes in zebrafish*.** Manuscript

Table of contents

Selected abbreviations

Aβ	Amyloid β
AD	Alzheimer's Disease
ADCA	Autosomal Dominant Cerebellar Ataxia
ALS	Amyotrophic Lateral Sclerosis
APP	Amyloid Precursor Protein
ARCA	Autosomal Recessive Cerebellar Ataxia
ATP	Adenosine Triphosphate
BAG	Bcl-2-associated Athanogene
CA	Cerebellar Ataxia
CHIP	Carboxy terminus of Hsp70-Interacting Protein
CNS	Central Nervous System
CRISPR	Clustered Regularly Interspaced Short Palindromic Repeats
HD	Huntington's Disease
HECT	Homologous to the E6-AP Carboxyl Terminus
Hip	Hsc70-Interacting Protein
Hsp70	70 kDa Heat Shock Protein
Hsp90	90 kDa Heat Shock Protein
ND	Neurodegenerative Diseases
PD	Parkinson's Disease
PQC	Protein Quality Control
PrP	Prion Protein
PTM	Post-Translation Modifications
RING	Really Interesting New Gene
SCA	Spinocerebellar Ataxia
SCAR 16	Autosomal Recessive Spinocerebellar Ataxia type-16
STUB1	STIP1 homology and U-box containing protein 1
TPR	Tetratricopeptide Repeat
UPP	Ubiquitin-Proteasome Pathway

1. Introduction

1.1. Neurodegeneration

Proper activity of multiple cellular protein networks is an essential requirement for the well-being of cells and organisms and depends on the correct folding and conformational structure of thousands of proteins in these networks. Protein conformational disorders, including the most common types of neurodegenerative diseases (NDs), develop due to protein misfolding and accumulation in the brain. Neurodegenerative diseases are a diverse group of heterogenous disorders in which neuronal cells of specific subtypes lose their function, structure, or both. Selective neuronal loss in motor, sensory, and cognitive systems affect memory, movements, emotional feelings and other abilities in ND patients. NDs can develop both hereditary and sporadic, with slow progression over time (1).

1.1.1. Protein aggregation in neurodegeneration

Despite variations in clinical symptoms and disease progression, a wide range of neurodegenerative diseases including Alzheimer's disease (AD), Parkinson's disease (PD), polyglutamine (polyQ) diseases (including Huntington's disease (HD) and several forms of spinocerebellar ataxia (SCA)), amyotrophic lateral sclerosis (ALS), and Prion diseases are reported with the common hallmark feature of cellular protein aggregates (2). These protein aggregates were first described in AD as amyloid plaques and neurofibrillary tangles. Later, it was found that sequential proteolysis of amyloid precursor protein (APP) results in the formation and accumulation of amyloid-β protein (Aβ) as the main component of amyloid plaques in the brain parenchyma and around cerebellar vessel walls (3), while tangles are aggregates of abnormally hyperphosphorylated forms of tau protein in the cytoplasm of degenerating neurons (4). In PD, inclusion bodies called Lewy bodies are mainly composed of aggregated α-synuclein proteins, and are widely distributed in the cytoplasm of substantia nigra and cortical neurons (5). Expansions of a CAG repeat encoding polyglutamine are known to form polyglutamine-rich deposits of proteins as the typical feature of brains with polyQ diseases. For example, polyglutamine stretches of 36 and more in the N-terminal of

huntingtin protein cause intracellular inclusions in the degenerating regions of a brain with HD (6), and SCA1 is associated with intranuclear inclusions containing ataxin-1 with expanded polyglutamine tracts (7). ALS patients are characterized by the aggregates of superoxide dismutase enzyme (SOD1) in the cytoplasm of motor neurons (8), and finally, extracellular accumulation of prion protein (PrP) in the form of aggregates and amyloid-like deposits are a common characteristic of animals and human brains with prion diseases (9).

Misfolded proteins and protein aggregates cause neurodegeneration by activating programmed cell death and neuronal apoptosis (10). Selective neuronal loss in different regions of the brain determines the clinical symptoms of associated neurodegenerative disease. The loss of memory in patients with AD, for example, is connected with neuronal death in hippocampus, amygdala, and entorhinal cortex (11). There are three main hypotheses regarding the role of protein aggregates in neuronal apoptosis and neurodegeneration (12). According to the first hypothesis, "**The loss-of-function hypothesis",** neurodegeneration develops due to the loss of activity of a native protein following its depletion during protein misfolding and aggregation. This model has been used to describe pathogenesis of HD (13). Huntingtin is a caspase substrate, and *in vitro* studies have shown that wild-type huntingtin protects neurons from several death receptors and pro-apoptotic proteins. Homozygous knock-out mice for huntingtin have been shown to die early in embryonic development, while heterozygous mice displayed normal phenotypes in adulthood (13). The similarity of clinical features observed in HD patients carrying homozygous and heterozygous huntingtin mutations, however, stands as a strong argument against the loss-of-function hypothesis (12).

The second and most widely accepted hypothesis, called "**The gain-of-function hypothesis"**, suggests acquisition of a neurotoxic function by the misfolded and aggregated proteins through different cellular pathways. Aggregates of expanded polyglutamine proteins are found to resist proteasomal degradation (14) and induce cell toxicity through various mechanisms such as impaired protein homeostasis, mitochondrial dysfunction, and genotoxic stress (15). Extracellular aggregates are proposed to interact with cellular receptors and activate signaling pathways for apoptosis inside the cells. Fibrils of Aβ and PrP have been reported to interact with a

multi-ligand cell surface receptor and trigger the nuclear factor-κB cellular stress pathway (16). The Aβ and PrP neurotoxicity is also reported via depolarization of membrane by formation of ion channels, which results in disruption of ion homeostasis and cell death (17, 18). Induction of oxidative stress by producing free radical species is proposed as another cell toxicity mechanism by Aβ, as well as α-synuclein aggregates, which results in oxidation of proteins and lipids, and further dysfunction of mitochondria (19, 20). The toxicity of protein aggregates has been questioned lately as clinical symptoms have been detected before formation of protein aggregates in transgenic mice with mutant ataxin-1 and APP (21, 22). Also, inhibitors of protein aggregation did not prevent cell death in a number of studies, indicating that misfolding and oligomerization of proteins could have a more deleterious effect than mature aggregates on cells (23, 24). This theory was further supported by studies showing a similar or more toxicity of purified oligomers and protofibrils compared to amyloid-like fibrils (23, 25, 26). In fact, formation of protein deposits is suggested to serve as a protective cellular mechanism for sequestering and isolating toxic misfolded intermediates (27). However, it is also possible that fibril deposits damage the cells through other ways such as destroying neuronal connections and occupying tissue space (12).

Finally, abnormal protein aggregates are thought to cause inflammatory reactions in the brain as irritants, leading to synaptic alterations and neuronal death (28). The third hypothesis, termed as "**The brain inflammatory hypothesis"**, is evidenced by the presence of activated microglia and astrocytes around protein deposits (29), accumulation of released inflammatory proteins such as cytokines, proteases and protease inhibitors in cerebral protein aggregates (28), and decreased incidence of AD in animal models and humans treated by anti-inflammatory drugs (30). In contrast, inflammation has been reported to be beneficial in neurodegeneration by other studies describing increased plaque load in response to inhibition of the inflammatory component C3 in mice (31), and improved behavioral and cognitive impairments in animal models vaccinated with Aβ (32). Although, the latter approach resulted in several cases of meningoencephalitis in human (33). Brain inflammation is, therefore, suggested

to act as a double-edged sword with both negative and positive effects in neurodegenerative diseases (34).

1.1.2. Protein misfolding and aggregation processes

Several studies have been performed to elucidate the mechanism of protein misfolding and aggregation in human diseases (35). In spite of process complexity and the presence of various types of aggregates involved in different diseases, *in vitro* structural studies have proposed a common molecular basis during protein aggregation. According to this theory, a native protein structure, usually containing α-helices and random structures, undergoes large conformational rearrangements and secondary structural alterations which lead to acquisition of a β-sheet-rich conformation (35). However, it is still unclear whether conformational changes trigger protein aggregation or if oligomerization of proteins induces misfolding and further aggregation. Kinetic modelling studies suggest that formation of protein aggregates might follow a nucleation-dependent polymerization mechanism, in which protein oligomers induce conformational rearrangements by acting as a nucleus and directing further polymerization and growth of aggregates (36). From an opposite point of view, induced conformational changes have been proposed to form misfolded proteins that might eventually aggregate (37). The most widely accepted hypothesis represents an intermediate viewpoint and suggests formation of intermediate oligomers by misfolded proteins to be essential for further growth of aggregates (38). According to this hypothesis, slight conformational changes in the structure of a native protein lead to the formation of a misfolded intermediate that is highly unstable due to the exposure of its hydrophobic segments to the aqueous environment. The misfolded intermediate has a high tendency for stabilization through interactions with other molecules. The small β-sheet oligomers formed from these intramolecular interactions will further grow by incorporation of additional monomers and produce protofibrils and amyloid-like fibrils (38). Exposure of certain hydrophobic fragments to the surface of the misfolded protein has been shown to be critical for aggregation of Aβ, PrP, and α-synuclein (39-41). However, in HD and other polyQ diseases, β-sheets are suggested to be formed by both hydrophobic interactions and polar hydrogen bonds among side-chain amide groups of glutamine expansions (42).

1.1.3. Causative factors in protein aggregation and neurodegeneration

Several genetic alterations and environmental factors can initiate protein misfolding and aggregation. Based on the nucleation hypothesis described in the previous section, mutations causing increased protein concentration can enhance the polymerization likelihood. For instance, triplication at the α-synuclein locus is known to cause familial PD (43), and an early deposition of Aβ plaques has been reported in Down's syndrome patients with an extra copy of the APP locus (44). Increased transcription and expression of disease-associated genes can also happen as a result of alterations in the promoter sites of these genes, or mutations that modify protein conformation and stability in favor of misfolding and aggregation (44). Expansion of the polyglutamine stretch in polyQ diseases are one such example.

In addition to genetic modifications, environmental factors such as metal ions, pH and oxidative stress, as well as post-translational modifications and pathological chaperone proteins may facilitate protein aggregation (12). Many of these factors are associated with aging, and thus, in agreement with the late-onset development of sporadic neurodegenerative diseases (45). Oxidative modifications and phosphorylation can promote α-synuclein aggregation (46, 47). Phosphorylation has also been implicated in aggregation of ataxin-1 in SCA1 and tau protein in AD (48). Proteolytic cleavage is involved in formation of amyloid fibrils in AD, and short N-terminal fragments of huntingtin in HD (49).

Molecular chaperones, together with several co-chaperones, play a major role in cellular protein quality control (PQC) system by regulating protein folding as well as preventing accumulation of damaged proteins (50). Different compartments of this system are described in more details in section 1.2. Deficiencies in the components of PQC machinery have been shown to impair the ability of cells to cope with protein misfolding and aggregation, and therefore promote neurodegeneration. For instance, the loss of E3 ubiquitin ligase activity of Parkin leads to accumulation of its substrates and development of PD (51). Also, polyglutamine expansions of the deubiquitinating enzyme ataxin-3 are reported to cause SCA3 following the induction of cellular stress (52, 53). Recently, several mutations have been identified in the STIP1 homology and U-box containing protein 1 (*STUB1*) gene encoding the co-chaperone and E3 ubiquitin

ligase Carboxy terminus of Hsp70-interacting protein (CHIP) in connection with the recessive and dominant types of hereditary cerebellar ataxia (CA) diseases (54). These mutations are described in section 1.4.2.

1.1.4. Cerebellar ataxias

Ataxia, or loss of coordination, can develop due to several diseases including metabolic disorders, cancer, brain injuries, as well as degeneration of neurons in the brain stem, cerebellar cortex, spinocerebellar tracts, and afferent/efferent connections (55). Ataxias involving cerebellum, brainstem, and spinocerebellar tracts are generally referred to as "cerebellar ataxias" (56). Gait impairments, poor balance, lack of upper limb coordination, eye movement abnormalities, and dysarthria (motor speech disorder) are considered as the main phenotypes of patients with CA (56). CAs mostly develop sporadic by non-genetic causative factors such as toxicity, immune-mediated diseases, and vitamin deficiencies (57). Hereditary ataxias are rare, and can develop through autosomal recessive, autosomal dominant, X-linked, and mitochondrial modes of inheritance (58). A complete list of currently known hereditary CA subtypes are provided in Appendix A (58). Various types of mutations contribute to the complexity of hereditary CAs. For example, CAG repeat expansions are responsible for development of more common inherited CA diseases including many forms of dominant CAs, while point mutations, deletions and duplications cause some rare dominant CAs and most of the recessive CAs (59).

Autosomal recessive cerebellar ataxias (ARCAs), with the estimated global prevalence of approximately 3 per 100,000 individuals, are a large group of rare neurological disorders with early-onset usually before the age of 20 (58, 60). Several types of ARCAs with overlapping phenotypes have been discovered during the past few years following identification of associated genes and loci (Appendix A), and different classifications have been proposed based on clinical, pathological and genetic criteria (61). Many of these disorders are extremely rare, involving single families and few known pathogenic variants, but some are more common with well characterized genetic basis and pathogenic pathways (58). Friedreich's ataxia (FA), with the estimated prevalence of 1:30,000 in Europe (56) and 1:176,000 in Norway (62), is the most

common type of ARCA mainly resulting from homozygous expansion of GAA repeats above a normal threshold in the first intron of the *FXN* gene. Mutated gene results in deficiencies of the mitochondrial protein frataxin (56), and dysfunction of mitochondria further provokes bioenergetics failure and leads to cell death in FA (63). Ataxia telangiectasia (AT) is the second most common type of ARCAs and develops due to defects in the DNA repair system. Missense mutations in the *ATM* gene encoding phosphatidylinositol-3 kinase (PI3K) have been identified in connection with AT (56). PI3K is involved in early cellular responses to DNA damage (64). Ataxia with oculomotor apraxia type 1 and 2 (AOA1, AOA2) are also considered as common ARCAs caused by mutations in the genes involved in DNA repair mechanisms and with neurological similarities to AT (56). In addition to those mentioned above, other disease mechanisms have been described for less common ARCAs including altered vesicular trafficking, malfunctioning of calcium-mediated chloride channels, mislocalization of synaptic nuclei and protein misfolding and aggregation following dysfunction of chaperones (56). The latter mechanism has been used to describe the pathogenesis of *STUB1*-mediated autosomal recessive cerebellar ataxia disease (56) (see section 1.4.2 for more details).

Autosomal dominant cerebellar ataxias (ADCAs) are a heterogenous group of progressive disorders with the estimated global prevalence of approximately 1-5 per 100,000 and the mean age of onset in the third to fourth decade of life (58, 60). Additional phenotypes including pyramidal and extrapyramidal signs as well as cognitive impairment are often associated with the cerebellar ataxia symptoms in these diseases (65). The term “spinocerebellar ataxia (SCA)” is generally used to designate dominant CAs. CAG repeats above a specific threshold in the coding and non-coding regions of genes underlie the majority of SCAs where the number of CAG repeats negatively correlates with the age of onset (59, 65). SCA3, also named as Machado-Joseph disease, is the most common subtype of the polyglutamine expansion SCAs which is associated with >51 CAG repeats in the *ATXN3* gene encoding ataxin-3 (66). A small proportion of SCAs are caused by conventional mutations in various associated genes. Missense and deletion mutations in the *SPTBN2* gene encoding B3-spectrin were reported for the first time in association with SCA5 (67). To date, more than 20 SCAs

have been reported due to mutations other than repeat expansions. A limited number of families identified with these mutations complicates correlations between genotype and phenotype in this group. Also, genetic heterogeneity among the subtypes results in difficulties in the pathogenicity analysis of these diseases (59, 65). A recently discovered subtype of this group, SCA48, has been reported in patients with heterozygous *STUB1* mutations (68) (see section 1.4.2 for more details).

1.2. Cellular protein quality control system

As mentioned in the previous section, proteins are continuously being subjected to misfolding and structural damages resulting from genetic alterations and environmental stressors. In a normal and healthy condition, misfolded and damaged proteins must be rapidly refolded into their native conformation or, alternatively, degraded before they start to accumulate and form toxic aggregates. At the same time, new polypeptide chains synthesized by cellular ribosomes ought to be properly folded and replace degraded proteins. The process of protein turnover is highly regulated by protein quality control (PQC) systems in the cytosol, endoplasmic reticulum, and other cell organelles (69). The PQC machinery allows for a selective and precise elimination of misfolded and damaged proteins through several common and compartment-specific mechanisms (69). Different components of the cytosolic PQC system in eukaryotic cells are described in the following subsections.

1.2.1. Molecular chaperones

At the first level of PQC, cells must be able to distinguish between native proteins and non-native structures including unfolded, partially unfolded, misfolded, and incorrectly modified proteins (70). Within the extremely crowded cellular environment, several new polypeptide chains and misfolded or damaged protein structures exist in close proximity, whose exposed hydrophobic residues and unstructured segments make them prone to interact with one another and form intramolecular aggregates. In order to avoid such dangers, a conserved network of molecular chaperones has evolved in both prokaryotic and eukaryotic cells, which can rapidly recognize the nascent chains of newly translated

polypeptides and hydrophobic surfaces of misfolded intermediates, and help them to fold/refold to their native conformation (71).

In a eukaryotic cytosol, the majority of small polypeptide chains can fold upon ribosomal release in association with nascent chain-associated complex (NAC) and without further assistance from chaperons (72). NAC does not show any ATPase activity or chaperoning functions *per se,* but it is known to generally interact with the short nascent chains emerging from the ribosomal exit site, and give signals for further protection of growing polypeptides by chaperone components (50). About 25% to 30% of nascent chains including longer polypeptides require participation of other co- and post-translational chaperones to achieve their native structure (50). Some of these chains such as cytoskeletal proteins actin and tubulin, are folded by the TCP-1 [T-complex 1] ring complex (TRiC) chaperonin through mechanisms that are not fully understood yet (50). Chaperonins are large, cylindrical protein complexes that provide a physically distinct environment for folding proteins while protecting them from other aggregating/non-native proteins. These substrates are reported to be captured in the central cavity of TRiC through hydrophobic interactions with several chaperonin subunits and further fold in an adenosine triphosphate (ATP)-dependent manner (50). Other newly synthesized chains (15-20%) are folded in reactions assisted by the family of **70 kDa heat shock protein (Hsp70)** chaperones (50).

Hsp70s play major roles in the mammalian PQC by assisting a wide range of folding processes during the post-translational assembly of newly synthesized proteins as well as quality control of misfolded and damaged proteins. The human Hsp70 family consists of at least eight homologous chaperones with distinct biological functions, residing in the cytosol and nucleus (Hsp701a, Hsp701b, Hsp70-1t, Hsp70-2, Hsp70-6, and Hsc70) as well as endoplasmic reticulum and mitochondria (Hsp70-5, Hsp70-9) (73). Some of the Hsp70s including Hsp70-1a, Hsp70-1b, and Hsp70-6 are stress-inducible proteins and cope with harmful aggregations and denatured proteins during stress (73). Yet, others are constitutively expressed, tissue-specific proteins with basal housekeeping functions. For example, the **cognate Hsp70 family member (Hsc70)** is known as an essential housekeeping protein with multiple chaperoning functions required for cell survival including folding new polypeptides, prevention of protein

aggregation, protein translocation across membranes, and chaperone-mediated autophagy (73).

Hsp70 proteins display a highly conserved domain structure in human and other species containing an N-terminal nucleotide binding domain (NBD) and a C-terminal substrate binding domain (SBD), which enable them to bind and release the exposed hydrophobic amino acid stretches on protein substrates in an ATP-dependent manner (74). Hsp70s also bind to the tetratricopeptide repeat (TPR) domain of heat shock proteins and co-chaperones through an EEVD motif in their C-terminal domain (74). The variety of functions in the Hsp70 family members can be explained by reduced number of conserved amino acids in their C-terminal domains (74).

Hsp70 chaperones function through cycling between two stable conformations with modulated affinities for polypeptide substrates (74) (Figure 1). In the ATP-bound state, Hsp70 has a "open" conformation with low affinity for the substrates and displays fast rates of peptide binding and release. Upon ATP hydrolysis, a conformational change in the lid traps the substrate within the substrate binding domain of Hsp70 and lowers the exchange rates for the substrates. Once adenosine diphosphate (ADP) is exchanged by ATP, Hsp70 switches back to its initial conformation which triggers substrate release and a new cycle of chaperoning (74). Unfolded chains released from Hsp70 are free to gain a native conformation. However, slow-folding intermediates often require rebinding to Hsp70 and further chaperoning cycles to avoid intramolecular misfolding and aggregation (50). Long polypeptide chain cycles are often mediated by the function of multiple Hsp70 chaperones on individual domains of the protein (50).

The activity of Hsp70 chaperones is tightly regulated by several regulatory co-factors (co-chaperones) which help Hsp70s to bind specific peptides and chaperones, or mediate substrate release through physical association with both Hsp70 and target proteins (75). The 40 kDa heat shock protein (Hsp40) family of J-domain proteins plays important co-chaperoning functions by recruiting Hsp70 to a distinct subset of client proteins and stimulating the ATPase activity of Hsp70 for subsequent binding to the substrate (76). Hsp40 and Hsp40-like proteins are defined by a common structural domain (J-domain) as the major binding site for their interacting partners, which contains structural features that determine the specificity of Hsp40-Hsp70 interactions

(76, 77). The ADP state of Hsp70 is stabilized by the Hsc70-interacting protein (Hip) which is a TPR domain-containing co-chaperone and keeps Hsp70 in the substrate-bound conformation to prevent release of the client protein before it is completely processed (75). Hip is known to function through antagonizing the interaction between Hsc70 and the human Bcl-2-associated athanogen-1 (BAG-1) co-chaperone which, together with several other classes of nucleotide exchange factors, catalyze the ADP-ATP exchange in the chaperone cycle (74, 75).

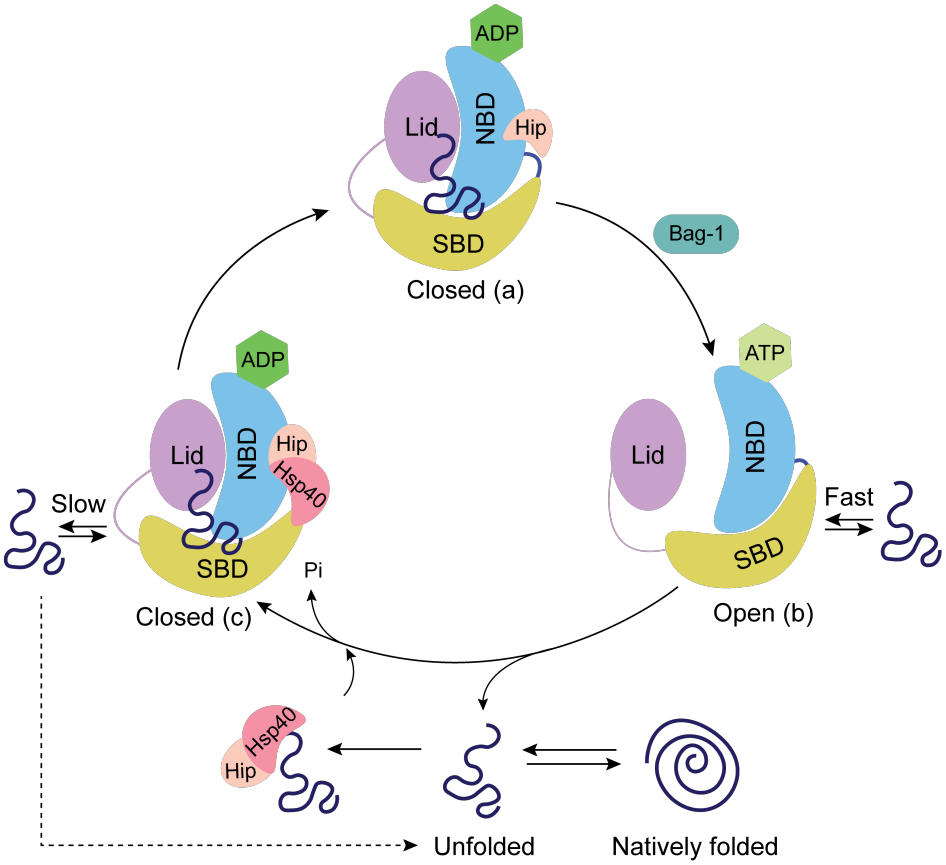

Figure 1. Hsp70 chaperones function through ATPase cycles of binding and release. In the ADP-bound state (a), Hsp70 gains a "closed" conformation with a high affinity towards the substrate. Once ADP is replaced by ATP, a conformational change in the lid results in an "open" structure for Hsp70 (b), which facilitates fast substrate binding and release. Released substrates either refold to their native conformation, or rebind to Hsp70 for another chaperoning cycle through interactions with the Hsp40 and Hip regulatory co-factors. Following ATP hydrolysis, Hsp70 returns to its "closed" conformation (c) with a lower rate of substrate exchange. This figure is adapted from (78).

The second key molecular chaperone in the cellular protein folding machinery is **90 kDa heat shock protein (Hsp90)**, which collaborates with Hsp70 and facilitates final maturation of proteins for a selected range of clients including protein kinases, transcription factors, and steroid hormone receptors (SHRs) (79). Therefore, it participates in various cellular processes including signal transduction and intracellular transport. Hsp90s are conserved homodimers containing an N-terminal ATP-binding domain (N-domain), a middle domain (M-domain), and a C-terminal dimerization domain (C-domain) (79). Residues in the M-domain contribute to ATP hydrolysis by formation of an ATPase site on Hsp90. M-domain is also essential for the interaction of Hsp90 with client proteins and some co-chaperones. Co-chaperones containing TPR domain interact with Hsp90 through a conserved MEEVD motif in the C-terminal of Hsp90 (79).

Similar to the Hsp70 chaperones, a conformational plasticity in the structure of Hsp90 is critical for its chaperoning function on various client proteins and allows for a dynamic equilibrium between "open" and "closed" conformations under the regulation of different co-chaperone complexes (79) (Figure 2). The steps of Hsp90 functional cycle are well studied in case of SHRs: in the first stage, the client protein is transferred to Hsp90 from an "early complex" (where it was initially processed by Hsp70 and Hsp40 chaperones) through collaborative activities of Hsp70-Hsp90 organizing protein (Hop), stress inducible protein-1 (StiI) and other client-specific co-chaperones. The Hop/StiI complex is also known to stabilize the "open" conformation of Hsp90 together with members of the peptidylpropyl isomerase (PPIase) family. Once ATP is bound, a series of conformational changes in the N-terminal of Hsp90 changes its orientation towards the M-domain and leads to the formation of a more compact Hsp90 conformation. Stabilization of the "closed" conformation of Hsp90 is assisted by p23 and other PPIases such as cyclophilin 40 (Cyp40) which interfere with binding of the Hop/StiI complex to Hsp90 and form a "late complex" in association with Hsp90. Maturation of the client protein is facilitated at this stage, and folded proteins together with the co-chaperones are released from Hsp90 after hydrolysis of ATP (79). The activator of Hsp90 ATPase (AhaI) is known to play critical roles in the progression of Hsp90 cycles including

releasing the Hop/StiI complex, promoting the "closed" conformation of Hsp90 and stimulating the inherent ATPase activity of Hsp90 (79, 80).

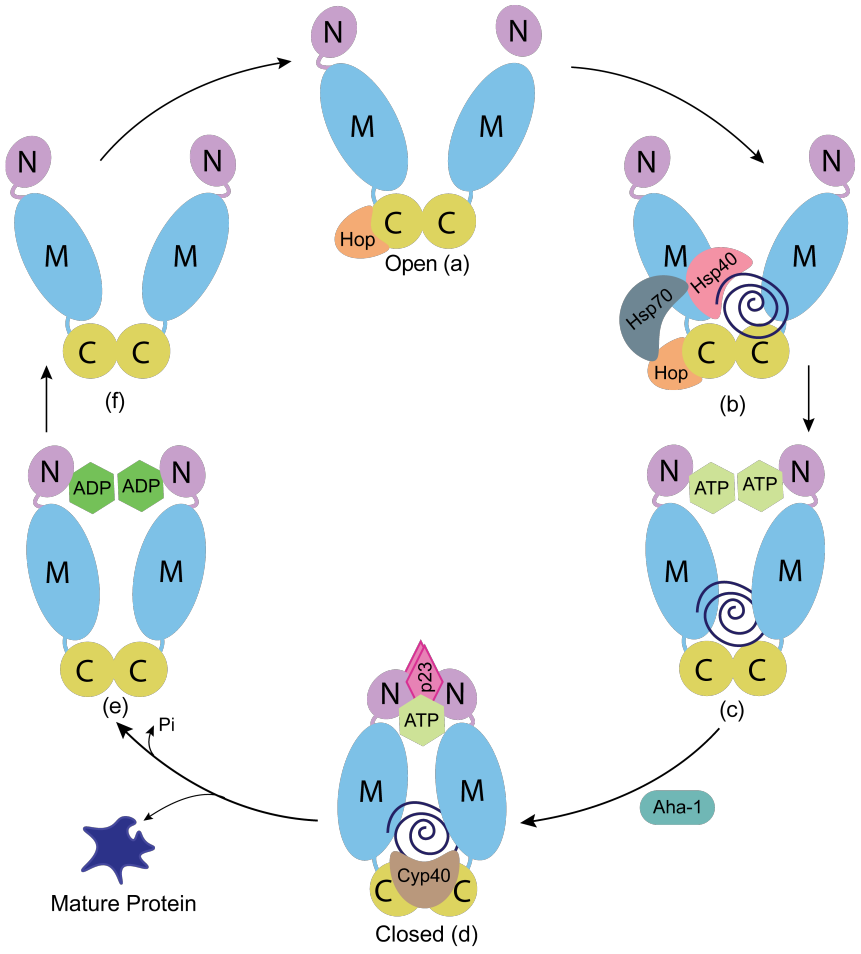

Figure 2. Hsp90 chaperoning cycle involves a dynamic equilibrium between the "closed" and "open" conformations. In a conformationally open state (a), Hsp90 receives the substrate from the Hsp70 complex. The "open" conformation of Hsp90 is stabilized by the activity of Hop and other co-chaperones at this stage (b). In the ATP-bound state (c), conformational changes are induced to keep the substrate inside a compact Hsp90 structure, which is stabilized by p23 and Cyp40 co-chaperones (d). Upon ATP hydrolysis, Hsp90 undergoes further conformational changes (e) resulting in the mature substrate to release. Hsp90 regains its "open" conformation (f) to start another cycle of chaperoning. This figure is adapted from (81).

1.2.2. The ubiquitin-proteasome pathway

Proteins successfully (re)folded to their native states are removed from the pool of non-native proteins in the cell. These proteins can no longer be recognized by components of the PQC system as their hydrophobic segments are buried inside the native structure. Other non-native proteins and folding intermediates, which are released from the chaperones without reaching their native forms, can rebind to the chaperones for another refolding attempt. However, some of these structures can be recognized by proteases before they get another chance of refolding, and thus be fated for complete degradation. Destruction of abnormal proteins had first evolved in the prokaryotic cells by intracellular proteolytic systems including different types of energy-dependent proteases which function in the cytosol or extracellular environment to digest a wide range of protein substrates (82). Throughout evolution, cells have been developed with an ability to destroy certain misfolded and damaged proteins without targeting non-specific proteins and cellular elements via more complex systems (82).

The ubiquitin-proteasome pathway (UPP) functions at the second level of the eukaryotic PQC system in a close relationship with the molecular chaperone networks, targeting unfolded or misfolded proteins for proteasomal degradation. In fact, components of the UPP and chaperones compete for recognition and further refolding or degradation of non-native substrates prior to formation of aggregates (70). In the UPP, substrates are selectively recognized in a ubiquitin enzymatic cascade which facilitates transfer of conserved 76-residue ubiquitin molecules on the substrates, marking them for subsequent degradation by proteasomes (83). The ubiquitination reaction, defined as the *iso*-peptide binding of ubiquitin through its C-terminal (Gly76) to the ε-amino group of a lysine residue on the substrate, is mediated by sequential actions of three enzymes (Figure 3A). First a **ubiquitin-activating enzyme (E1)** forms a thiol ester with the carboxyl group of Gly76 and activates C-terminal of ubiquitin. Activated ubiquitin is then transiently carried by a **ubiquitin-conjugating enzyme (E2)**, and ultimately transferred to a lysine residue on the substrate or other ubiquitin molecules by a **ubiquitin-protein ligase (E3)** (83).

E1 activates ubiquitin through formation of a Mg-ATP-bound ubiquitin (ubiquitin adenylate) intermediate, which subsequently hydrolyzes ATP to adenosine

monophosphate (AMP) to form a thioester bond with a cysteine in the E1 active site (84). A high rate of ATP-AMP exchange by E1 allows for efficient activation of ubiquitin for the entire downstream conjugation reactions. Each E1 interacts with a significant, but limited number of E2s, and each E2 make interactions with a much larger number of E3s (85). In human, around 40 E2s are reported to participate in protein ubiquitination, all sharing a ubiquitin-binding core domain of 150 amino acids containing an E2 active site and an E3 binding site (86). Additional N- and/or C-terminal extensions on some E2s determine the specificity of their interactions with E3s (86). Ubiquitin transport from E1 to the cysteine residue of E2 is mainly catalyzed by side-chain groups located in the E1 active site (85). The E2/E3 binding surface mediates the interaction through the really interesting new gene (RING) and homologous to the E6-AP carboxyl terminus (HECT) domains of E3s (86).

The majority of E3 ligases with more than 600 members are RING-type E3s, containing the RING domain or RING-related structures termed as U-box domain, which interacts with both E2-ubiquitin conjugate and a substrate, facilitating ubiquitin transfer directly from the E2 active site to the substrate without chemical participation in the reaction (83). However, HECT-type E3s (~30 members) together with a third smaller class of RING-between-RINGs (RBRs) are known to form an E3-ubiquitin intermediate prior to ultimate ligation to the substrate (83) (Figure 3B). Many E3s mediate both ubiquitin-substrate and ubiquitin-ubiquitin ligations. Yet, polyubiquitination of some substrates requires further catalytic activity of an **elongation factor (E4)** which enhances the activity of E3 ubiquitin ligases and ensures the assembly of polyubiquitin chains with sufficient length for proteasomal degradation of the substrate (87). E4s are also considered as specialized types of E3s with the ability of targeting the protein-bound, polyubiquitin chains for further ubiquitination (88).

Protein ubiquitination regulates several intracellular mechanisms depending on the subcellular localization of the substrate, as well as the number and topology of conjugated ubiquitin molecules (85). For example, substrates bound to a polyubiquitin chain on Lys63 are implicated in autophagic degradation and non-proteolytic pathways including ribosomal function, DNA repair, and inflammatory responses. Polyubiquitin chains conjugated through Lys48 are destined for proteasomal degradation, although

certain substrates marked with one or a few ubiquitin molecules on Lys48 are alternatively degraded through endocytosis and lysosomal degradation pathways (see section 1.2.3 for more details) (85).

Proteins modified with chains of at least four ubiquitin molecules can be recognized by the **26S proteasome** as a major cellular protease in eukaryotic cells (89). (Figure 3C). The 26S proteasome is composed of two sub-complexes: the base and lid regulatory particle (19S) and the cylindrical-shaped core particle (20S). Small structural changes upon substrate binding initiate an unfolding process in the 19S proteasome lid. The polypeptide is then translocated to the 20S core for further degradation by the trypsin- and caspase-like peptidase activity of core subunits. In the end, small oligopeptides resulting from protein cleavage emerge from the proteasome, and are further broken down to free amino acids. The six ATPase rings located at the base of 19S proteasome supply the energy for the whole process from protein unfolding to amino acid release (89, 90). Deubiquitinating subunits in the proteasome lid function to release ubiquitin chains from the target protein during or after its degradation, providing free ubiquitin molecules to be used in a new conjugating cascade (90).

At another level of PCQ, deubiquitination by ubiquitin isopeptidases results in the disassembly of degradation signals and regeneration of the protein substrate as a final protection mechanism against proteolysis of poorly or perhaps wrongly ubiquitinated proteins (91).

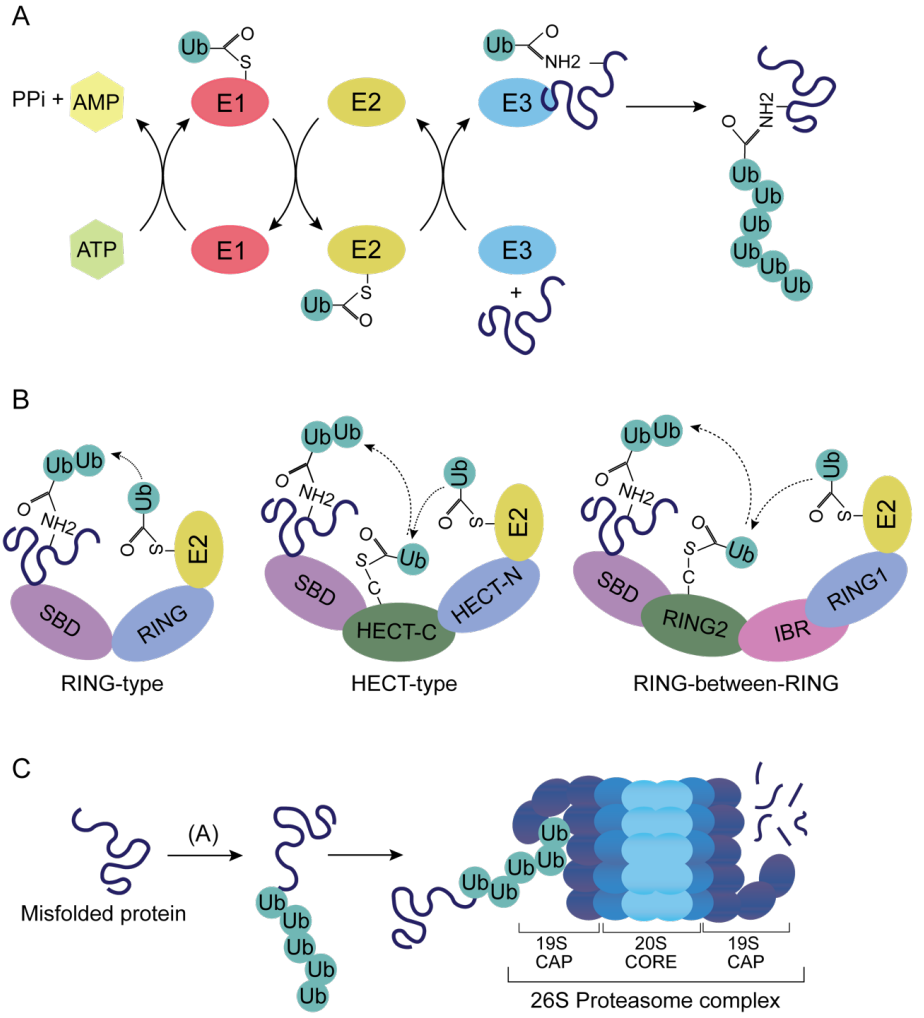

Figure 3. The ubiquitin-proteasome system mediates selective degradation of misfolded and damaged proteins. A) Selected substrates are polyubiquitinated during an enzymatic cascade mediated by a sequential action of ubiquitin activating enzyme (E1), ubiquitin conjugating enzyme (E2), and ubiquitin-protein ligase (E3). B) RING-type E3 ligases act as scaffolds and facilitate direct transfer of ubiquitin molecules from E2s to the substrates, while HECT-type E3 ligases and RBR ligases participate in the ubiquitination reaction by formation of E3-ubiquitin intermediates. C) Substrates marked with four or more ubiquitin molecules are recognized by the 26S proteasome lid, and translocated to the core complex for ATP-dependent degradation by peptidases. Free amino acids and ubiquitin molecules released from the proteasome base will be reused in another ubiquitination reaction. Ub, Ubiquitin molecule; SBD, substrate binding domain; IBR, in-between RING. This figure is adapted from (92).

1.2.3. Lysosomal degradation pathway

In addition to the ubiquitin-proteasome system, which is mainly responsible for elimination of short-lived and damaged proteins, the eukaryotic PQC is equipped with another degradative pathway for destruction of long-lived, aggregated proteins and cellular organelles (including mitochondria, peroxisomes, and ribosomes), called autophagy (93).

During autophagy, the target protein (cargo) is degraded by multiple enzymes inside the lysosomal lumen through three distinct mechanisms. Large portions of the cytoplasm and organelles are delivered to the lysosome through a pathway called macroautophagy where the substrates are first sequestered by a double membrane vesicle (autophagosome) which, subsequently, is fused with the lysosome (Figure 4A). During microautophagy, a small portion of the cytosol, together with its contents, is engulfed by the lysosomal membrane (Figure 4B). Higher eukaryotes have been characterized with a third autophagy pathway called chaperone-mediated autophagy (CMA) in which the target substrate is first recognized by the cytosolic chaperone Hsc70 and associated co-chaperones (including BAG1, Hip, Hop, and Hsp40), and then delivered to the lysosome as the chaperone binds to the lysosomal associated-membrane protein 2A (LAMP2A) receptors on the lysosomal membrane (Figure 4C) (93).

For a long period of time, the UPP and autophagy were regarded as two distinct pathways of the eukaryotic PQC. However, new findings are now strongly suggesting the presence of many interfering elements leading to several orchestrated activities for these pathways (94). At the first level of crosstalk, ubiquitination serves as a signal for both proteasomal degradation and selective autophagy. In this case, the fate of a protein for degradation via each pathway depends on the exact type of ubiquitin modification (94) (as mentioned in section 1.2.2), and is decided by certain co-chaperones with linking activity such as BAG family, CHIP and/or adaptor molecules like p62 and neighbor of BRCA1 (NBR1). These proteins are capable of interacting with both ubiquitin and components of proteasome/autophagic machinery, and thus provide the correct type of link for a given substrate (93, 94). Another association between the UPP and autophagy is through compensatory mechanisms, in which the impairment of one pathway can cause upregulation of the other pathway. Several hypotheses have been

proposed to explain this crosstalk. For example, accumulation of misfolded proteins has been suggested to induce the endoplasmic reticulum stress signaling pathway, resulting in the activation of autophagy (95).

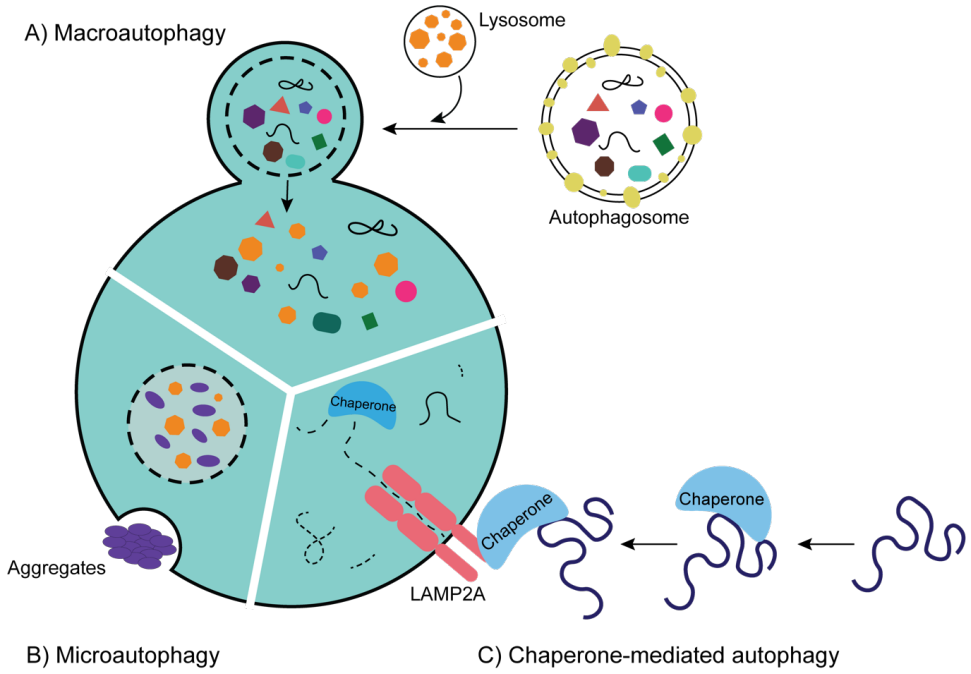

Figure 4. Aggregated proteins and larger organelles are eliminated through autophagy pathways. A) Macroautophagy: large organelles are isolated inside an autophagosome which subsequently fuses with the lysosome. B) Microautophagy: smaller portions of cytosol are directly engulfed by the lysosomal membrane. C) Chaperone-mediated autophagy: some substrates are delivered to the lysosome in complex with the chaperones binding to the LAMP2A receptors on the lysosomal membrane. This figure is adapted from (96).

1.3. The Carboxy terminus of Hsp70-Interacting Protein (CHIP)

In 1998, Ballinger and colleagues discovered a novel 35 kDa cytoplasmic protein while searching for all TPR domain-containing proteins in the human cDNA library. This protein was found to directly interact with the carboxy terminal of both Hsc70 and Hsp70 chaperones, thus it was termed as “the carboxy terminus of Hsp70-interacting protein (CHIP)” (97). Through this interaction, CHIP was reported to block the

Hsc70/Hsp70 substrate binding cycle, and therefore, negatively regulate their folding activity. In another study by the same group, CHIP was found to interact with Hsp90 and inhibit activation of the glucocorticoid receptor (GR) substrate through dissociation of the Hsp90 co-chaperone, p23. Instead, CHIP induced ubiquitination followed by proteasomal degradation of the GR substrate (98). The ubiquitination activity of CHIP is mediated by the C-terminal U-box domain which functions as an E3 ubiquitin ligase towards protein substrates associated with Hsp90 and Hsc70 chaperones (99). Therefore, it was suggested that CHIP is a chaperone-dependent E3 ligase that acts as a link between protein folding and degradation of a chaperone substrate, regulating the balance between these two arms of the PQC system (98, 99).

CHIP is a protein composed of 303 amino acids, and is encoded by the STIP1 homology and U-box containing gene 1 (*STUB1*) located on chromosome 16 (100). The full-length *STUB1* pre-mRNA (NM_005861.4) contains seven exons and six introns (Figure 5A). Another protein-coding isoform (NM_001293197.2) has been predicted with the start codon located in the second exon of *STUB1*, which encodes a protein isoform of 231 amino acids with a shorter TPR domain. However, no experimental evidence is available for this transcript (National Centre for Biotechnology Information [NCBI], available from: ncbi.nlm.nih.gov).

1.3.1. Structural organization of CHIP

The primary structure of CHIP comprises an N-terminal TPR domain, a C-terminal U-box domain, and a central helical hairpin (HH) region (Figure 5A) (97, 101). CHIP dimeric structure, in association with the Hsp90 chaperone and ubiquitin conjugating enzyme 13 (Ubc13), has been described by Zhang *et al.*, using crystallized structure of mouse CHIP (102). For this reason, residues provided based on these data in this section correspond to the mouse CHIP amino acid sequence which differ from the human CHIP sequence by +1 amino acid from Ser20 (NCBI) (102). Equivalent residues in human CHIP are therefore assumed as (n-1), where (n) presents the amino acid position in the mouse CHIP.

The TPR domain includes three pair of TPR repeats, each consisting of two antiparallel α-helices separated by a turn (Figure 5B). The ability of CHIP for protein-

protein interactions with molecular chaperones is facilitated by the hydrophobic surface of the TPR motifs. The TPR binding site is provided by side chains of Lys31, Asn35, Phe38, Asn66, Leu69, Lys73, Lys96, and Asp135 as well as a hydrophobic pocket formed by side chains of Lys96, Phe99, Phe100, Phe132, and Ile136. Differences in the conformation of bound residues upstream of the EEVD motif explain the specificity of CHIP interactions with Hsp70 and Hsp90 chaperones (102).

The U-box domain consists of a pair of β-hairpins followed by a short α-helix and another hairpin, leading to an α-helix at the C-terminal (Figure 5B). As mentioned in section 1.2.2, U-boxes are considered as members of the RING-type E3 ligases with minor structural modifications compared to the RING fingers. In the CHIP protein structure, this domain acts as a scaffold by positioning the chaperone substrate (bound to the TPR domain) in close proximity to the E2 conjugating enzyme for completing the ubiquitination process. The U-box domain interacts with E2s through a hydrophobic groove comprising the short α-helix (254-265) and small parts of two β-hairpins (234-239 and 269-274) (102). The middle region of CHIP is formed of helical hairpins, and is known to be crucial for its structural stability, dimerization and functioning (101, 102).

The structure of a mouse CHIP is described as an asymmetric homodimer with each protomer adopting a different conformation in the dimer (102). CHIP dimerization occurs via two separate segments of polypeptides located at the helical hairpins and the U-box domain. At the U-box core of interface, dimerization happens via symmetrical interactions between Asn284 side chains and their surrounding hydrophobic clusters (Tyr231, Leu285, Ala286, Met287, Val290, and Phe294 and Ile246, Pro248, Gly250, and Ile282) in each protomer. Residues on the surface of helical hairpins from the N-terminal arm of one protomer (Leu162, Tyr165, Leu166, Leu169, and Ile170) and the C-terminal arm of the opposite protomer (Tyr208, Met212, Leu215, Phe216, and Val219) pack against each other and form the second dimer junction. The asymmetric structure of the helical linker is demonstrated as a straight α-helix (from Asp134 to Arg183) in one protomer and another α-helix broken into two parallel helices (Asp134–Arg155 and Glu161–Arg183) in the other protomer (Figure 5B). The broken α-helix causes the TPR domain to adopt a different orientation which inhibits binding of E2

enzymes to the associated U-box domain and results in a half-of-site activity for CHIP (102) (Figure 5C). Further investigations on the conformational dynamics of human CHIP revealed a symmetric dimer structure with a highly flexible broken segment in the middle domain, which might rapidly alternate between the helical and the unfolded state, and thus provide asymmetric and symmetric conformations sequentially (103). The interaction of CHIP with molecular chaperones can restrict this flexibility and lead to a stabilized TPR domain which overlaps partly with its attached U-box domain (103).

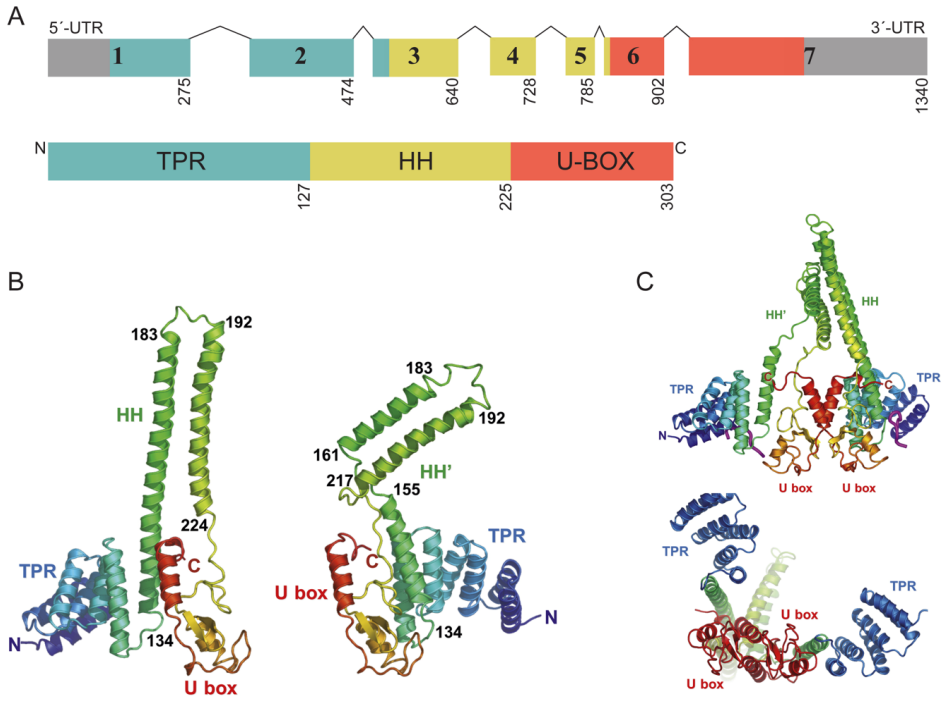

Figure 5. CHIP is a 303-amino acid protein with an asymmetric homodimer structure. A) There are three main domains in the primary structure of human CHIP, translated from seven exons of the *STUB1* mRNA (NM_005861.4). B) At the N-terminal, three pairs of antiparallel α-helices comprise the TPR domain (in blue). The central dimerization domain (in yellow) contains a helical hairpin with broken segments in one protomer, causing asymmetry in the conformation of CHIP. The U-box domain (in red) consists of three β-hairpins and two α-helices. C) The asymmetric structure of dimerization domain causes one of the TPR domains to adopt a different orientation towards the associated U-box domain, and leads to half-of-site activity for CHIP. This figure is adapted from (102).

1.3.2. CHIP interactions and mechanisms of function

CHIP is a multifaceted protein with regulatory roles over a large network of substrates, both as a co-chaperone and an E3 ubiquitin ligase. CHIP can modulate the activity of chaperones and their associated co-factors in connection with various substrate proteins. As mentioned, CHIP inhibits folding activity of Hsp90 towards substrates like glucocorticoid receptor (98) and erythroblastic leukemia viral oncogene homolog-2 (ErbB2) (104) by releasing the p23 co-chaperone. Similarly, CHIP can regulate Hsp70 chaperoning functions by antagonizing the effect of its co-chaperones Hsp40 and Hip (97).

CHIP associates with Hsp70 or Hsp90 through its TPR domain and, at the same time, participates in the ubiquitination and proteasomal degradation of the chaperone-bound substrates by recruiting E2 enzymes to the chaperone complex. This mostly happens through direct interaction of the CHIP U-box domain, as an E3 ligase, with the E2 enzymes (Figure 6A). A vast array of proteins has been reported to be degraded by CHIP through this mechanism. These substrates are implicated in multiple cellular pathways and pathologies including development, transcription, signaling, neurodegeneration, and cancer (105) (Table 1). In addition to these proteins, CHIP has been reported to target Hsp70/Hsp90 chaperones and itself as a part of auto-regulation mechanism during stress recovery (106).

In a few cases, CHIP has been shown to co-operate with other E3 ligases as an E4 co-factor and facilitate ubiquitination of the chaperone substrates in a TPR domain-mediated (U-box-independent) manner (Figure 6B). CHIP was first identified as an E4 enzyme in complex with Hsp70, Parkin, and Parkin-associated endothelin receptor-like receptor (Pael-R), where it facilitates Parkin-mediated Pael-R ubiquitination through dissociation of Hsp70 from Parkin (107). The E4 activity of CHIP has also been reported in association with the S-phase kinase-associated protein1 (Skp1)/Cullin/F-box (SCF) ubiquitin ligase complex, where it cooperates with the F-box E3 ligase (Fbx2) for ubiquitination and degradation of Fbx2-bound glycoproteins like the N-methyl-D-aspartate receptor subunit NR2A (108).

Table 1. CHIP substrates are involved in multiple cellular pathways.

Cellular Pathway	Substrate	Degradation Mechanism	ref.
Cancer	Smad1/ Smad4	Proteasomal	(109)
	Akt		(110)
	LKB1		(111)
	ErbB2		(112)
	c-Myc		(113)
	P53		(114)
	MIF		(115)
	eIF4E		(116)
	PTEN		(117)
	PTK6		(118)
	Src		(119)
	Menin		(120)
	AIF		(121)
	Filamin	Lysosomal	(122)
Neurodegeneration	nNOS	Proteasomal	(123)
	Ataxin-3		(124)
	β-amyloid		(125)
	Hsp70/Hsp90		(106, 126)
	Huntingtin		(124)
	SOD1		(127)
	LRRK2		(128)
	BAG3	Lysosomal	(129)
	Tau	Proteasomal/Lysosomal	(130)
	α-synuclein		(131)
Signaling	AR	Proteasomal	(132)
	ASK1		(133)
	Src		(119)
	MEKK2		(134)
	DLK		(135)
	SGK		(136)
	GHR	Lysosomal	(137)
Transcription	FoxO1	Proteasomal	(138)
	c-Myc		(113)
	GUCY		(139)
	P53		(114)
	ER		(140)
	SENP3		(141)
	HIF-1α	Proteasomal/Lysosomal	(142)
Development	Katanin p60	Proteasomal	(143)
	Profilin		(144)
	RUNX		(145, 146)
	SirT6		(147)
	Keratin		(148)
	MKKS		(149)
	Myocardin		(150)

This table is adapted from (105). Abbreviations: Smad, Sma-mother against decapentaplegic; Akt, AKR/J thyoma protein kinase; LKB1, liver kinase B 1; c-myc, cellular myelocytomatosis viral oncogene homolog; MIF, migration inhibitory factor; eIF4E, eukaryotic translation initiation factor 4E; PTEN, phosphatase and tensin homolog deleted on chromosome TEN; PTK6, protein tyrosine kinase 6; Src, sarcoma viral oncogene homolog; AIF, apoptosis-inducing factor; nNOS, neuronal enzymes like neuronal nitric oxide synthase; SOD1, superoxide dismutase1; LRRK2, leucine-rich repeat kinase 2; AR, androgen receptor; ASK1, apoptosis signal-regulating kinase 1; MEKK2, MAPK/ERK kinase kinase 2; DLK, dual leucine zipper- bearing kinase; SGK1, serum and glucocorticoid-regulated kinase-1; GHR, growth hormone receptor; FoxO1, fork head transcription factor 1; GUCY, guanylate cyclase; ER, estrogen receptor; SENP3, SUMO/sentrin protease 3; Runx1, runt-related transcription factor 1; SirT6, Sirtuin6; MKKS, McKusick-Kaufman syndrome protein.

While the majority of CHIP substrates are targeted to the proteasome, degradation of some proteins has been reported through the autophagy pathway (105). In these cases, CHIP binds to the substrate directly via its U-box domain and mediates ubiquitination and lysosomal degradation independent of the TPR domain and molecular chaperones (Figure 6C). For instance, degradation of the hypoxia-inducible factor-1 alpha (HIF1α) transcription factor in the lysosome has been reported to require CHIP to mediate the interaction between HIF1α and the LAMP2A receptor (142). CHIP is known to cause degradation of a few substrates such as HIF1α, α-synuclein and tau both in the TPR domain-dependent (proteasomal degradation) and U-box domain-dependent (lysosomal degradation) manners (131) (Table 1).

Localization of the CHIP substrates in different cellular compartments consequently leads to a distributed cellular expression pattern for CHIP. CHIP was first identified in the cytoplasm as a component of the quality control system for cytoplasmic proteins (97). Later, it was found to ubiquitinate mitochondrial proteins like leucine-rich repeat kinase 2 (LRRK2) (128) as well as proteins localized in the Golgi complex such as β-APP (125). In addition, CHIP has been detected in the nucleus where it activates the heat shock factor-1 (HSF1) (151), and on the endoplasmic reticulum membrane in association with the cystic-fibrosis transmembrane-conductance regulator (CFTR) substrate (152).

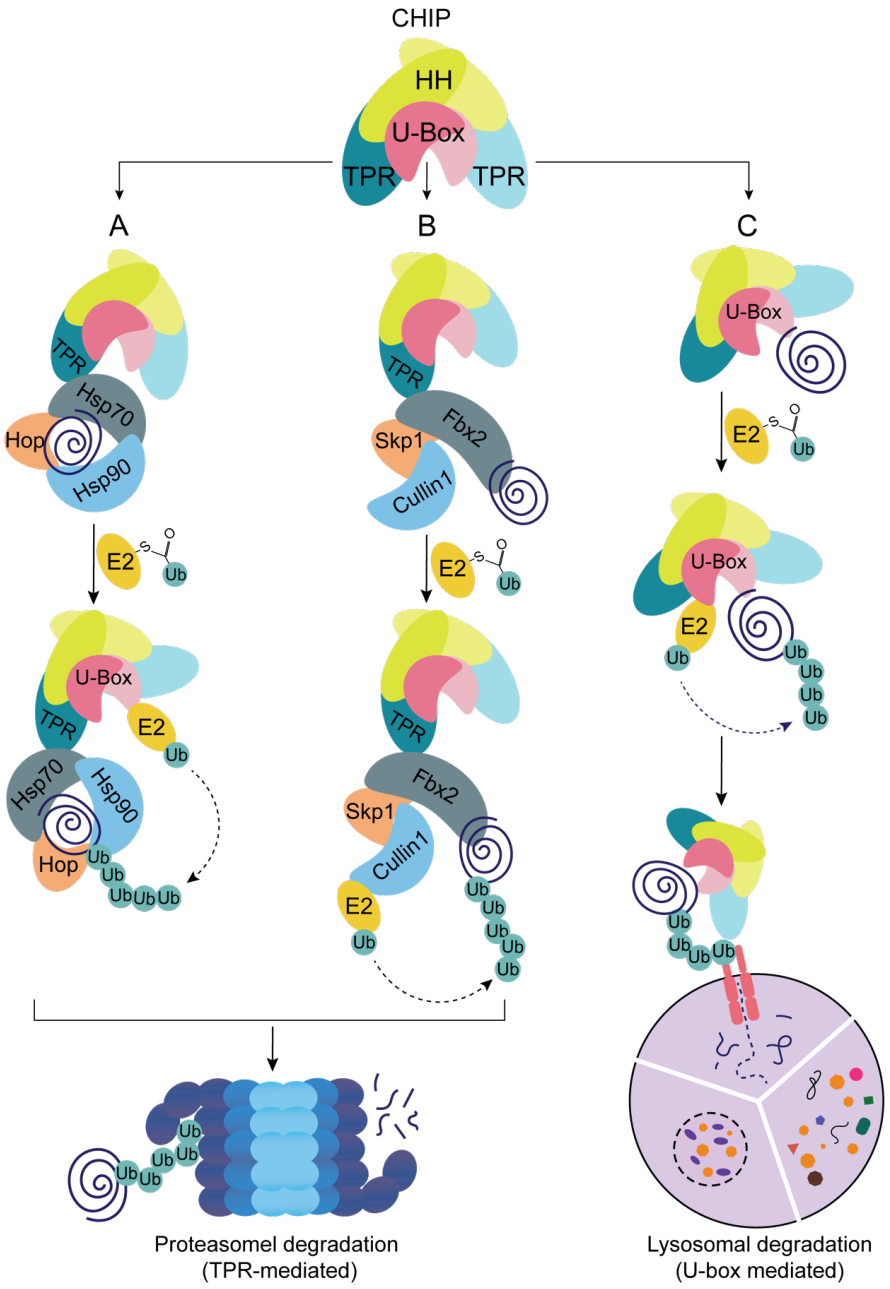

Figure 6. CHIP participates in the ubiquitination and degradation of substrates through different mechanisms. A) In the majority of cases, CHIP acts as an E3 ligase to ubiquitinate substrates bound to the Hsp70/Hsp90 chaperones for further degradation by 26S proteasome. This mechanism is mediated both by the TPR domain and the U-box domain of CHIP. B) For

some substrates, CHIP functions as an E4 co-chaperone through its TPR domain, and facilitates ubiquitination and proteasomal degradation of substrates in complex with other E3 ligases. C) In a few cases, CHIP mediates ubiquitination of the substrate directly through its U-box domain and independent of the TPR domain. These substrates will further be degraded through the chaperone-mediated autophagy pathway.

1.3.3. Regulation of CHIP

Expression profiling of *STUB1* shows a ubiquitous pattern with the highest levels in the metabolically active tissues skeletal muscle, heart, and brain, which supports the regulatory function of CHIP in protein homeostasis pathways (153). Under normal conditions, the basal levels of Hsp70/Hsp90 chaperones and their co-chaperones are sufficient to maintain cellular protein homeostasis. However, the expression of these proteins must be rapidly adjusted in response to various stress conditions such as heat-shock, oxidative damage and different human pathologies including neurodegenerative diseases, muscular dystrophies and heart diseases (154).

Regulation of *STUB1* expression **at the transcriptional level** has been linked to a number of human malignancies and inflammatory responses including Toll-like receptor (TLR) signaling, T-cell activation, and formation of dendritic-cell aggresome-like inducible structures (154). The TLR2 receptor has been shown to upregulate expression of *STUB1* through the c-Jun N-terminal kinases (JNK) inflammatory pathway (155). In addition, downregulated levels of *STUB1* mRNA and protein are reported in tissues with breast (156), colorectal (157), and gastric cancer (158). **At the post-transcriptional level**, CHIP downregulation has been observed during osteoblast differentiation in calvarial and osteoblast progenitor cells, where the microRNA miR-764-5p binds to the 3′-UTR of *STUB1* mRNA and inhibits its translation (159). The activity of CHIP can be regulated **at the post-translational level** through different mechanisms. Posttranslational modifications (PTMs) are known to regulate the ubiquitination activity of CHIP by recruiting other co-factors to the chaperone complex, which modulate the type and length of ubiquitin chains on the substrate (154). For example, monoubiquitination of CHIP at Lys2 results in association of the deubiquitinating enzyme Ataxin-3 which limits the length of ubiquitin chains on CHIP's substrates and terminates the ubiquitination reaction by deubiquitinating CHIP (160).

Regulation of CHIP by modifications other than ubiquitination is not directly evidenced, although associations have been reported between CHIP and phosphatase Laforin (161) as well as extracellular signal-regulated kinase-5 (ERK5) and Lim kinase-1 (LIMK1) (162, 163). The ERK5-CHIP interaction is proposed to be essential for CHIP ubiquitin ligase activity towards inducible cAMP early repressor (ICER) substrate, and the activity of CHIP is shown to be increased in the presence of ERK5 possibly due to changes in the conformation of CHIP (163).

Other mechanisms of regulation involves CHIP interactions with a number of proteins including Ca^{2+}/S100 protein (164), hepatitis B virus X-associated protein (Xap2) (165), Obg-like ATPase-1 (OLA-1) (166), Ataxin-3 (160) and members of the BAG family (154). Some of these proteins have been reported to regulate CHIP activity by competing either with protein substrates for binding to the TPR domain of CHIP (Ca^{2+}/S100), or with CHIP for binding to Hsp70 (OLA-1) and Hsp90 (Xap2) through their own TPR domain. Other proteins modulate CHIP ligase activity through association with the chaperone complexes in a non-competitive manner. BAG1 and BAG3 are known to stimulate CHIP activity through simultaneous interaction with Hsc70 and proteasome (167, 168). By contrast, BAG2 is shown to inhibit ubiquitination process by interfering with the interaction between CHIP and E2s. (169). A similar inhibitory effect has also been reported for BAG5 towards α-synuclein, although the mechanism of this effect is not understood yet (170).

1.4. CHIP and neurodegenerative diseases

1.4.1. CHIP as a guardian

Inability of neuronal cells to regenerate themselves highlights the added value of protein quality control in the brain compared to other tissues. During neurodegeneration, different components of the PQC system are recruited to the sites of protein deposits, where they function to prevent or remove protein aggregates. From this perspective, CHIP has been linked to a number of diseases including AD, ALS, PD, and polyQ disorders (105). In AD, CHIP has been shown to ubiquitinate phosphorylated tau at Lys48 and Lys63, thus directing its degradation via both proteasome and autophagy pathways (130). In addition, CHIP has been reported to suppress accumulation of toxic

β-amyloid by stabilizing normal APP as well as proteasomal removal of toxic β-amyloids (125). Lysosomal degradation of mutant SOD1 in ALS involves participation of CHIP in a complex with Hsc70, HspB8, and BAG3 (171). CHIP has also been found in association with the protein inclusions of Pael-R (107), α-synuclein (131), and LRRK2 (128) in PD. CHIP is known to switch between proteasomal and lysosomal degradation of α-synuclein by polyubiquitinating or monoubiquitinating this substrate, respectively (170). Oligomeric forms of α-synuclein are reported to be targeted preferentially for degradation in a TPR domain-dependent manner, suggesting an ability for CHIP to distinguish between different species of α-synuclein for processing via different pathways (172). The protecting role of CHIP in polyQ diseases has been demonstrated in connection with HD, SCA1, and SCA3, where CHIP was shown to promote ubiquitination and proteasomal degradation of polyglutamine aggregates of huntingtin, ataxin-1, and ataxin-3 as well as unexpanded forms of ataxin-1 in cooperation with Hsp70 (124, 173).

1.4.2. CHIP as a threat

From a different point of view, failure or insufficient functioning of the PQC system to eliminate misfolded and damaged proteins can result in the development of many neurodegenerative diseases. In a similar manner, *STUB1* mutations have been reported in connection with cerebellar ataxia diseases (see section 1.1.4 for more details).

Progressive cerebellar ataxias caused by homozygous and compound heterozygous mutations in the *STUB1* gene are categorized in a rare group of ARCAs named as **autosomal recessive spinocerebellar ataxia type-16 (SCAR16)** (100). Similar to other forms of ARCA, SCAR16 most often begins around the age of 20, although earlier and later onset have been reported in some cases (174, 175). *STUB1* was first reported as a novel causative gene for ARCA by Shi *et al.* in 2013 (100). They identified one homozygous (c.493C>T/p.Leu165Phe) and two compound heterozygous *STUB1* mutations (c.389A>T/p.Asn130Ile and c.441G>T/p.Trp147Cys; c.621C>G/ p.Tyr207* and c.707G>C/p.Ser236Thr) in three separate Chinese families with ARCA history. All affected patients showed cerebellar ataxia associated with cerebellar atrophy, and two related patients were detected with signs of cognitive impairment.

Impaired ability of CHIP to promote degradation of NR2A was further suggested as an underlying mechanism for development of SCAR16 in these patients (100).

At the same time, another group reported a different homozygous *STUB1* mutation (c.737C>T/p.Thr246Met) in two siblings with cerebellar ataxia from China (176). These patients displayed severe ataxia associated with clinical features overlapping with the Gordon Holmes syndrome including cognitive impairments and hypogonadotropic hypogonadism. Similar to the first report, loss of CHIP function was hypothesized to directly contribute to the disease phenotypes (176). Further studies revealed several other pathogenic mutations in *STUB1* associated with SCAR16 including our previous study in which a homozygous (c.194A>G/p.Asn65Ser) and a compound heterozygous (c.82G>A/p.Glu28Lys and c.430A>T/p.Lys144*) mutation were identified in two families originally from Middle East (174).

To date, more than 30 *STUB1* mutations have been reported in association with SCAR16 in different domains of CHIP (177-179) (Figure 7). Many of these mutations are characterized by negative effects on the activity, interactions, and protein stability of CHIP (180). In **paper I,** the structural instability of CHIP has been investigated as an underlying mechanism of SCAR16 for six *STUB1* mutations located in the TPR domain (Glu28Lys and Asn65Ser), the central HH region (Lys145Gln and Met211Ile) and the U-box domain of CHIP (Ser236Thr and Thr246Met) (Figure 7).

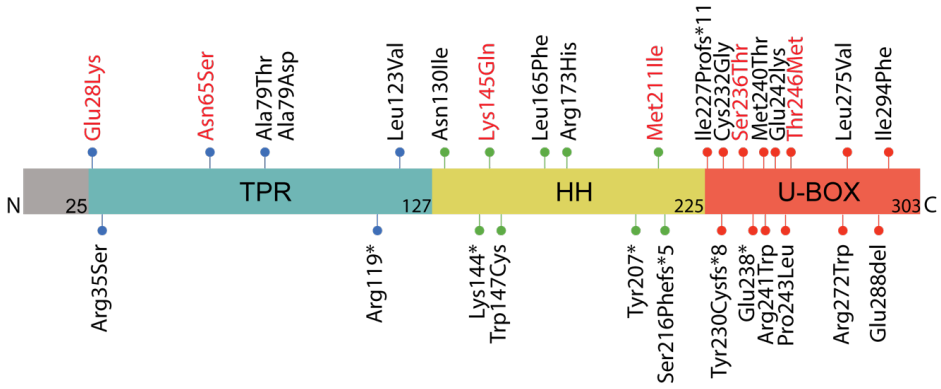

Figure 7. Homozygous and compound heterozygous *STUB1* mutations are associated with SCAR16. So far, 30 mutations are reported in association with SCAR16 (177-179). The six mutations characterized in paper I are indicated in red. This figure is adapted from (54).

Heterozygous mutations in *STUB1* have been recently reported to cause ADCA in a number of families with late-onset SCA and variably associated phenotypes (68). Genis *et al.* described **Spinocerebellar ataxia type-48 (SCA48)** for the first time in 2018, following identification of a frame-shift heterozygous *STUB1* variant (c.823_824delCT/ p.L275Dfs*16) in six patients from a Spanish family with developed cerebellar ataxia and cognitive impairment (68). MRI data showed atrophy in the cerebellar areas related to cognition and emotion. Spatial cognition disorder, language difficulties, and significant behavioral changes lead to characterization of the cerebellar cognitive/affective syndrome (CCAS) in addition to SCA in these patients.

More SCA48 cases were further reported in ten Italian families with more complex syndromes including ataxia in all the patients and several associated phenotypes such as chorea, parkinsonism, dystonia, cognitive-psychiatric disorder, epilepsy, hypogonadism and other endocrine dysfunctions (181, 182). Some of these clinical features including movement and endocrine abnormalities have also been found in SCAR16, suggesting continuous and overlapping clinical spectra for the *STUB*1-related disorders.

So far, 18 heterozygous *STUB1* mutations have been reported in families with SCA48 (178) (Figure 8). We have reported and characterized three novel *STUB1* heterozygous mutations found in patients with SCA48 in **paper II**.

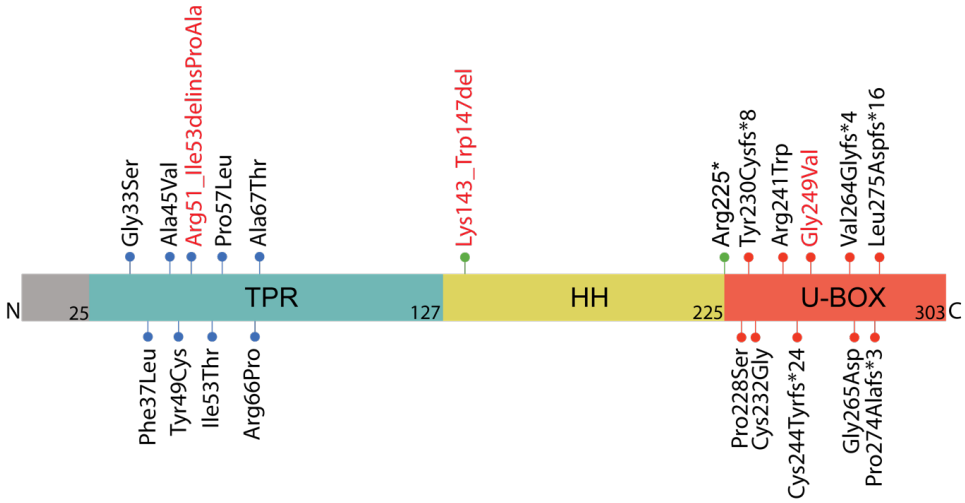

Figure 8. Heterozygous *STUB1* mutations have been reported in patients with SCA48. So far, 18 mutations are reported in association with SCA48 (178). The three mutations reported in paper II are indicated in red. This figure is adapted from (54).

1.5. Modeling neurodegeneration in zebrafish

Zebrafish, *Danio rerio*, is a tropical bony fish belonging to the infraclass of teleost and native to south Asia. Zebrafish are found in a wide range of environmental conditions in clear or turbid water with temperatures from 10 to 40 °C, pH from 6 to 10, and conductivity from 10 to 271 μS/cm (183). Laboratory strains of zebrafish have been maintained in a stable husbandry conditions for at least 25 years (183).

Zebrafish have been increasingly used as a model organism for the study of developmental processes and human diseases due to several advantages that these animals provide over other vertebrate models (184). The small body size and short generation time (2-3 months) of zebrafish facilitate quick and cheap production of large batches without requirements for large areas. Zebrafish produce large clutches of externally-fertilized eggs that are optically transparent and develop rapidly, allowing for direct *in vivo* visualization and large-scale analyses during early development (184). In addition, the small size and large clutches of zebrafish eggs enable high-throughput gene screening approaches for identification of mutations in genetic studies (185).

1.5.1. Anatomy of zebrafish cerebellum

During recent years, zebrafish larvae have been found with neurological phenotypes comparable to those observed in human including sleeping, learning, and drug addiction, which rapidly drew the attentions to the use of these animals in neurobehavioral studies (186). The zebrafish central nervous system (CNS) is similarly organized to that of other vertebrates dividing into forebrain (Telencephalon and Diencephalon), midbrain (Mesencephalon), hindbrain (Cerebellum and Medulla oblongata), and spinal cord (Figure 9A and B). In spite of a major difference of scale, the main regions of the zebrafish CNS including spinal cord, medulla, cerebellum, hypothalamus, optic tectum (superior colliculus) and olfactory system show obvious structural homology to their human counterparts (187).

The cerebellum mainly functions to control motor movements, and is also involved in several cognitive and emotional processes by integrating sensory inputs associated with motor commands (188). Different types of cerebellar neurons use either glutamate (glutamatergic/excitatory neurons) or gamma aminobutyric acid (GABA) and/or

glycine (GABAergic/glycinergic/inhibitory neurons) as their major neurotransmitter, and are arranged in a three-layer structure including the molecular layer (ML), the Purkinje cell layer (PCL), and the granular layer (GL) in both mammalian and zebrafish cerebellum (188) (Figure 9C and D). The Purkinje cells of PCL are key inhibitory neurons that receive and integrate information from outside of the cerebellum through excitatory neurons including climbing fibers and axons of granule cells (parallel fibers), as well as inhibitory stellate interneurons and project axons to the adjacent Purkinje cells or to other regions of brain via excitatory eurydendroid cells (188) (Figure 9E).

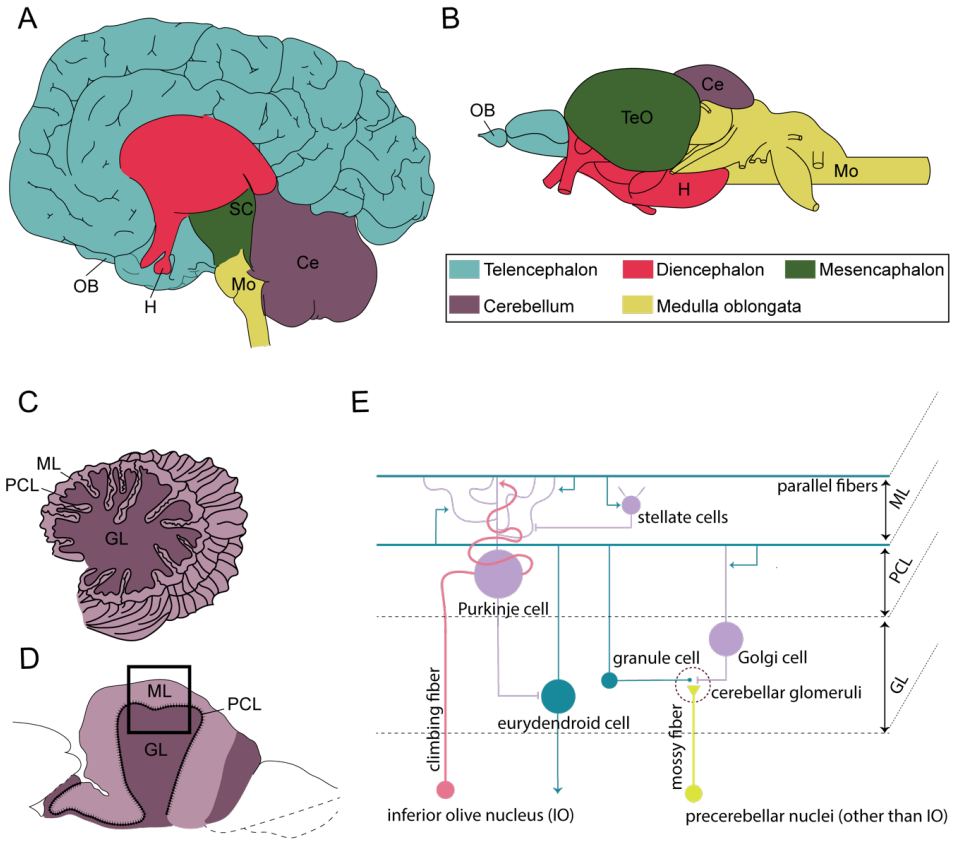

Figure 9. The structure and function of the cerebellum is highly conserved between mammalian species and zebrafish. The central nervous system presents highly similar structures in human (A) and zebrafish (B), consisting the main regions of Telencephalon, Diencephalon, midbrain, Cerebellum, and Medulla oblongata. This similarity also includes different layers of the cerebellum indicated as: ML (molecular layer), PCL (Purkinje cell layer)

and GL (granular layer) in the cross sections of the human (C) and zebrafish (D) cerebellum. E) Schematic illustration of neuronal circuits and connections in three layers of zebrafish cerebellum, indicating Purkinje cells as key neurons involved in integration and projection of sensory information to other parts of nervous system. This figure is adapted from (188, 189). MO, medulla oblongata; Ce, cerebellum; H, hypothalamus; TeO, optic tectum; OB, olfactory bulb; SC, superior colliculus.

A few structural differences have been reported between zebrafish and mammalian cerebellum such as the lack of eurydendroid cells for which the deep cerebellar nuclei (DCN) plays a functional homologous role in mammals (188). Yet, despite the differences, these species are reported with similar expression profiles of the GABAergic and glutamatergic neurons, indicating the presence of a similar molecular machinery for cerebellar development and functions (188).

1.5.2. Gene editing in zebrafish

In addition to the advantages mentioned earlier, the zebrafish genome shows 50-80% homology with most human genes, which enables an effective and simplified manipulation of gene expression and function for many human gene orthologs (184). However, this process can be complicated due to duplication of many genes in zebrafish during evolution (184).

To date, different tools have been introduced for genetic manipulation of zebrafish. Knock-out and knockdown techniques include chemical mutagenesis or injections with anti-sense morpholinos (MOs) which block translation or splicing of pre-mRNAs, as well as interfering RNAs that bind to and further destroy the mRNA of interest (190). Injection of synthetic protein-coding mRNAs or expression plasmids into early embryos are standard methods for global overexpression or transgenic expression of proteins of interest in zebrafish (191). Sequence-specific manipulation of zebrafish genome by designed endonucleases has been emerged as a golden technique for efficient targeted mutagenesis during recent years. In targeted genome editing techniques, different nucleases including zinc finger nucleases (ZFNs), transcription activator-like effector nucleases (TALENs), and clustered regularly interspaced short palindromic repeats (CRISPR) associated protein 9 (Cas9) endonucleases are used to generate a double-

strand break (DSB) in the target site (191). DSB repair by non-homologous end joining (NHEJ) mechanism is error prone and can result in frameshifts and early stop codons by introducing random insertions/deletions. In a more precise method of mutagenesis, DSB repair can be directed through homologous recombination (HR)-mediated pathway, leading to site-directed integration or substitution of nucleotide(s) (191).

The *STUB1* zebrafish orthologue (*stub1*) encodes a 287 amino acid Chip protein (NP_955968.2, NCBI) with 77% sequence identity to the human CHIP. At the C-terminal, zebrafish Chip is ten amino acids shorter than the human CHIP, however the U-box domain structure as well as key residues involved in the interactions with E2 enzymes are reported to remain conserved in zebrafish (192). In **paper III**, we have characterized Chip expression pattern and enzymatic function in zebrafish and also generated and characterized mutant zebrafish with a truncated U-box domain of Chip for the first time by using CRISPR/Cas9 technique.

2. Aims of the study

STUB1 mutations have recently been reported in spinocerebellar ataxia patients with recessive (SCAR16) and dominant (SCA48) types of inheritance. These mutations are located in regions encoding different domains of the CHIP protein (see section 1.4.2 for more details). The molecular mechanisms by which *STUB1* mutations cause the disease and the relationship between *STUB1* variants and different clinical manifestations are not well understood yet. Our group has recently described three novel *STUB1* variants in families with SCAR16 (174). These mutations were suggested to impact CHIP protein expression levels as well as its ubiquitin ligase activity and interactions.

The overarching aims of this thesis were to characterize the molecular properties of CHIP under the effect of recently reported recessive and dominant *STUB1* mutations, and to establish a stable, mutant zebrafish line for investigation of the *STUB1*-mediated disease mechanisms.

Specific objectives were determined as follows:

1- To study the structural and functional significances of *STUB1* mutations mediating SCAR16, using *in vitro* biochemical assays (**paper I**)
2- To describe novel heterozygous *STUB1* mutations in patients with SCA48 and further characterize the structural and functional consequences of these mutations, using *in vitro* biochemical assays (**paper II**)
3- To investigate the pathogenic effects of impaired CHIP ubiquitin ligase activity by generation and characterization of mutant zebrafish lacking the Chip functional U-box domain (**paper III**)

3. Summary of results

3.1. Paper I

In vitro characterization of six STUB1 variants in spinocerebellar ataxia 16 reveals altered structural properties for the encoded CHIP proteins.

Several bi-allelic mutations have been described in the *STUB1* gene in association with the autosomal recessive spinocerebellar ataxia 16 (SCAR16) disease. Some of these mutations have been proposed to cause SCAR16 through disruption of CHIP ubiquitin ligase activity, protein levels and interactions with the substrates (100, 174, 176). However, the effect of these mutations on the structural properties of CHIP has not been fully recognized yet. In this paper, we investigated the effect of six *STUB1* mutations (Glu28Lys, Asn65Ser, Lys145Gln, Met211Ile, Ser236Thr, Thr246Met) on CHIP ubiquitin ligase activity, structural stability, and conformational states. These variants were expressed as recombinant proteins and examined *in vitro* by using ubiquitin ligase activity, limited proteolysis, size-exclusion chromatography, native gel electrophoresis and circular dichroism assays.

We observed impaired ubiquitination of the Hsc70 substrate by the Asn65Ser and Thr246Met variants. The Thr246Met variant was also impaired for self-ubiquitination activity. However, the other variants of CHIP displayed similar activities as the wild-type protein. Limited proteolysis data revealed decreased structural stability for five variants of CHIP (Glu28Lys, Lys145Gln, Met211Ile, Ser236Thr, Thr246Met) with increased rates of trypsin degradation among which, the Glu28Lys and Thr246Met variants had the highest degradation rates. On the other hand, the Asn65Ser variant was associated with slower degradation compared to the wild-type CHIP, indicating a more stable protein structure for this variant. The oligomeric structure of CHIP protein was mostly altered in case of the Glu28Lys, Asn65Ser, and Thr146Met variants: size-exclusion chromatography of CHIP demonstrated increased amount of high-oligomeric forms and less dimers for the Glu28Lys variant compared to the wild-type CHIP. Asn65Ser, in contrast, showed elevated levels of dimeric structures and Thr246Met was associated with high levels of large oligomeric and monomeric structures, but little

amount of dimeric CHIP. Higher-order oligomers were also detected as the major conformational state of Thr246Met by native polyacrylamide gel electrophoresis, while other variants presented similar patterns of protein migration as the wild-type CHIP. Finally, using circular dichroism spectroscopy, increased molar ellipticity at 222 nm was observed for Asn65Ser compared to the wild-type protein and other variants, indicating elevated levels of secondary structure content for this variant. In contrast, Thr246Met was identified with a significant loss of secondary structures. This variant also displayed more alterations during thermal denaturation compared to what was observed for the wild-type CHIP and other variants. This was demonstrated by the absence of dimeric denaturation transition in the protein unfolding profile of Thr246Met which, in line with the previous findings, indicates less available dimeric structures for this variant.

Taken together, our results illustrate a profound impact for some of the *STUB1* mutations on the ubiquitin ligase activity and structural properties of CHIP. These data can be beneficial to the growing knowledge about the mechanisms behind the pathogenicity of SCAR16 disease.

3.2. Paper II

Genetic dominant variants in *STUB1*, segregating in families with SCA48, display *in vitro* functional impairments indistinctive from recessive variants associated with SCAR16.

Heterozygous mutations in the *STUB1* gene have been recently described in association with a new form of dominantly inherited cerebellar ataxia disease, spinocerebellar ataxia type 48 (SCA48). To date, 18 families are reported with SCA48, presenting cerebellar ataxia phenotypes often associated with cognitive-psychiatric disorder and some expanding features like dystonia and parkinsonism. However, molecular investigations elucidating the pathogenic effects of these variants as well as mechanisms underlying their dominant inheritance are still unknown. In this study, we reported three novel heterozygous variants of *STUB1* in families with SCA48, and for the first time,

characterized the structural and functional properties of these variants by *in vitro* assays on recombinant CHIP proteins.

Using whole exome sequencing, we identified the heterozygous *STUB1* variant c.152_158delinsCAGC (p.Arg51_Ile53delinsProAla) in the first proband, her father, and three siblings of the first family, the variant c.426_441delinsT (p. Lys143_Trp147del) in the second proband and her father, and the missense variant c.746G>T (p.Gly249Val) in the third proband and her mother. These patients presented with common SCA48 phenotypes including progressive cerebellar atrophy and dysarthria at the average age of 48, and some were also reported with cognitive and psychiatric disorders. However, phenotypes related to other organs such as eye movement abnormalities, urinary symptoms and hypergonadotropic hypogonadism were rarely reported.

In vitro functional analysis showed a complete lack of ubiquitin ligase activity towards the Hsc70 substrate for all the variants as well as impaired self-ubiquitination activity for the Gly249Val variant. Using circular dichroism spectroscopy, we observed decreased molar ellipticity at 222 nm as well as loss of one or two unfolding transitions in the thermal unfolding profiles of all the variants, which indicate a profound impact of the *STUB1* mutations on the structure and oligomerization of CHIP. Alterations in the oligomeric structure of CHIP variants were further verified by native polyacrylamide gel electrophoresis, where all the variants were associated with reduced dimeric structures and a remarkable increase in the amounts of higher-order oligomers compared to the wild-type CHIP.

Overall, our findings demonstrate deleterious effects of heterozygous *STUB1* mutations on the ubiquitin ligase activity as well as conformational structure of CHIP. These molecular data are found to be similar to those of the previously reported recessive *STUB1* variants associated with SCAR16. However, the healthy status of *STUB1* carriers in SCAR16 families complicates speculations on the genotype-phenotype correlations for these diseases. Therefore, we suggest performing additional genetic screenings as well as regular clinical follow-ups for carriers of SCAR16 variants. Future studies should also aim to investigate molecular effects of more SCA48

variants in order to understand the underlying mechanisms and relationships between the SCAR16 and SCA48 diseases.

3.3. Paper III

U-box domain truncation in the Chip protein affects Purkinje neuron morphology and leads to behavioral changes in zebrafish.

The pathogenic effects of CHIP deficiency have previously been investigated *in vivo* by using mammalian animal models (151, 176, 193-197). However, molecular mechanisms underlying CHIP-related diseases remain to be completely understood. In this study, we used zebrafish animals to investigate the phenotypes associated with impaired ubiquitin ligase activity of CHIP. We first characterized the zebrafish orthologue of *STUB1* (*stub1*) and further described zebrafish mutants of *stub1* with a truncated U-box domain.

Analysis of CHIP protein structure and function revealed a high degree of amino acid sequence similarity as well as conserved ubiquitin ligase activity between human and zebrafish. Transcripts of *stub1* were found to be ubiquitously expressed in zebrafish tissues, ranging from high levels in reproductive tissues and brain to the lower levels in liver, kidney and thyroid. *In situ* hybridization of brain sections using *stub1* cRNA probes demonstrated signals in the Purkinje cells and granular layer of the cerebellum, indicating a conserved expression pattern for *STUB1* between mammals and zebrafish. Using CRISPR/Cas9 technique, we generated homozygous mutant zebrafish with a 7-base pair deletion mutation in the last exon of the *stub1* gene, resulting in early stop codon and truncation of 28 amino acids from C-terminal of the Chip protein. Recombinant Chip proteins produced from the cDNA library of the homozygous mutant zebrafish brains were found to be impaired for the ubiquitin ligase activity towards the Hsc70 substrate as well as Chip itself. These fish were studied up to the age of 24 months, and examined for development of phenotypes associated with impaired activity of Chip. A progressive reduction of body size was observed for the mutant fish at 6, 12 and 24 months compared to their wild-type siblings. Magnetic resonance imaging of mutant brains at 24 months revealed no major atrophy of the cerebellum or other parts. However, a disturbed growth pattern and morphology was detected by immunostaining

for the Purkinje cell dendrites of the mutant fish with a significant reduction in the total number of distal filaments in the molecular layer of cerebellum at 24 months. Detailed examination of mutant Purkinje cell dendrites indicated no significant swelling while the number of spines on these filaments were observed with an increasing trend as compared to the wild-type dendrites. A significant loss of Purkinje cell bodies was also detected in the mutant fish at 6 and 24 months, and mutant cell bodies at 24 months displayed decreased size and irregular shapes. Examination of the 26S proteasome activity in zebrafish brains indicated a reduced activity in the mutant fish at 24 months although this reduction was not associated with increased levels of amyloid oligomers nor some of the known CHIP substrates including NR2A, α-synuclein and ataxin-3. Finally, analysis of fish behavior indicated less anxiety-like behavior for the mutant animals at 12 and 24 months of age compared to the wild-type fish, demonstrated by increased amount of time spent in the top zone of a novel tank. The average swimming velocity of these fish was also significantly increased at 24 months. Investigation of the locomotor activity as well as social behavior did not reveal any significant differences between the wild-type and mutant fish.

Overall, these findings demonstrate a conserved ubiquitin ligase activity as well as expression pattern of CHIP between human and zebrafish, and indicate that truncation of the Chip U-box domain in zebrafish results in the development of morphological, physiological, and behavioral abnormalities that are partially similar to those reported in CHIP-deficient mammalian models as well as SCAR16 human patients. Future studies on these models as well as knock-out zebrafish with total loss of Chip function will significantly improve our understanding of the pathogenic pathways behind SCAR16/SCA48 as well as other *STUB1*-mediated diseases.

4. Discussion

Today, neurodegenerative diseases are a matter of great concern as major threats to human health, and effective treatments to overcome these destructive diseases require a deep understanding of the causes and underlying mechanisms. Therefore, it is important to study neurodegeneration from several perspectives to gain a better overview of how it affects the overall status of a healthy organism. To this end, we investigate spinocerebellar ataxia diseases (SCAR16/SCA48) mediated by variants of the *STUB1* gene through a set of *in vitro*, *in vivo*, and clinical studies. Our findings from this thesis add to the growing knowledge about protein characteristics of CHIP variants and introduce a new mutant animal model for future studies on SCAR16/SCA48 as well as other *STUB1*-related diseases.

4.1. The unknowns of SCAR16 and SCA48 diseases

In **paper I**, we characterized the biochemical consequences of six *STUB1* mutations previously reported in SCAR16 patients (198). Our functional data confirmed previous studies where Asn65Ser mutation was shown to impair ubiquitination activity of CHIP towards the Hsc70 substrate (174), and Thr246Met variant was reported with a complete loss of ubiquitin ligase activity towards chaperone substrates as well as itself (176). We also provided the first *in vitro* evidence regarding the effect of these mutations on CHIP structural properties, which indicated significant structural alterations affecting CHIP's stability for the Asn65Ser and Thr246Met variants. These data were later supported in a similar study by Kanack *et al*., indicating that the majority of *STUB1* mutations affect the ubiquitin ligase activity of CHIP through reducing its structural stability and steady-state levels (180). They further suggested that defects in the mutant CHIP structure and function are often correlated with the location of corresponding mutation(s). For example, a direct disruption of interactions through reduction of CHIP's affinity for the chaperones was shown for some mutations located in the TPR domain such as Asn65Ser, explaining the inability of this variant to ubiquitinate Hsp70 chaperone despite being intact for self-ubiquitination (180). Likewise, the ability of the U-box variant Tht246Met, with a complete loss of ubiquitination activity, to maintain

chaperone interactions with Hsp70 was previously shown and suggested to be due to the presence of an intact TPR domain in this variant (176). In another study, the Lys145Gln variant, located in the central domain of CHIP, was predicted to affect CHIP structure and stability due to the critical location of the affected amino acid residue in CHIP dimerization interface (199). However, our data from size-exclusion chromatography and native gel electrophoresis did not indicate any changes in the oligomeric state of the Lys145Gln variant. We rather observed changes in oligomerization of Thr246Met and Glu28Lys, demonstrated by a significantly higher levels of oligomers for the Thr246Met variant and, to a lesser extent, Glu28Lys. Similar findings were also reported for these two variants in the study by Kanack *et al*.(180).

Taken these data together, we suggest that mutation-specific loss-of-function in CHIP through impaired chaperone interactions and/or reduced protein levels is the underlying mechanism of several SCAR16 variants, while elevated levels of oligomerization in variants Glu28Lys and Thr246Met might also be deleterious through gain-of-a toxic function mechanism. The functional effect of some variants including Lys145Gln, Met211Ile, and Ser236Thr, with similar structural and functional properties to those of the wild-type CHIP, remains unknown. It could be speculated that the presence of the other *STUB1* nonsense mutation in the compound heterozygous state acts together with these variants thereby contributing to the development of SCAR16 in these patients.

In **paper II,** we reported three novel heterozygous *STUB1* mutations detected in patients referred for genetic testing and investigated their putative role in SCA48. We characterized the biochemical effects of these mutations on the ubiquitin ligase activity and structural properties of CHIP, and noticed remarkable similarities in these data and our previous findings for the recessive SCAR16 variants. We found an intact ability of the Arg51_Ile53delinsProAla (located in the TPR domain) and Lys143_Trp147del (located in the dimerization domain) variants for self-ubiquitination, while being impaired for ubiquitination of the Hsc70 substrate. A complete loss of ubiquitin ligase activity was identified for the Gly249Val (located in the U-box domain) variant. These data are consistent with the previously suggested correlation between the location of

STUB1 mutations and resulting defects in the structure and function of CHIP (180). In addition, we observed a high tendency for formation of higher-order oligomers in these variants as we had reported for the recessive Thr246Met variant in paper I (198). The Thr246Met mutation was first described by Shi *et al*. in a family affected with ataxia and cognitive impairments (176). Cognitive involvement has also been frequently reported in SCA48 patients in paper III and other studies (178), which could point out a potential connection between aggregates of CHIP and development of this phenotype. However, current data regarding the functional implications of SCA48 variants are limited to our study, and further investigations on a larger number of mutations are required to examine these speculations.

CHIP functions in a dimeric form. The reported pathogenicity of one mutated *STUB1* allele in SCA48 patients suggests that, in heterodimers of CHIP, the product of the abnormal allele could adversely affect the functional monomer produced from the wild-type allele, resulting in CHIP total functional deficiencies. The so called "dominant negative effect" of SCA48 variants can be examined in heterozygous mutant systems (see section 6 for more details). On the other hand, in SCAR16 families, carriers of *STUB1* variants do not seem to be affected by the disease while homozygous or compound heterozygous patients present cerebellar ataxia phenotypes with earlier onset and more severity than that of SCA48 patients. With this said, it would be rational to propose that *STUB1* mutations lead to location-specific clinical features where, in some cases, the presence of one pathogenic allele is enough for the development of cerebellar ataxia while, in other cases, it seems as if both alleles need to be mutated in order for the disease to manifest. However, such assumptions can be questioned by our earlier observations indicating similar functional and structural impacts for the SCAR16 and SCA48 variants, as well as by two studies reporting previously described SCAR16 variants to cause SCA48 in other families (54, 200).

We suggest that the disease status of *STUB1* carriers should be verified at least in these families, and clinical follow-ups should be planned to search for possible signs of late-onset phenotypes. Further functional investigations on other SCA48 variants will also be critical to gain a more complete overview of their biochemical significance compared to the SCAR16 variants. In addition, as suggested by Roux *et al.* (200), the

penetrance of *STUB1* variants in SCA48 families could be influenced by other factors such as sex, variants of other ataxia-related genes or even the polygenic background of the person. Although this hypothesis has not so far been verified, future studies should still consider examining the potential contributing effect of these factors in the development of SCA48.

4.2. The significance of U-box domain in the pathogenesis of CHIP

In the studies by Heimdal *et al*. and Madrigal *et al*., it was hypothesized that mutations in certain domains of CHIP with specific biochemical activities are associated with distinct clinical features (174, 201). They found that variants of the U-box domain such as Thr246Met and Met240Thr can have severe effects on CHIP ubiquitin ligase activity, and are strongly associated with additional phenotypes related to cognitive dysfunction in SCAR16 patients. Likewise, our findings in paper I and II illustrate more severe biochemical impacts for the Thr246Met and Gly249Val variants compared to other variants examined, resulting in a complete loss of CHIP ubiquitination function and significant structural alterations (198).

In an attempt to investigate the effect of a non-functional U-box domain on development of cerebellar ataxia, we, in **paper III**, developed the first mutant zebrafish with a truncation at the C-terminal of Chip. Our initial investigations indicate a high degree of conservation in the function and expression pattern of wild-type CHIP between zebrafish and mammalian orthologs, highlighting the potential of zebrafish as a model system in CHIP-related studies. Mutant zebrafish lacking the U-box domain presented significant deviations in the morphology of cerebellum as well as patterns of behavior, consistent with what was previously observed in SCAR16 patients and *Stub1* knock-out mouse models (176, 202).

Purkinje cell pathology is a common observation in patients with cerebellar ataxia. The aberrant function and degeneration of Purkinje cells in spinocerebellar ataxias are suggested to be due to altered expression or activity of proteins and membrane channels, which result in downstream changes in calcium homeostasis and synaptic input from climbing and parallel fibers (203). Neuropathological examination of the cerebellum in SCAR16 patients with compound heterozygous mutations in *STUB1* (Met211Ile and

Glu238*) indicates severe decrease in Purkinje cells and neurons of the granular layer (202). *Stub1* $^{-/-}$ mice were also reported with loss of Purkinje cells and swollen dendrites in the cerebellum (176). Likewise, we could demonstrate a progressive disorganization of the dendrites with a decrease in the number and size of cell bodies in the Purkinje cells of the mutant fish up to 24 months of age, assuming that larger perturbations might happen at later ages. We did, however, not observe evidence of major atrophy of the cerebellum or other regions in mutant brains by 24 months of age, although this is a common phenotype in patients with *STUB1*-mediated cerebellar ataxia. Considering the average maximum lifespan of 3-5 years for laboratory zebrafish, observation of age-related phenotypes can also be expected after 24 months. On the other hand, it cannot be ruled out that the MRI system of our choice could potentially limit our ability to detect smaller deviations between the cerebellum structure of wild-type and mutant zebrafish as it is primarily designed for visualization of the brain anatomy in larger animals such as mice and rats. Development of new imaging tools specialized for zebrafish brain would therefore be advantageous for a more precise characterization of the morphology of the cerebellum in these animals in future.

Behavioral data indicated changes related to a reduced level of anxiety in the mutant fish, demonstrated by increased time spent in the top zone of a novel tank. Similar pattern of behavior has previously been reported for mice with total loss of CHIP function, and was suggested to indicate an abnormal exploration pattern in a novel environment (176). The exploratory behavior is known as an intrinsic behavior important for survival. Investigations of a novel environment or novel objects in a familiar environment require high levels of sensory processing in the cerebellum (204), and has been hypothesized to be related to cognitive functions (205). In addition, degeneration of the cerebellum and neuronal circuits can result in an increased activity or repetitive and stereotypical behaviors due to disruption of inhibitory control, and hyperactivity has been reported in patients with dementia and attention deficit disorders (206, 207). Although the locomotion behavior studies revealed similar findings in the overall activity of the wild-type and mutant fish, a significant increase was observed in the average velocity of these fish in the novel tank at 24 months of age, which might be an early indicator of a tendency for more activity. Thereby, we propose that the

abnormal behavior observed for the mutant fish in the novel tank diving experiment can possibly be related to the cognitive dysfunction often seen in SCAR16 patients with impaired U-box domain of CHIP. However, these data should be considered as preliminary and future studies are required on these fish to understand if the phenotypes persist and increase in severity at later ages. In addition, we do not exclude the possibility that the intact N-terminal of Chip in the mutant fish might have a compensating effect for the impaired U-box domain by targeting at least a few substrates for ubiquitination via the TPR domain, as previously reported for α-synuclein and NR2A substrates (108, 131). Therefore, future experiments should be designed to investigate the pathogenic effect of total loss of CHIP function as well as disease-associated variants of different CHIP domains by using knock-out and knock-in animal models (see section 6 for more details).

4.3. The power of zebrafish in neurodegeneration science

While working at the University of Oregon in 1970s, **George Streisinger** recognized the vast potential of zebrafish for the first time in developmental and genetics research. He is known as the founding father of zebrafish research, and published the very first method for the use of zebrafish in screening mutants among a pathogenic population (208). His valuable discovery has been spread to over 300 research laboratories as of today.

Modelling human diseases in primary model organisms with a completely sequenced genome allows for a fast screening of mutations and a better understanding of protein interactions and regulatory pathways within the context of a simpler biological system. For instance, worms and fruit flies are common transgenic systems to study toxic mechanisms underlying neurodegenerative diseases (209). Zebrafish, as a vertebrate, has developed a more similar nervous system to those of mammalian species. The anatomical and structural similarities of CNS, together with the presence of a more comparable genetic background containing orthologs of many human genes have led to the use of these animals in modelling a wide range of neurodegenerative diseases (187).

Zebrafish models of Alzheimer's disease have been generated by loss of APP function, resulting in reduced body length and impaired movements during early development (210). Stable transgenic zebrafish lines expressing mutant human tau proteins have also been established that show pathologic phenotypes of tauopathies such as hyperphosphorylation and accumulation of tau within the brain and neurodegeneration in spinal cord. Zebrafish embryos expressing mutant tau are reported with disruption of escape behavior in response to touch stimulus (211, 212).

Models of Parkinsonism are well established in zebrafish by injection with neurotoxins like 1-methyl-4-phenyl-1,2,3,6-tetra-hydropyridine (MPTP) and 6-hydroxydopamine6-(OHDA). These animals are reported with typical neurochemical and behavioral phenotypes of PD including reduced velocity and traveled distance, reflecting impaired motor coordination, as well as deficiencies in memory and learning (213, 214). Transgenic and knock-out zebrafish models of PD have also been generated for some disease-associated genes (215, 216). For example, knockdown of *pink1* resulted in reduced swimming behavior and alterations in mitochondrial function (217). Zebrafish with *parkin* deficiencies were reported with loss of dopaminergic neurons and impaired mitochondrial respiratory chain while transgenic overexpression of *parkin* suggested a protective role against cell death (218, 219). Transient expression of another PD-associated gene, *snca*, is reported to cause axon swelling followed by cell death in zebrafish sensory neurons, indicating the toxicity of the encoded protein, α-synuclein, in the axonal compartment (220). In addition, heterozygous zebrafish with glucocerebrosidase1 deficiencies showed degeneration of dopaminergic neurons and reduced motor activity (221).

Huntingtin loss-of-function in zebrafish resulted in blood hypochromia and reduced hemoglobin production due to altered iron metabolism as a pathological mechanism of HD. Moreover, morphant zebrafish displayed reduced sensory neurons in telencephalic tissues where huntingtin is mainly believed to function (222). Loss of huntingtin function were associated with small eyes and head as well as abnormal jaw in other zebrafish models of HD (223).

Zebrafish are also known to have a great potential in behavioral research by presenting conserved behavioral patterns, similar to what has been reported in

mammalian species. The recently developed powerful video-tracking tools enable high-throughput screening of behavior for both larval and adult zebrafish. Several studies have described zebrafish responses to various drugs such as fluoxetine (224) and ethanol (225), and reported behavioral phenotypes of adult fish in connection to different diseases including social behavior (226), addiction (227), sleeping (228), memory and learning (229). The exposure of zebrafish to an unfamiliar environment, as well as some pharmacological agents, have been reported to evoke a robust response consistent with previous findings in rodents, supporting the capacity of zebrafish as a valid model of anxiety and exploratory behaviors (230, 231).

Despite several advantages of zebrafish as a model organism for neurodegenerative diseases, one should also consider the limitations associated with these animals as a potential determining factor in translational research. The presence of more than one copy of several genes in the zebrafish genome as a result of a whole genome duplication complicates identification of human homologs and the process of gene editing in zebrafish (184). In such cases, the function of a gene could be divided between the two duplicated genes or completely lost for one of the genes. Therefore, it is important to consider a possible compensating effect of the duplicated gene for the loss of function of a homolog targeted for knockdown or knock-out (184). The lack of high-quality antibodies against various zebrafish proteins represents another obstacle for the use of these animals in different immunoassays such as immunohistochemistry, western blotting, and immunoprecipitation. Technical and economic investments for generation of new specific antibodies would, therefore, be beneficial to the use of zebrafish in an increasing number of research projects. As previously mentioned, the simple structure of nervous system in non-mammalian species enables a better understanding of human diseases. Although, this applies to conditions where the underlying mechanisms are phylogenetically conserved to a sufficient level. Several lines of evidence indicate that observations in zebrafish models of different diseases are clinically applicable due to the presence of conserved CNS structures between zebrafish and human (187). However, there are a few striking differences reported between mammalian and zebrafish brain. The ability of zebrafish nervous system for continued growth and generation of new neuronal circuits after injury or a disease, for instance, is

in contrast to the inhibitory environment of mammalian CNS for regeneration (232). It is not clear whether the repairing capacity of zebrafish brain can hamper the power of this organism in modelling degenerative diseases (187).

Overall, initial zebrafish models of several neurodegenerative diseases indicate the development of key morphological and biochemical features shared with human diseases, which provide an excellent outlook for application of zebrafish to study the pathogenesis of these diseases. However, it is also possible that early findings could not yet fully represent the degree to which human diseases are acting. Optimization of current models and assays are hence critical to generate a valuable progress in this important field of neurology.

5. Concluding remarks

The work presented in this thesis highlights the key role of the CHIP protein in the maintenance of protein homeostasis for normal cellular functions. Our findings illustrate the molecular basis of genetic defects in CHIP structure and function, and provide further insights into the role of aberrant ubiquitin ligase function in CHIP-mediated diseases by using *stub1* mutant zebrafish.

Characterization of the *STUB1* mutations associated with the recessive SCAR16 and dominant SCA48 diseases in **paper I** and **paper II** demonstrated similar biochemical impacts on CHIP ubiquitin ligase activity and oligomerization properties. However, the presence of unaffected heterozygous carriers reported in SCAR16 families opens up new questions regarding the validity of current data on the disease status of SCAR16 parents and highlight the importance of future studies focusing on the exact mechanisms behind the pathogenesis of each of these variants.

The study of homozygous mutant zebrafish expressing Chip with a truncated, non-functional U-box domain in **paper III** revealed severe alterations in the body size and cerebellum structure, as well as behavioral changes related to anxiety and exploration patterns. These findings indicate deleterious effects of impaired ubiquitin ligase activity of CHIP and moreover, suggest zebrafish as a new potential animal model for the study of *STUB1*-mediated cerebellar ataxias.

6. Future perspectives

Our findings in **paper I** and **paper II** indicate that *STUB1* mutations can affect ubiquitin ligase activity as well as the structural stability and oligomerization of CHIP to different extents. However, the underlying mechanisms through which these mutations cause the disease are not fully understood yet. Therefore, future work should focus on unravelling the pathogenesis of SCAR16 and SCA48 disorders, and also investigate how *STUB1* mutations of different type and location contribute to specific clinical expressions.

STUB1 mutations have been mostly reported to cause a loss-of-function in CHIP, either directly through affecting its ubiquitination activity, or by impairing CHIP structure and interactions (180). In this respect, the use of high-throughput RNA sequencing and protein-protein interaction screenings can serve as a starting point to identify a wider range of substrates and cellular processes regulated by CHIP, and therefore, enable a better characterization of impaired interaction networks mediated by CHIP variants. On the other hand, formation of higher order oligomers and protein aggregates have been reported for some of the CHIP variants by our group as well as in other studies (180), which indicate a potential gain-of-function mechanism for the disease. This can further be investigated in neuronal cell cultures and animal models by using approaches such as cytotoxicity and cell viability assays.

STUB1 variants have been suggested to cause a dominant negative effect on CHIP function in SCA48 patients (54). However, the healthy status of heterozygous parents to SCAR16 patients argues against this hypothesis. Therefore, we suggest that future functional studies aim to elucidate mutation-specific effects of *STUB1* variants associated with both SCAR16 and SCA48 diseases. The dominant negative effect of mutations can be also examined in heterologous expression systems by using cell lines simultaneously transfected with wild-type and mutant *STUB1* plasmids, as well as *in vivo* models heterozygous for the *STUB1* mutations. On the other hand, carriers of recessive *STUB1* variants should be verified for the disease status in the SCAR16 families where heterozygous parents or siblings of the proband are available, and clinical examinations are required to check for the development of late-onset phenotypes in these individuals. Whole exome sequencing of heterozygous SCA48 patients in order

to search for variants of other ataxia-related genes, as was performed in paper II for families with Arg51_Ile53delinsProAla and Lys143_Trp147del variants, would also be beneficial to the identification of potential contributing factors in the development of SCA48. In addition, common genetic polymorphism has recently been suggested as a risk factor for the development of cognitive dysfunction in ALS patients. Therefore, investigations determining the polygenic risk score of SCA48 are highly suggested (233).

We have reported a progressive development of abnormal phenotypes associated with impaired U-box domain of Chip in the homozygous mutant zebrafish in **paper III**. Our data highlight the potential for zebrafish as new models of SCAR16/SCA48. Future studies should focus on investigating the progressive effect of truncated U-box domain in these fish after 24 months of age, and to characterize cellular pathways behind their phenotypes. For example, severe disorganization of Purkinje cell dendrites and loss of Purkinje cell bodies in the mutant cerebellum should be studied more in-depth. Also, it would be interesting to analyze the differential expression of Chip and its substrates in these fish. Therefore, obtaining a specific antibody against zebrafish Chip is considered a priority.

In an attempt to explore whether total loss of CHIP function may have different phenotypic consequences compared to CHIP with a non-functional U-box domain, we have recently established a *stub1* knock-out zebrafish line by targeting the third exon of the *stub1* gene for CRSPR/Cas9 mutagenesis. Preliminary results from characterization of the homozygous and heterozygous mutant offspring at 6 and 12 months of age show alterations in certain phenotypes, partly similar to those we reported for the U-box-truncated fish in paper III. Further analyses of these fish will be necessary to determine the pathogenic effect of total loss of Chip function, and also to distinguish the clinical features of heterozygous and homozygous mutant fish. Moreover, generation of knock-in zebrafish with disease-associated mutations in the *stub1* gene could be a very powerful approach to study the connections between defects in different domains of CHIP and specific phenotype manifestations both in the heterozygous and homozygous

states. Such studies might also be useful for understanding of the underlying pathogenesis pathways and connections between SCAR16 and SCA48 diseases.

From the broader perspective, CHIP acts as a key protein to regulate cellular homeostasis and ensure quality control in several pathways and networks. The possibility of using CHIP as a biomarker and therapeutic agent has been tested in a number of human cancers such as breast cancer and gastric cancer (234). Likewise, the protective role of CHIP during neurodegeneration calls attentions for its potential to benefit the treatment of neurodegenerative diseases. Upregulation of CHIP expression by small-molecule agonists of CHIP such as sulforaphane, for instance, has been suggested as a promising therapeutic target for the treatment of neurological disorders (235). Future work to understand the extent of CHIP ubiquitin ligase activity and co-chaperoning functions in different cellular processes, and to improve current knowledge regarding the underlying mechanisms of CHIP functioning allows for the use of this multifaceted protein as a possible therapeutic molecule in various treatment strategies.

7. References

1. Przedborski S. Neurodegeneration. In: Ikezu T, Gendelman HE, editors. Neuroimmune Pharmacology. Cham: Springer International Publishing; 2017. p. 345-54.

2. Martin JB. Molecular basis of the neurodegenerative disorders. The New England journal of medicine. 1999;340(25):1970-80.

3. Glenner GG, Wong CW. Alzheimer's disease: initial report of the purification and characterization of a novel cerebrovascular amyloid protein. 1984. Biochemical and biophysical research communications. 2012;425(3):534-9.

4. Grundke-Iqbal I, Iqbal K, Quinlan M, Tung YC, Zaidi MS, Wisniewski HM. Microtubule-associated protein tau. A component of Alzheimer paired helical filaments. The Journal of biological chemistry. 1986;261(13):6084-9.

5. Spillantini MG, Schmidt ML, Lee VM, Trojanowski JQ, Jakes R, Goedert M. Alpha-synuclein in Lewy bodies. Nature. 1997;388(6645):839-40.

6. DiFiglia M, Sapp E, Chase KO, Davies SW, Bates GP, Vonsattel JP, et al. Aggregation of huntingtin in neuronal intranuclear inclusions and dystrophic neurites in brain. Science (New York, NY). 1997;277(5334):1990-3.

7. Orr HT, Zoghbi HY. SCA1 molecular genetics: a history of a 13 year collaboration against glutamines. Human molecular genetics. 2001;10(20):2307-11.

8. Bruijn LI, Houseweart MK, Kato S, Anderson KL, Anderson SD, Ohama E, et al. Aggregation and motor neuron toxicity of an ALS-linked SOD1 mutant independent from wild-type SOD1. Science (New York, NY). 1998;281(5384):1851-4.

9. Bolton DC, McKinley MP, Prusiner SB. Identification of a protein that purifies with the scrapie prion. Science (New York, NY). 1982;218(4579):1309-11.

10. Mattson MP. Apoptosis in neurodegenerative disorders. Nature reviews Molecular cell biology. 2000;1(2):120-9.

11. Hyman BT, Van Hoesen GW. Neuron numbers in Alzheimer's disease: cell-specific pathology. Neurobiology of aging. 1987;8(6):555-6.

12. Soto C. Unfolding the role of protein misfolding in neurodegenerative diseases. Nature reviews Neuroscience. 2003;4(1):49-60.

13. Cattaneo E, Rigamonti D, Goffredo D, Zuccato C, Squitieri F, Sipione S. Loss of normal huntingtin function: new developments in Huntington's disease research. Trends in neurosciences. 2001;24(3):182-8.

14. Verhoef LG, Lindsten K, Masucci MG, Dantuma NP. Aggregate formation inhibits proteasomal degradation of polyglutamine proteins. Human molecular genetics. 2002;11(22):2689-700.

15. Takahashi T, Katada S, Onodera O. Polyglutamine Diseases: Where does Toxicity Come from? What is Toxicity? Where are We Going? Journal of Molecular Cell Biology. 2010;2(4):180-91.

16. Yan SD, Zhu H, Zhu A, Golabek A, Du H, Roher A, et al. Receptor-dependent cell stress and amyloid accumulation in systemic amyloidosis. Nature medicine. 2000;6(6):643-51.

17. Arispe N, Rojas E, Pollard HB. Alzheimer disease amyloid beta protein forms calcium channels in bilayer membranes: blockade by tromethamine and aluminum. Proceedings of the National Academy of Sciences of the United States of America. 1993;90(2):567-71.

18. Lin MC, Mirzabekov T, Kagan BL. Channel formation by a neurotoxic prion protein fragment. The Journal of biological chemistry. 1997;272(1):44-7.

19. Hsu LJ, Sagara Y, Arroyo A, Rockenstein E, Sisk A, Mallory M, et al. alpha-synuclein promotes mitochondrial deficit and oxidative stress. The American journal of pathology. 2000;157(2):401-10.

20. Behl C, Davis JB, Lesley R, Schubert D. Hydrogen peroxide mediates amyloid beta protein toxicity. Cell. 1994;77(6):817-27.

21. Klement IA, Skinner PJ, Kaytor MD, Yi H, Hersch SM, Clark HB, et al. Ataxin-1 nuclear localization and aggregation: role in polyglutamine-induced disease in SCA1 transgenic mice. Cell. 1998;95(1):41-53.

22. Moechars D, Dewachter I, Lorent K, Reverse D, Baekelandt V, Naidu A, et al. Early phenotypic changes in transgenic mice that overexpress different mutants of amyloid precursor protein in brain. The Journal of biological chemistry. 1999;274(10):6483-92.

23. Hartley DM, Walsh DM, Ye CP, Diehl T, Vasquez S, Vassilev PM, et al. Protofibrillar intermediates of amyloid beta-protein induce acute electrophysiological changes and progressive neurotoxicity in cortical neurons. The Journal of neuroscience : the official journal of the Society for Neuroscience. 1999;19(20):8876-84.

24. Lambert MP, Barlow AK, Chromy BA, Edwards C, Freed R, Liosatos M, et al. Diffusible, nonfibrillar ligands derived from Abeta1-42 are potent central nervous system neurotoxins. Proceedings of the National Academy of Sciences of the United States of America. 1998;95(11):6448-53.

25. Bucciantini M, Giannoni E, Chiti F, Baroni F, Formigli L, Zurdo J, et al. Inherent toxicity of aggregates implies a common mechanism for protein misfolding diseases. Nature. 2002;416(6880):507-11.

26. Walsh DM, Klyubin I, Fadeeva JV, Cullen WK, Anwyl R, Wolfe MS, et al. Naturally secreted oligomers of amyloid beta protein potently inhibit hippocampal long-term potentiation in vivo. Nature. 2002;416(6880):535-9.

27. Goldberg MS, Lansbury PT, Jr. Is there a cause-and-effect relationship between alpha-synuclein fibrillization and Parkinson's disease? Nature cell biology. 2000;2(7):E115-9.

28. McGeer PL, McGeer EG. The inflammatory response system of brain: implications for therapy of Alzheimer and other neurodegenerative diseases. Brain research Brain research reviews. 1995;21(2):195-218.

29. Itagaki S, McGeer PL, Akiyama H, Zhu S, Selkoe D. Relationship of microglia and astrocytes to amyloid deposits of Alzheimer disease. Journal of neuroimmunology. 1989;24(3):173-82.

30. McGeer PL, Schulzer M, McGeer EG. Arthritis and anti-inflammatory agents as possible protective factors for Alzheimer's disease: a review of 17 epidemiologic studies. Neurology. 1996;47(2):425-32.

31. Wyss-Coray T, Yan F, Lin AH, Lambris JD, Alexander JJ, Quigg RJ, et al. Prominent neurodegeneration and increased plaque formation in complement-inhibited Alzheimer's mice. Proceedings of the National Academy of Sciences of the United States of America. 2002;99(16):10837-42.

32. Janus C, Pearson J, McLaurin J, Mathews PM, Jiang Y, Schmidt SD, et al. A beta peptide immunization reduces behavioural impairment and plaques in a model of Alzheimer's disease. Nature. 2000;408(6815):979-82.

33. Schenk D. Amyloid-beta immunotherapy for Alzheimer's disease: the end of the beginning. Nature reviews Neuroscience. 2002;3(10):824-8.

34. Wyss-Coray T, Mucke L. Inflammation in neurodegenerative disease--a double-edged sword. Neuron. 2002;35(3):419-32.

35. Soto C. Protein misfolding and disease; protein refolding and therapy. FEBS letters. 2001;498(2-3):204-7.

36. Lansbury PT, Jr. Structural neurology: are seeds at the root of neuronal degeneration? Neuron. 1997;19(6):1151-4.

37. Carrell RW, Gooptu B. Conformational changes and disease--serpins, prions and Alzheimer's. Current opinion in structural biology. 1998;8(6):799-809.

38. Kelly JW. Alternative conformations of amyloidogenic proteins govern their behavior. Current opinion in structural biology. 1996;6(1):11-7.

39. Castano EM, Ghiso J, Prelli F, Gorevic PD, Migheli A, Frangione B. In vitro formation of amyloid fibrils from two synthetic peptides of different lengths homologous to Alzheimer's disease beta-protein. Biochemical and biophysical research communications. 1986;141(2):782-9.

40. Tagliavini F, Prelli F, Verga L, Giaccone G, Sarma R, Gorevic P, et al. Synthetic peptides homologous to prion protein residues 106-147 form amyloid-like fibrils in vitro. Proceedings of the National Academy of Sciences of the United States of America. 1993;90(20):9678-82.

41. Serpell LC, Berriman J, Jakes R, Goedert M, Crowther RA. Fiber diffraction of synthetic alpha-synuclein filaments shows amyloid-like cross-beta conformation. Proceedings of the National Academy of Sciences of the United States of America. 2000;97(9):4897-902.

42. Perutz MF, Johnson T, Suzuki M, Finch JT. Glutamine repeats as polar zippers: their possible role in inherited neurodegenerative diseases. Proceedings of the National Academy of Sciences of the United States of America. 1994;91(12):5355-8.

43. Singleton AB, Farrer M, Johnson J, Singleton A, Hague S, Kachergus J, et al. alpha-Synuclein locus triplication causes Parkinson's disease. Science (New York, NY). 2003;302(5646):841.

44. Singleton A, Myers A, Hardy J. The law of mass action applied to neurodegenerative disease: a hypothesis concerning the etiology and pathogenesis of complex diseases. Human molecular genetics. 2004;13 Spec No 1:R123-6.

45. Kumar A, Gibbs JR, Beilina A, Dillman A, Kumaran R, Trabzuni D, et al. Age-associated changes in gene expression in human brain and isolated neurons. Neurobiology of aging. 2013;34(4):1199-209.

46. Conway KA, Rochet JC, Bieganski RM, Lansbury PT, Jr. Kinetic stabilization of the alpha-synuclein protofibril by a dopamine-alpha-synuclein adduct. Science (New York, NY). 2001;294(5545):1346-9.

47. Okochi M, Walter J, Koyama A, Nakajo S, Baba M, Iwatsubo T, et al. Constitutive phosphorylation of the Parkinson's disease associated alpha-synuclein. The Journal of biological chemistry. 2000;275(1):390-7.

48. Emamian ES, Kaytor MD, Duvick LA, Zu T, Tousey SK, Zoghbi HY, et al. Serine 776 of ataxin-1 is critical for polyglutamine-induced disease in SCA1 transgenic mice. Neuron. 2003;38(3):375-87.

49. Lunkes A, Lindenberg KS, Ben-Haiem L, Weber C, Devys D, Landwehrmeyer GB, et al. Proteases acting on mutant huntingtin generate cleaved products that differentially build up cytoplasmic and nuclear inclusions. Molecular cell. 2002;10(2):259-69.

50. Hartl FU, Hayer-Hartl M. Molecular chaperones in the cytosol: from nascent chain to folded protein. Science (New York, NY). 2002;295(5561):1852-8.

51. Dawson TM, Dawson VL. The role of parkin in familial and sporadic Parkinson's disease. Movement disorders : official journal of the Movement Disorder Society. 2010;25 Suppl 1(0 1):S32-9.

52. Kawaguchi Y, Okamoto T, Taniwaki M, Aizawa M, Inoue M, Katayama S, et al. CAG expansions in a novel gene for Machado-Joseph disease at chromosome 14q32.1. Nature genetics. 1994;8(3):221-8.

53. Dantuma NP, Herzog LK. Machado-Joseph Disease: A Stress Combating Deubiquitylating Enzyme Changing Sides. Advances in experimental medicine and biology. 2020;1233:237-60.

54. De Michele G, Galatolo D, Barghigiani M, Dello Iacovo D, Trovato R, Tessa A, et al. Spinocerebellar ataxia type 48: last but not least. Neurol Sci. 2020;41(9):2423-32.

55. Matilla-Duenas A, Corral-Juan M, Volpini V, Sanchez I. The spinocerebellar ataxias: clinical aspects and molecular genetics. Advances in experimental medicine and biology. 2012;724:351-74.

56. Vermeer S, van de Warrenburg BP, Willemsen MA, Cluitmans M, Scheffer H, Kremer BP, et al. Autosomal recessive cerebellar ataxias: the current state of affairs. Journal of medical genetics. 2011;48(10):651-9.

57. Klockgether T. Chapter 2 Acquired Cerebellar Ataxias and Differential Diagnosis. In: Brice A, Pulst S-M, editors. Blue Books of Neurology. 31: Butterworth-Heinemann; 2007. p. 61-77.

58. Bird TD. Hereditary Ataxia Overview. In: Adam MP, Ardinger HH, Pagon RA, Wallace SE, Bean LJH, Stephens K, et al., editors. GeneReviews((R)). Seattle (WA)1993.

59. Hersheson J, Haworth A, Houlden H. The inherited ataxias: genetic heterogeneity, mutation databases, and future directions in research and clinical diagnostics. Human mutation. 2012;33(9):1324-32.

60. Ruano L, Melo C, Silva MC, Coutinho P. The global epidemiology of hereditary ataxia and spastic paraplegia: a systematic review of prevalence studies. Neuroepidemiology. 2014;42(3):174-83.

61. Palau F, Espinós C. Autosomal recessive cerebellar ataxias. Orphanet journal of rare diseases. 2006;1:47.

62. Wedding IM, Kroken M, Henriksen SP, Selmer KK, Fiskerstrand T, Knappskog PM, et al. Friedreich ataxia in Norway - an epidemiological, molecular and clinical study. Orphanet journal of rare diseases. 2015;10:108.

63. Bradley J, Blake J, Chamberlain S, Thomas P, Cooper J, Schapira A. Clinical, biochemical and molecular genetic correlations in Friedreich's ataxia. Human molecular genetics. 2000;9(2):275-82.

64. Savitsky K, Bar-Shira A, Gilad S, Rotman G, Ziv Y, Vanagaite L, et al. A single ataxia telangiectasia gene with a product similar to PI-3 kinase. Science (New York, NY). 1995;268(5218):1749-53.

65. Durr A. Autosomal dominant cerebellar ataxias: polyglutamine expansions and beyond. The Lancet Neurology. 2010;9(9):885-94.

66. Gu W, Ma H, Wang K, Jin M, Zhou Y, Liu X, et al. The Shortest Expanded Allele of the MJD1 Gene in a Chinese MJD Kindred with Autonomic Dysfunction. European Neurology. 2004;52(2):107-11.

67. Ranum LP, Schut LJ, Lundgren JK, Orr HT, Livingston DM. Spinocerebellar ataxia type 5 in a family descended from the grandparents of President Lincoln maps to chromosome 11. Nature genetics. 1994;8(3):280-4.

68. Genis D, Ortega-Cubero S, San Nicolas H, Corral J, Gardenyes J, de Jorge L, et al. Heterozygous STUB1 mutation causes familial ataxia with cognitive affective syndrome (SCA48). Neurology. 2018;91(21):e1988-e98.

69. Buchberger A, Bukau B, Sommer T. Protein quality control in the cytosol and the endoplasmic reticulum: brothers in arms. Molecular cell. 2010;40(2):238-52.

70. Wickner S, Maurizi MR, Gottesman S. Posttranslational quality control: folding, refolding, and degrading proteins. Science (New York, NY). 1999;286(5446):1888-93.

71. Young JC, Agashe VR, Siegers K, Hartl FU. Pathways of chaperone-mediated protein folding in the cytosol. Nature reviews Molecular cell biology. 2004;5(10):781-91.

72. Hartl FU. Molecular chaperones in cellular protein folding. Nature. 1996;381(6583):571-9.

73. Daugaard M, Rohde M, Jaattela M. The heat shock protein 70 family: Highly homologous proteins with overlapping and distinct functions. FEBS letters. 2007;581(19):3702-10.

74. Kabani M, Martineau CN. Multiple hsp70 isoforms in the eukaryotic cytosol: mere redundancy or functional specificity? Current genomics. 2008;9(5):338-248.

75. Mayer MP, Bukau B. Hsp70 chaperones: cellular functions and molecular mechanism. Cellular and molecular life sciences : CMLS. 2005;62(6):670-84.

76. Hennessy F, Nicoll WS, Zimmermann R, Cheetham ME, Blatch GL. Not all J domains are created equal: implications for the specificity of Hsp40-Hsp70 interactions. Protein science : a publication of the Protein Society. 2005;14(7):1697-709.

77. Kelley WL. The J-domain family and the recruitment of chaperone power. Trends in biochemical sciences. 1998;23(6):222-7.

78. Radons J. The human HSP70 family of chaperones: where do we stand? Cell stress & chaperones. 2016;21(3):379-404.

79. Li J, Buchner J. Structure, function and regulation of the hsp90 machinery. Biomedical journal. 2013;36(3):106-17.

80. Lotz GP, Lin H, Harst A, Obermann WM. Aha1 binds to the middle domain of Hsp90, contributes to client protein activation, and stimulates the ATPase activity of the molecular chaperone. The Journal of biological chemistry. 2003;278(19):17228-35.

81. Chua CS, Low H, Sim TS. Co-chaperones of Hsp90 in Plasmodium falciparum and their concerted roles in cellular regulation. Parasitology. 2014;141(9):1177-91.

82. Goldberg AL. Protein degradation and protection against misfolded or damaged proteins. Nature. 2003;426(6968):895-9.

83. Zheng N, Shabek N. Ubiquitin Ligases: Structure, Function, and Regulation. Annual Review of Biochemistry. 2017;86(1):129-57.

84. Haas AL, Rose IA. The mechanism of ubiquitin activating enzyme. A kinetic and equilibrium analysis. The Journal of biological chemistry. 1982;257(17):10329-37.

85. Pickart CM. Mechanisms underlying ubiquitination. Annu Rev Biochem. 2001;70:503-33.

86. Stewart MD, Ritterhoff T, Klevit RE, Brzovic PS. E2 enzymes: more than just middle men. Cell research. 2016;26(4):423-40.

87. Koegl M, Hoppe T, Schlenker S, Ulrich HD, Mayer TU, Jentsch S. A novel ubiquitination factor, E4, is involved in multiubiquitin chain assembly. Cell. 1999;96(5):635-44.

88. Hatakeyama S, Yada M, Matsumoto M, Ishida N, Nakayama KI. U box proteins as a new family of ubiquitin-protein ligases. The Journal of biological chemistry. 2001;276(35):33111-20.

89. Bedford L, Paine S, Sheppard PW, Mayer RJ, Roelofs J. Assembly, structure, and function of the 26S proteasome. Trends in cell biology. 2010;20(7):391-401.

90. Voges D, Zwickl P, Baumeister W. The 26S proteasome: a molecular machine designed for controlled proteolysis. Annu Rev Biochem. 1999;68:1015-68.

91. Lam YA, Xu W, DeMartino GN, Cohen RE. Editing of ubiquitin conjugates by an isopeptidase in the 26S proteasome. Nature. 1997;385(6618):737-40.

92. Burger AM, Seth AK. The ubiquitin-mediated protein degradation pathway in cancer: therapeutic implications. European journal of cancer. 2004;40(15):2217-29.

93. Lilienbaum A. Relationship between the proteasomal system and autophagy. International journal of biochemistry and molecular biology. 2013;4(1):1-26.

94. Korolchuk VI, Menzies FM, Rubinsztein DC. Mechanisms of cross-talk between the ubiquitin-proteasome and autophagy-lysosome systems. FEBS letters. 2010;584(7):1393-8.

95. Høyer-Hansen M, Jäättelä M. Connecting endoplasmic reticulum stress to autophagy by unfolded protein response and calcium. Cell death and differentiation. 2007;14(9):1576-82.

96. Xu W, Ocak U, Gao L, Tu S, Lenahan CJ, Zhang J, et al. Selective autophagy as a therapeutic target for neurological diseases. Cellular and Molecular Life Sciences. 2021;78(4):1369-92.

97. Ballinger CA, Connell P, Wu Y, Hu Z, Thompson LJ, Yin LY, et al. Identification of CHIP, a novel tetratricopeptide repeat-containing protein that interacts with heat shock proteins and negatively regulates chaperone functions. Molecular and cellular biology. 1999;19(6):4535-45.

98. Connell P, Ballinger CA, Jiang J, Wu Y, Thompson LJ, Höhfeld J, et al. The co-chaperone CHIP regulates protein triage decisions mediated by heat-shock proteins. Nature cell biology. 2001;3(1):93-6.

99. Murata S, Minami Y, Minami M, Chiba T, Tanaka K. CHIP is a chaperone-dependent E3 ligase that ubiquitylates unfolded protein. EMBO reports. 2001;2(12):1133-8.

100. Shi Y, Wang J, Li JD, Ren H, Guan W, He M, et al. Identification of CHIP as a novel causative gene for autosomal recessive cerebellar ataxia. PloS one. 2013;8(12):e81884.

101. Nikolay R, Wiederkehr T, Rist W, Kramer G, Mayer MP, Bukau B. Dimerization of the human E3 ligase CHIP via a coiled-coil domain is essential for its activity. The Journal of biological chemistry. 2004;279(4):2673-8.

102. Zhang M, Windheim M, Roe SM, Peggie M, Cohen P, Prodromou C, et al. Chaperoned ubiquitylation--crystal structures of the CHIP U box E3 ubiquitin ligase and a CHIP-Ubc13-Uev1a complex. Molecular cell. 2005;20(4):525-38.

103. Graf C, Stankiewicz M, Nikolay R, Mayer MP. Insights into the conformational dynamics of the E3 ubiquitin ligase CHIP in complex with chaperones and E2 enzymes. Biochemistry. 2010;49(10):2121-9.

104. Xu W, Marcu M, Yuan X, Mimnaugh E, Patterson C, Neckers L. Chaperone-dependent E3 ubiquitin ligase CHIP mediates a degradative pathway for c-ErbB2/Neu. Proceedings of the National Academy of Sciences of the United States of America. 2002;99(20):12847-52.

105. Joshi V, Amanullah A, Upadhyay A, Mishra R, Kumar A, Mishra A. A Decade of Boon or Burden: What Has the CHIP Ever Done for Cellular Protein Quality Control Mechanism Implicated in Neurodegeneration and Aging? Frontiers in molecular neuroscience. 2016;9:93.

106. Qian SB, McDonough H, Boellmann F, Cyr DM, Patterson C. CHIP-mediated stress recovery by sequential ubiquitination of substrates and Hsp70. Nature. 2006;440(7083):551-5.

107. Imai Y, Soda M, Hatakeyama S, Akagi T, Hashikawa T, Nakayama KI, et al. CHIP is associated with Parkin, a gene responsible for familial Parkinson's disease, and enhances its ubiquitin ligase activity. Molecular cell. 2002;10(1):55-67.

108. Nelson RF, Glenn KA, Miller VM, Wen H, Paulson HL. A novel route for F-box protein-mediated ubiquitination links CHIP to glycoprotein quality control. The Journal of biological chemistry. 2006;281(29):20242-51.

109. Li R-F, Shang Y, Liu D, Ren Z-S, Chang Z, Sui S-F. Differential Ubiquitination of Smad1 Mediated by CHIP: Implications in the Regulation of the Bone Morphogenetic Protein Signaling Pathway. Journal of Molecular Biology. 2007;374(3):777-90.

110. Dickey CA, Koren J, Zhang YJ, Xu YF, Jinwal UK, Birnbaum MJ, et al. Akt and CHIP coregulate tau degradation through coordinated interactions. Proceedings of the National Academy of Sciences of the United States of America. 2008;105(9):3622-7.

111. Gaude H, Aznar N, Delay A, Bres A, Buchet-Poyau K, Caillat C, et al. Molecular chaperone complexes with antagonizing activities regulate stability and activity of the tumor suppressor LKB1. Oncogene. 2012;31(12):1582-91.

112. Jung Y, Xu W, Kim H, Ha N, Neckers L. Curcumin-induced degradation of ErbB2: A role for the E3 ubiquitin ligase CHIP and the Michael reaction acceptor activity of curcumin. Biochimica et biophysica acta. 2007;1773(3):383-90.

113. Paul I, Ahmed SF, Bhowmik A, Deb S, Ghosh MK. The ubiquitin ligase CHIP regulates c-Myc stability and transcriptional activity. Oncogene. 2013;32(10):1284-95.

114. Esser C, Scheffner M, Höhfeld J. The chaperone-associated ubiquitin ligase CHIP is able to target p53 for proteasomal degradation. The Journal of biological chemistry. 2005;280(29):27443-8.

115. Schulz R, Dobbelstein M, Moll UM. HSP90 inhibitor antagonizing MIF: The specifics of pleiotropic cancer drug candidates. Oncoimmunology. 2012;1(8):1425-6.

116. Murata T, Shimotohno K. Ubiquitination and proteasome-dependent degradation of human eukaryotic translation initiation factor 4E. The Journal of biological chemistry. 2006;281(30):20788-800.

117. Ahmed SF, Deb S, Paul I, Chatterjee A, Mandal T, Chatterjee U, et al. The chaperone-assisted E3 ligase C terminus of Hsc70-interacting protein (CHIP) targets PTEN for proteasomal degradation. The Journal of biological chemistry. 2012;287(19):15996-6006.

118. Kang SA, Cho HS, Yoon JB, Chung IK, Lee ST. Hsp90 rescues PTK6 from proteasomal degradation in breast cancer cells. Biochem J. 2012;447(2):313-20.

119. Yang M, Wang C, Zhu X, Tang S, Shi L, Cao X, et al. E3 ubiquitin ligase CHIP facilitates Toll-like receptor signaling by recruiting and polyubiquitinating Src and atypical PKC{zeta}. J Exp Med. 2011;208(10):2099-112.

120. Yaguchi H, Ohkura N, Takahashi M, Nagamura Y, Kitabayashi I, Tsukada T. Menin missense mutants associated with multiple endocrine neoplasia type 1 are rapidly degraded via the ubiquitin-proteasome pathway. Molecular and cellular biology. 2004;24(15):6569-80.

121. Kim C, Yun N, Lee J, Youdim MBH, Ju C, Kim WK, et al. Phosphorylation of CHIP at Ser20 by Cdk5 promotes tAIF-mediated neuronal death. Cell Death & Differentiation. 2016;23(2):333-46.

122. Arndt V, Dick N, Tawo R, Dreiseidler M, Wenzel D, Hesse M, et al. Chaperone-assisted selective autophagy is essential for muscle maintenance. Curr Biol. 2010;20(2):143-8.

123. Peng HM, Morishima Y, Jenkins GJ, Dunbar AY, Lau M, Patterson C, et al. Ubiquitylation of neuronal nitric-oxide synthase by CHIP, a chaperone-dependent E3 ligase. The Journal of biological chemistry. 2004;279(51):52970-7.

124. Jana NR, Dikshit P, Goswami A, Kotliarova S, Murata S, Tanaka K, et al. Co-chaperone CHIP associates with expanded polyglutamine protein and promotes their degradation by proteasomes. The Journal of biological chemistry. 2005;280(12):11635-40.

125. Kumar P, Ambasta RK, Veereshwarayya V, Rosen KM, Kosik KS, Band H, et al. CHIP and HSPs interact with beta-APP in a proteasome-dependent manner and influence Abeta metabolism. Human molecular genetics. 2007;16(7):848-64.

126. Morales JL, Perdew GH. Carboxyl terminus of hsc70-interacting protein (CHIP) can remodel mature aryl hydrocarbon receptor (AhR) complexes and mediate ubiquitination of both the AhR and the 90 kDa heat-shock protein (hsp90) in vitro. Biochemistry. 2007;46(2):610-21.

127. Choi J-S, Lee DH. CHIP promotes the degradation of mutant SOD1 by reducing its interaction with VCP and S6/S6′ subunits of 26S proteasome. Animal cells and systems. 2010;14(1):1-10.

128. Ding X, Goldberg MS. Regulation of LRRK2 stability by the E3 ubiquitin ligase CHIP. PloS one. 2009;4(6):e5949.

129. Gamerdinger M, Carra S, Behl C. Emerging roles of molecular chaperones and co-chaperones in selective autophagy: focus on BAG proteins. J Mol Med (Berl). 2011;89(12):1175-82.

130. Petrucelli L, Dickson D, Kehoe K, Taylor J, Snyder H, Grover A, et al. CHIP and Hsp70 regulate tau ubiquitination, degradation and aggregation. Human molecular genetics. 2004;13(7):703-14.

131. Shin Y, Klucken J, Patterson C, Hyman BT, McLean PJ. The co-chaperone carboxyl terminus of Hsp70-interacting protein (CHIP) mediates alpha-synuclein degradation decisions between proteasomal and lysosomal pathways. The Journal of biological chemistry. 2005;280(25):23727-34.

132. Sarkar S, Brautigan DL, Parsons SJ, Larner JM. Androgen receptor degradation by the E3 ligase CHIP modulates mitotic arrest in prostate cancer cells. Oncogene. 2014;33(1):26-33.

133. Hwang JR, Zhang C, Patterson C. C-terminus of heat shock protein 70-interacting protein facilitates degradation of apoptosis signal-regulating kinase 1 and inhibits apoptosis signal-regulating kinase 1-dependent apoptosis. Cell stress & chaperones. 2005;10(2):147-56.

134. Maruyama T, Kadowaki H, Okamoto N, Nagai A, Naguro I, Matsuzawa A, et al. CHIP-dependent termination of MEKK2 regulates temporal ERK activation required for proper hyperosmotic response. The EMBO journal. 2010;29(15):2501-14.

135. Daviau A, Proulx R, Robitaille K, Di Fruscio M, Tanguay RM, Landry J, et al. Down-regulation of the mixed-lineage dual leucine zipper-bearing kinase by heat shock protein 70 and its co-chaperone CHIP. The Journal of biological chemistry. 2006;281(42):31467-77.

136. Belova L, Sharma S, Brickley DR, Nicolarsen JR, Patterson C, Conzen SD. Ubiquitin-proteasome degradation of serum- and glucocorticoid-regulated kinase-1 (SGK-1) is mediated by the chaperone-dependent E3 ligase CHIP. Biochem J. 2006;400(2):235-44.

137. Slotman JA, da Silva Almeida AC, Hassink GC, van de Ven RH, van Kerkhof P, Kuiken HJ, et al. Ubc13 and COOH terminus of Hsp70-interacting protein (CHIP) are required for growth hormone receptor endocytosis. The Journal of biological chemistry. 2012;287(19):15533-43.

138. Li F, Xie P, Fan Y, Zhang H, Zheng L, Gu D, et al. C terminus of Hsc70-interacting protein promotes smooth muscle cell proliferation and survival through ubiquitin-mediated degradation of FoxO1. The Journal of biological chemistry. 2009;284(30):20090-8.

139. Xia T, Dimitropoulou C, Zeng J, Antonova GN, Snead C, Venema RC, et al. Chaperone-dependent E3 ligase CHIP ubiquitinates and mediates proteasomal degradation of soluble guanylyl cyclase. Am J Physiol Heart Circ Physiol. 2007;293(5):H3080-7.

140. Fan M, Park A, Nephew KP. CHIP (carboxyl terminus of Hsc70-interacting protein) promotes basal and geldanamycin-induced degradation of estrogen receptor-alpha. Mol Endocrinol. 2005;19(12):2901-14.

141. Yan S, Sun X, Xiang B, Cang H, Kang X, Chen Y, et al. Redox regulation of the stability of the SUMO protease SENP3 via interactions with CHIP and Hsp90. The EMBO journal. 2010;29(22):3773-86.

142. Ferreira JV, Fôfo H, Bejarano E, Bento CF, Ramalho JS, Girão H, et al. STUB1/CHIP is required for HIF1A degradation by chaperone-mediated autophagy. Autophagy. 2013;9(9):1349-66.

143. Yang SW, Oh KH, Park E, Chang HM, Park JM, Seong MW, et al. USP47 and C terminus of Hsp70-interacting protein (CHIP) antagonistically regulate katanin-p60-mediated axonal growth. The Journal of neuroscience : the official journal of the Society for Neuroscience. 2013;33(31):12728-38.

144. Choi YN, Lee SK, Seo TW, Lee JS, Yoo SJ. C-Terminus of Hsc70-interacting protein regulates profilin1 and breast cancer cell migration. Biochemical and biophysical research communications. 2014;446(4):1060-6.

145. Li X, Huang M, Zheng H, Wang Y, Ren F, Shang Y, et al. CHIP promotes Runx2 degradation and negatively regulates osteoblast differentiation. J Cell Biol. 2008;181(6):959-72.

146. Shang Y, Zhao X, Xu X, Xin H, Li X, Zhai Y, et al. CHIP functions an E3 ubiquitin ligase of Runx1. Biochemical and biophysical research communications. 2009;386(1):242-6.

147. Ronnebaum SM, Wu Y, McDonough H, Patterson C. The ubiquitin ligase CHIP prevents SirT6 degradation through noncanonical ubiquitination. Molecular and cellular biology. 2013;33(22):4461-72.

148. Löffek S, Wöll S, Höhfeld J, Leube RE, Has C, Bruckner-Tuderman L, et al. The ubiquitin ligase CHIP/STUB1 targets mutant keratins for degradation. Human mutation. 2010;31(4):466-76.

149. Hirayama S, Yamazaki Y, Kitamura A, Oda Y, Morito D, Okawa K, et al. MKKS is a centrosome-shuttling protein degraded by disease-causing mutations via CHIP-mediated ubiquitination. Molecular biology of the cell. 2008;19(3):899-911.

150. Xie P, Fan Y, Zhang H, Zhang Y, She M, Gu D, et al. CHIP represses myocardin-induced smooth muscle cell differentiation via ubiquitin-mediated proteasomal degradation. Molecular and cellular biology. 2009;29(9):2398-408.

151. Dai Q, Zhang C, Wu Y, McDonough H, Whaley RA, Godfrey V, et al. CHIP activates HSF1 and confers protection against apoptosis and cellular stress. The EMBO journal. 2003;22(20):5446-58.

152. Meacham GC, Patterson C, Zhang W, Younger JM, Cyr DM. The Hsc70 co-chaperone CHIP targets immature CFTR for proteasomal degradation. Nature cell biology. 2001;3(1):100-5.

153. McDonough H, Patterson C. CHIP: a link between the chaperone and proteasome systems. Cell stress & chaperones. 2003;8(4):303-8.

154. Paul I, Ghosh MK. The E3 ligase CHIP: insights into its structure and regulation. Biomed Res Int. 2014;2014:918183.

155. Meng Y, Chen C, Wang L, Wang X, Tian C, Du J, et al. Toll-like receptor-2 ligand peptidoglycan upregulates expression and ubiquitin ligase activity of CHIP through JNK pathway. Cellular physiology and biochemistry : international journal of experimental cellular physiology, biochemistry, and pharmacology. 2013;32(4):1097-105.

156. Kajiro M, Hirota R, Nakajima Y, Kawanowa K, So-ma K, Ito I, et al. The ubiquitin ligase CHIP acts as an upstream regulator of oncogenic pathways. Nature cell biology. 2009;11(3):312-9.

157. Wang Y, Ren F, Wang Y, Feng Y, Wang D, Jia B, et al. CHIP/Stub1 functions as a tumor suppressor and represses NF-κB-mediated signaling in colorectal cancer. Carcinogenesis. 2014;35(5):983-91.

158. Gan L, Liu DB, Lu HF, Long GX, Mei Q, Hu GY, et al. Decreased expression of the carboxyl terminus of heat shock cognate 70 interacting protein in human gastric cancer and its clinical significance. Oncology reports. 2012;28(4):1392-8.

159. Guo J, Ren F, Wang Y, Li S, Gao Z, Wang X, et al. miR-764-5p promotes osteoblast differentiation through inhibition of CHIP/STUB1 expression. Journal of bone and mineral research : the official journal of the American Society for Bone and Mineral Research. 2012;27(7):1607-18.

160. Scaglione KM, Zavodszky E, Todi SV, Patury S, Xu P, Rodríguez-Lebrón E, et al. Ube2w and ataxin-3 coordinately regulate the ubiquitin ligase CHIP. Molecular cell. 2011;43(4):599-612.

161. Sengupta S, Badhwar I, Upadhyay M, Singh S, Ganesh S. Malin and laforin are essential components of a protein complex that protects cells from thermal stress. Journal of cell science. 2011;124(Pt 13):2277-86.

162. Lim MK, Kawamura T, Ohsawa Y, Ohtsubo M, Asakawa S, Takayanagi A, et al. Parkin interacts with LIM Kinase 1 and reduces its cofilin-phosphorylation activity via ubiquitination. Experimental cell research. 2007;313(13):2858-74.

163. Woo CH, Le NT, Shishido T, Chang E, Lee H, Heo KS, et al. Novel role of C terminus of Hsc70-interacting protein (CHIP) ubiquitin ligase on inhibiting cardiac apoptosis and dysfunction via regulating ERK5-mediated degradation of inducible cAMP early repressor. FASEB journal : official publication of the Federation of American Societies for Experimental Biology. 2010;24(12):4917-28.

164. Shimamoto S, Kubota Y, Yamaguchi F, Tokumitsu H, Kobayashi R. Ca2+/S100 proteins act as upstream regulators of the chaperone-associated ubiquitin ligase CHIP (C terminus of Hsc70-interacting protein). The Journal of biological chemistry. 2013;288(10):7158-68.

165. Lees MJ, Peet DJ, Whitelaw ML. Defining the role for XAP2 in stabilization of the dioxin receptor. The Journal of biological chemistry. 2003;278(38):35878-88.

166. Mao RF, Rubio V, Chen H, Bai L, Mansour OC, Shi ZZ. OLA1 protects cells in heat shock by stabilizing HSP70. Cell death & disease. 2013;4(2):e491.

167. Alberti S, Demand J, Esser C, Emmerich N, Schild H, Hohfeld J. Ubiquitylation of BAG-1 suggests a novel regulatory mechanism during the sorting of chaperone substrates to the proteasome. The Journal of biological chemistry. 2002;277(48):45920-7.

168. Behl C. BAG3 and friends: co-chaperones in selective autophagy during aging and disease. Autophagy. 2011;7(7):795-8.

169. Arndt V, Daniel C, Nastainczyk W, Alberti S, Höhfeld J. BAG-2 acts as an inhibitor of the chaperone-associated ubiquitin ligase CHIP. Molecular biology of the cell. 2005;16(12):5891-900.

170. Kalia LV, Kalia SK, Chau H, Lozano AM, Hyman BT, McLean PJ. Ubiquitinylation of α-synuclein by carboxyl terminus Hsp70-interacting protein (CHIP) is regulated by Bcl-2-associated athanogene 5 (BAG5). PloS one. 2011;6(2):e14695.

171. Crippa V, Sau D, Rusmini P, Boncoraglio A, Onesto E, Bolzoni E, et al. The small heat shock protein B8 (HspB8) promotes autophagic removal of misfolded proteins involved in amyotrophic lateral sclerosis (ALS). Human molecular genetics. 2010;19(17):3440-56.

172. Tetzlaff JE, Putcha P, Outeiro TF, Ivanov A, Berezovska O, Hyman BT, et al. CHIP targets toxic alpha-Synuclein oligomers for degradation. The Journal of biological chemistry. 2008;283(26):17962-8.

173. Al-Ramahi I, Lam YC, Chen HK, de Gouyon B, Zhang M, Pérez AM, et al. CHIP protects from the neurotoxicity of expanded and wild-type ataxin-1 and promotes their ubiquitination and degradation. The Journal of biological chemistry. 2006;281(36):26714-24.

174. Heimdal K, Sanchez-Guixe M, Aukrust I, Bollerslev J, Bruland O, Jablonski GE, et al. STUB1 mutations in autosomal recessive ataxias - evidence for mutation-specific clinical heterogeneity. Orphanet journal of rare diseases. 2014;9:146.

175. Hayer SN, Deconinck T, Bender B, Smets K, Züchner S, Reich S, et al. STUB1/CHIP mutations cause Gordon Holmes syndrome as part of a widespread multisystemic neurodegeneration: evidence from four novel mutations. Orphanet journal of rare diseases. 2017;12(1):31.

176. Shi CH, Schisler JC, Rubel CE, Tan S, Song B, McDonough H, et al. Ataxia and hypogonadism caused by the loss of ubiquitin ligase activity of the U box protein CHIP. Human molecular genetics. 2014;23(4):1013-24.

177. Stenson PD, Mort M, Ball EV, Evans K, Hayden M, Heywood S, et al. The Human Gene Mutation Database: towards a comprehensive repository of inherited mutation data for medical research, genetic diagnosis and next-generation sequencing studies. Human genetics. 2017;136(6):665-77.

178. Ravel JM, Benkirane M, Calmels N, Marelli C, Ory-Magne F, Ewenczyk C, et al. Expanding the clinical spectrum of STIP1 homology and U-box containing protein 1-associated ataxia. J Neurol. 2021.

179. Chiu HH, Hsaio CT, Tsai YS, Liao YC, Lee YC, Soong BW. Clinical and Genetic Characterization of Autosomal Recessive Spinocerebellar Ataxia Type 16 (SCAR16) in Taiwan. Cerebellum. 2020;19(4):544-9.

180. Kanack AJ, Newsom OJ, Scaglione KM. Most mutations that cause spinocerebellar ataxia autosomal recessive type 16 (SCAR16) destabilize the protein quality-control E3 ligase CHIP. The Journal of biological chemistry. 2018;293(8):2735-43.

181. De Michele G, Lieto M, Galatolo D, Salvatore E, Cocozza S, Barghigiani M, et al. Spinocerebellar ataxia 48 presenting with ataxia associated with cognitive, psychiatric, and extrapyramidal features: A report of two Italian families. Parkinsonism & related disorders. 2019;65:91-6.

182. Lieto M, Riso V, Galatolo D, De Michele G, Rossi S, Barghigiani M, et al. The complex phenotype of spinocerebellar ataxia type 48 in eight unrelated Italian families. European journal of neurology. 2020;27(3):498-505.

183. Aleström P, D'Angelo L, Midtlyng PJ, Schorderet DF, Schulte-Merker S, Sohm F, et al. Zebrafish: Housing and husbandry recommendations. Laboratory Animals. 2020;54(3):213-24.

184. Kabashi E, Brustein E, Champagne N, Drapeau P. Zebrafish models for the functional genomics of neurogenetic disorders. Biochimica et biophysica acta. 2011;1812(3):335-45.

185. Nichols JT. Chapter 50 - Zebrafish as a Platform for Genetic Screening. In: Cartner SC, Eisen JS, Farmer SC, Guillemin KJ, Kent ML, Sanders GE, editors. The Zebrafish in Biomedical Research: Academic Press; 2020. p. 649-57.

186. Best JD, Alderton WK. Zebrafish: An in vivo model for the study of neurological diseases. Neuropsychiatric disease and treatment. 2008;4(3):567-76.

187. Sager JJ, Bai Q, Burton EA. Transgenic zebrafish models of neurodegenerative diseases. Brain Struct Funct. 2010;214(2-3):285-302.

188. Bae YK, Kani S, Shimizu T, Tanabe K, Nojima H, Kimura Y, et al. Anatomy of zebrafish cerebellum and screen for mutations affecting its development. Dev Biol. 2009;330(2):406-26.

189. Kozol RA, Abrams AJ, James DM, Buglo E, Yan Q, Dallman JE. Function Over Form: Modeling Groups of Inherited Neurological Conditions in Zebrafish. Frontiers in molecular neuroscience. 2016;9:55.

190. Rubinstein AL. Zebrafish: from disease modeling to drug discovery. Curr Opin Drug Discov Devel. 2003;6(2):218-23.

191. Sassen WA, Köster RW. A molecular toolbox for genetic manipulation of zebrafish. Advances in Genomics and Genetics. 2015;5:151.

192. Xu Z, Kohli E, Devlin KI, Bold M, Nix JC, Misra S. Interactions between the quality control ubiquitin ligase CHIP and ubiquitin conjugating enzymes. BMC Struct Biol. 2008;8:26.

193. Shi CH, Rubel C, Soss SE, Sanchez-Hodge R, Zhang S, Madrigal SC, et al. Disrupted structure and aberrant function of CHIP mediates the loss of motor and cognitive function in preclinical models of SCAR16. PLoS Genet. 2018;14(9):e1007664.

194. Min JN, Whaley RA, Sharpless NE, Lockyer P, Portbury AL, Patterson C. CHIP deficiency decreases longevity, with accelerated aging phenotypes accompanied by altered protein quality control. Molecular and cellular biology. 2008;28(12):4018-25.

195. McLaughlin B, Buendia MA, Saborido TP, Palubinsky AM, Stankowski JN, Stanwood GD. Haploinsufficiency of the E3 ubiquitin ligase C-terminus of heat shock cognate 70 interacting protein (CHIP) produces specific behavioral impairments. PloS one. 2012;7(5):e36340.

196. Dickey CA, Yue M, Lin WL, Dickson DW, Dunmore JH, Lee WC, et al. Deletion of the ubiquitin ligase CHIP leads to the accumulation, but not the aggregation, of both endogenous phospho- and caspase-3-cleaved tau species. The Journal of neuroscience : the official journal of the Society for Neuroscience. 2006;26(26):6985-96.

197. Palubinsky AM, Stankowski JN, Kale AC, Codreanu SG, Singer RJ, Liebler DC, et al. CHIP Is an Essential Determinant of Neuronal Mitochondrial Stress Signaling. Antioxid Redox Signal. 2015;23(6):535-49.

198. Pakdaman Y, Sanchez-Guixé M, Kleppe R, Erdal S, Bustad HJ, Bjørkhaug L, et al. In vitro characterization of six STUB1 variants in spinocerebellar ataxia 16 reveals altered structural properties for the encoded CHIP proteins. Biosci Rep. 2017;37(2).

199. Depondt C, Donatello S, Simonis N, Rai M, van Heurck R, Abramowicz M, et al. Autosomal recessive cerebellar ataxia of adult onset due to STUB1 mutations. Neurology. 2014;82(19):1749-50.

200. Roux T, Barbier M, Papin M, Davoine C-S, Sayah S, Coarelli G, et al. Clinical, neuropathological, and genetic characterization of STUB1 variants in cerebellar ataxias: a frequent cause of predominant cognitive impairment. Genetics in Medicine. 2020;22(11):1851-62.

201. Madrigal SC, McNeil Z, Sanchez-Hodge R, Shi CH, Patterson C, Scaglione KM, et al. Changes in protein function underlie the disease spectrum in patients with CHIP mutations. The Journal of biological chemistry. 2019;294(50):19236-45.

202. Bettencourt C, de Yébenes JG, López-Sendón JL, Shomroni O, Zhang X, Qian SB, et al. Clinical and Neuropathological Features of Spastic Ataxia in a Spanish Family with Novel Compound Heterozygous Mutations in STUB1. Cerebellum. 2015;14(3):378-81.

203. Robinson KJ, Watchon M, Laird AS. Aberrant Cerebellar Circuitry in the Spinocerebellar Ataxias. Front Neurosci. 2020;14:707.

204. Kelley AE, Cador M, Stinus L. Exploration and Its Measurement. In: Boulton AA, Baker GB, Greenshaw AJ, editors. Psychopharmacology. Totowa, NJ: Humana Press; 1989. p. 95-144.

205. Siwak CT, Tapp PD, Milgram NW. Effect of age and level of cognitive function on spontaneous and exploratory behaviors in the beagle dog. Learn Mem. 2001;8(6):317-25.

206. Snowden J. Fronto-temporal dementia. Frontotemporal lobar degeneration; Frontotemporal dementia, progressive aphasia, semantic dementia. 1996.

207. Pierce K, Courchesne E. Evidence for a cerebellar role in reduced exploration and stereotyped behavior in autism. Biological Psychiatry. 2001;49(8):655-64.

208. Varga M. The Doctor of Delayed Publications: The Remarkable Life of George Streisinger (1927-1984). Zebrafish. 2018;15(3):314-9.

209. Di Carlo M. Simple model systems: a challenge for Alzheimer's disease. Immun Ageing. 2012;9(1):3.

210. Joshi P, Liang JO, DiMonte K, Sullivan J, Pimplikar SW. Amyloid precursor protein is required for convergent-extension movements during Zebrafish development. Dev Biol. 2009;335(1):1-11.

211. Bai Q, Garver JA, Hukriede NA, Burton EA. Generation of a transgenic zebrafish model of Tauopathy using a novel promoter element derived from the zebrafish eno2 gene. Nucleic Acids Res. 2007;35(19):6501-16.

212. Paquet D, Bhat R, Sydow A, Mandelkow EM, Berg S, Hellberg S, et al. A zebrafish model of tauopathy allows in vivo imaging of neuronal cell death and drug evaluation. J Clin Invest. 2009;119(5):1382-95.

213. Anichtchik OV, Kaslin J, Peitsaro N, Scheinin M, Panula P. Neurochemical and behavioural changes in zebrafish Danio rerio after systemic administration of 6-hydroxydopamine and 1-methyl-4-phenyl-1,2,3,6-tetrahydropyridine. J Neurochem. 2004;88(2):443-53.

214. Bortolotto JW, Cognato GP, Christoff RR, Roesler LN, Leite CE, Kist LW, et al. Long-term exposure to paraquat alters behavioral parameters and dopamine levels in adult zebrafish (Danio rerio). Zebrafish. 2014;11(2):142-53.

215. Nabinger DD, Altenhofen S, Bonan CD. Zebrafish models: Gaining insight into purinergic signaling and neurological disorders. Prog Neuropsychopharmacol Biol Psychiatry. 2020;98:109770.

216. Xi Y, Noble S, Ekker M. Modeling neurodegeneration in zebrafish. Curr Neurol Neurosci Rep. 2011;11(3):274-82.

217. Anichtchik O, Diekmann H, Fleming A, Roach A, Goldsmith P, Rubinsztein DC. Loss of PINK1 Function Affects Development and Results in Neurodegeneration in Zebrafish. The Journal of Neuroscience. 2008;28(33):8199-207.

218. Flinn L, Mortiboys H, Volkmann K, Köster RW, Ingham PW, Bandmann O. Complex I deficiency and dopaminergic neuronal cell loss in parkin-deficient zebrafish (Danio rerio). Brain. 2009;132(Pt 6):1613-23.

219. Fett ME, Pilsl A, Paquet D, Bebber Fv, Haass C, Tatzelt J, et al. Parkin Is Protective against Proteotoxic Stress in a Transgenic Zebrafish Model. PloS one. 2010;5.

220. O'Donnell KC, Lulla A, Stahl MC, Wheat ND, Bronstein JM, Sagasti A. Axon degeneration and PGC-1α-mediated protection in a zebrafish model of α-synuclein toxicity. Dis Model Mech. 2014;7(5):571-82.

221. Cota-Coronado JA, Sandoval-Ávila S, Gaytan-Dávila YP, Diaz NF, Vega-Ruiz B, Padilla-Camberos E, et al. New transgenic models of Parkinson's disease using genome editing technology. Neurología (English Edition). 2019.

222. Henshall TL, Tucker B, Lumsden AL, Nornes S, Lardelli MT, Richards RI. Selective neuronal requirement for huntingtin in the developing zebrafish. Human molecular genetics. 2009;18(24):4830-42.

223. Diekmann H, Anichtchik O, Fleming A, Futter M, Goldsmith P, Roach A, et al. Decreased BDNF levels are a major contributor to the embryonic phenotype of huntingtin knockdown zebrafish. The Journal of neuroscience : the official journal of the Society for Neuroscience. 2009;29(5):1343-9.

224. Airhart MJ, Lee DH, Wilson TD, Miller BE, Miller MN, Skalko RG. Movement disorders and neurochemical changes in zebrafish larvae after bath exposure to fluoxetine (PROZAC). Neurotoxicol Teratol. 2007;29(6):652-64.

225. Loucks E, Carvan MJ, 3rd. Strain-dependent effects of developmental ethanol exposure in zebrafish. Neurotoxicol Teratol. 2004;26(6):745-55.

226. Bass SL, Gerlai R. Zebrafish (Danio rerio) responds differentially to stimulus fish: the effects of sympatric and allopatric predators and harmless fish. Behav Brain Res. 2008;186(1):107-17.

227. Darland T, Dowling JE. Behavioral screening for cocaine sensitivity in mutagenized zebrafish. Proceedings of the National Academy of Sciences of the United States of America. 2001;98(20):11691-6.

228. Cirelli C, Tononi G. Differential expression of plasticity-related genes in waking and sleep and their regulation by the noradrenergic system. The Journal of neuroscience : the official journal of the Society for Neuroscience. 2000;20(24):9187-94.

229. Colwill RM, Raymond MP, Ferreira L, Escudero H. Visual discrimination learning in zebrafish (Danio rerio). Behav Processes. 2005;70(1):19-31.

230. Egan RJ, Bergner CL, Hart PC, Cachat JM, Canavello PR, Elegante MF, et al. Understanding behavioral and physiological phenotypes of stress and anxiety in zebrafish. Behav Brain Res. 2009;205(1):38-44.

231. Champagne DL, Hoefnagels CC, de Kloet RE, Richardson MK. Translating rodent behavioral repertoire to zebrafish (Danio rerio): relevance for stress research. Behav Brain Res. 2010;214(2):332-42.

232. Becker CG, Becker T. Adult zebrafish as a model for successful central nervous system regeneration. Restor Neurol Neurosci. 2008;26(2-3):71-80.

233. Placek K, Benatar M, Wuu J, Rampersaud E, Hennessy L, Van Deerlin VM, et al. Machine learning suggests polygenic risk for cognitive dysfunction in amyotrophic lateral sclerosis. EMBO Mol Med. 2021;13(1):e12595.

234. Sun C, Li HL, Shi ML, Liu QH, Bai J, Zheng JN. Diverse roles of C-terminal Hsp70-interacting protein (CHIP) in tumorigenesis. J Cancer Res Clin Oncol. 2014;140(2):189-97.

235. Zhang S, Hu Z-w, Mao C-y, Shi C-h, Xu Y-m. CHIP as a therapeutic target for neurological diseases. Cell death & disease. 2020;11(9):727.

236. Coutelier M, Burglen L, Mundwiller E, Abada-Bendib M, Rodriguez D, Chantot-Bastaraud S, et al. GRID2 mutations span from congenital to mild adult-onset cerebellar ataxia. Neurology. 2015;84(17):1751-9.

237. Corcia P, Vourc'h P, Guennoc AM, Del Mar Amador M, Blasco H, Andres C, et al. Pure cerebellar ataxia linked to large C9orf72 repeat expansion. Amyotroph Lateral Scler Frontotemporal Degener. 2016;17(3-4):301-3.

238. Krygier M, Kwarciany M, Wasilewska K, Pienkowski VM, Krawczyńska N, Zielonka D, et al. A study in a Polish ataxia cohort indicates genetic heterogeneity and points to MTCL1 as a novel candidate gene. Clin Genet. 2019;95(3):415-9.

Appendix A. Classification of hereditary CA disorders.

Disease		Associated Clinical Features	Gene/locus	OMIM
ADCA	SCA1	Pyramidal/extrapyramidal signs Peripheral neuropathy Dementia	*ATXN1*	164400
	SCA2	Pyramidal/extrapyramidal signs Peripheral neuropathy Dementia Retinal degeneration	*ATXN2*	183090
	SCA3 (MJD)	Pyramidal/extrapyramidal signs	*ATXN3*	109150
	SCA4	Axonal sensory neuropathy Hypo/areflexia	16q22.1	600223
	SCA5	Tremor Hyperreflexia	*SPTBN2*	600224
	SCA6	Vibratory and sensory loss	*CACNA1A*	183086
	SCA7	Pigmental macular dystrophy	*ATXN7*	164500
	SCA8	Mild aspiration Spasticity	*ATXN8*	608768
	SCA10	Seizures Pyramidal signs	*ATXN10*	603516
	SCA11	Pyramidal signs	*TTBK2*	604432
	SCA12	Pyramidal/extrapyramidal signs Dementia	*PPP2R2B*	604326
	SCA13	Moderate intellectual disability Mild developmental delay Pyramidal signs	*KCNC3*	605259
	SCA14	Cognitive deficits	*PRKCG*	605361
	SCA15/16	Pyramidal signs Tremor	*ITPR1*	606658
	SCA17	Pyramidal/Extrapyramidal signs Intellectual impairments Dementia Seizures	*TBP*	607136
	SCA18	Early sensorymotor neuropathy Hyporeflexia	7q22-q32	607458
	SCA19/22	Cognitive impairment /Pyramidal Extrapyramidal signs	*KCND3*	607346
	SCA20	Spasmodic dysphonia Pyramidal signs	11q12	608687

Disease		Associated Clinical Features	Gene/locus	OMIM
ADCA	SCA21	Cognitive impairment Extrapyramidal signs	*TMEM240*	607454
	SCA23	Peripheral sensory neuropathy	*PDYN*	610245
	SCA25	Peripheral sensory neuropathy	*SCA25*	608703
	SCA26		*EEF2*	609306
	SCA27	Early-onset tremor	*FGF14*	609307
	SCA28	Hyperreflexia	*AFG3L2*	610246
	SCA29	Learning deficits Tremor	*ITPR1*	117360
	SCA30	Hyperreflexia	4q34.3-q35.1	613371
	SCA31	Reduced muscle tone	*BEAN1*	117210
	SCA34	Pyramidal signs	*ELOVL4*	133190
	SCA35	Pyramidal signs Tremor	*TGM6*	613908
	SCA36	Tongue atrophy Hyperreflexia Motor neuropathy	*NOP56*	614153
	SCA37		1P32	615945
	SCA38	Axonal neuropathy	*ELOVL5*	615957
	SCA40	Tremor Hyperreflexia	*CCDC88C*	616053
	SCA41		*TRPC3*	616410
	SCA42		*CACNA1G*	616795
	SCA43	Peripheral neuropathy Hyporeflexia Tremor	*MME*	617018
	SCA44	Dysphagia Hyperreflexia Spasticity	*GRM1*	617691
	SCA45		*FAT2*	617769
	SCA46	Sensory neuropathy	*PLD3*	617770
	SCA47	Dyplopia Hypotonia	*PUM1*	617931
	SCA48	**Cognitive-affective impairments** **Dysphagia** **Anxiety** **Urinary symptoms**	***STUB1***	**618093**

Disease		Associated Clinical Features	Gene/locus	OMIM
ADCA	DRPLA	Extrapyramidal signs Seizures Dementia	*ATN1*	125370
	ADCADN	Deafness Sensory neuropathy Psychosis, depression	*DNMT1*	604121
	HLD6	Extrapyramidal signs Spasticity Learning disability	*TUBB4A*	612438
	GRID2-related SCA	Cognitive delay Hearing loss	*GRID2*	(236)
	Pure CA		*C9orf72*	(237)
	DEE47	Infantile seizures Axial hypotonia Microcephaly Intellectual disability	*FGF12*	617166
	CAPOS	Episodic encephalopathy Hypotonia areflexia Hearing loss Optic atrophy	*ATP1A3*	601338
	EA1	Myokymia Tremor attacks	*KCNA1*	160120
	EA2	Dizziness attacks	*CACNA1A*	108500
	EA3	Vertigo Tinnitus Myokymia	1q42	606554
	EA4	Vertigo attacks Diplopia	—	606552
	EA5	Vertigo attacks	*CACNB4*	613855
	EA6	Seizures Slurred speech Vertigo, diplopia, nausea, vomiting	*SLC1A3*	612656
	EA7	Weakness	19q13	611907
	EA8	Weakness Tremor	1p36.13-p34.3	616055
	EA9	Headache Dizziness Vomiting	*SCN2A*	618924
	SPAX1	Spasticity, Hyperreflexia Pes cavus Dystonia/Hypertonia	*VAMP1*	108600

Disease		Associated Clinical Features	Gene/locus	OMIM
ARCA	SCAR10	Hyperreflexia	*ANO10*	613728
	EAOH (AOA 1)	Oculomotor apraxia Choreoathetosis Peripheral neuropathy	*APTX*	208920
	AT	Conjuctival telangiectasia Oculomotor apraxia Immune deficiency	*ATM*	208900
	IOSCA	Sensory neuropathy Hearing loss Seizures Muscular hypotonia Thetosis	*C10orf2*	271245
	CTX	Pyramidal/extrapyramidal signs Cataracts Mental disability Tendon xanthomata	*CYP27A1*	213700
	FRDA	Babinski responses Cardiomyopathy	*FXN*	229300
	RD	Peripheral neuropathy Hearing loss Anosmia Cataracts Retinopathy Cardic dysfunction	*PHYN* *PEX7*	266500
	BNHS	Hypogonadotropic hypogonadism Chorioretinal dystrophy	*PNPLA6*	215470
	CANVAS	Sensory neuropathy Impaired vestibular reflex	*RFC1*	614575
	SACS	Pyramidal signs Retinopathy Peripheral neuropathy	*SACS*	270550
	SCAN2 (AOA 2)	Pyramidal/extrapyramidal signs Oculomotor apraxia Peripheral neuropathy sensory neuropathy	*SETX*	606002
	MSS	Cataracts Somatic and mental retardation Hypergonadotropic Hypogonadism Myopathy	*SIL1*	248800
	BVVLS2	Deafness Tongue fasciculation Respiratory distress	*SLC52A2*	614707
	SCAR20	Intellectual disability Absent speech Pyramidal signs	*SNX14*	616354

Disease		Associated Clinical Features	Gene/locus	OMIM
ARCA	SCAR8	Extrapyramidal signs Optic atrophy	*SYNE1*	610743
	VED	Vitamin E deficiency Areflexia Friedreich's ataxia	*TTPA*	277460
	WFS1	Juvenile diabetes Optic atrophy Hearing impairment Dementia or Mental retardation	*WFS1*	222300
	PHARC	Refsum disease (RD)	*ABHD12*	612674
	ICRD	Hypotonia Muscle atrophy Seizures Optic atrophy	*ACO2*	614559
	SCAR9	Seizures Intellectual/cognitive regression Extrapyramidal signs	*COQ8A*	612016
	ATCAY	Tremor	*ATCAY*	601238
	SCAR25		*ATG5*	617584
	CAMRQ4	Mental retardation	*ATP8A2*	615268
	SPG76	Spasticity Hyperreflexia Foot deformities	*CAPN1*	616907
	LKPAT	Visual defects Learning disabilities Headaches	*CLCN2*	615651
	CLN5	Myoclonic epilepsy Dementia Visual failure	*CLN5*	256731
	SCAR17	Hypotonia/dystonia Impaired intellectual development	*CWF19L1*	616127
	AXPC1	Retinitis pigmentosa Sensory loss	*FLVCR1*	609033
	SCAR27	Spasticity Cognitive impairment	*GDAP2*	618369
	EMP6	Myoclonus epilepsy	*GOSR2*	614018
	SCAR18	Intellectual disability Hypotonia	*GRID2*	616204
	SCAR13	Intellectual deficits Poor/absent speech Hyperreflexia	*GRM1*	614831

Disease		Associated Clinical Features	Gene/locus	OMIM
ARCA	SESAMES	Hearing loss Seizures Mental retardation	*KCNJ10*	612780
	SCAR15	Cognitive impairment Developmental delay Seizures	*KIAA0226*	615705
	PTBHS	Retinal dystrophy	*LAMA1*	615960
	Early-onset ataxia	Intellectual disability Seizures	*MTCL1*	(238)
	DMJDS1	Intellectual disability Spasticity Dystonia Microcephaly Visual impairments Seizures	*PCDH12*	251280
	SCAR2	Delayed cognitive development Intellectual disability	*PMPCA*	213200
	AOA 4	Dystonia Oculomotor apraxia Peripheral neuropathy Cognitive impairment	*PNKP*	616267
	MTDPS4A MTDPS4B SANDO PEOB1	Epilepsy Mental retardation Axonal neuropathy Myopathy Sensory ataxia	*POLG*	203700 613662 607459 258450
	HLD7 HLD8	Spasticity Tremor Hypotonia Cognitive regression Hypogonadotropic hypogonadism	*POLR3A* *POLR3B*	607694 614381
	PACA	Neonatal diabetes Facial dysmorphism	*PTF1A*	609069
	GDHS	Cognitive decline Hypogonadotropic hypogonadism Chorea	*RNF216*	212840
	LIKNS	Sensorineural hearing loss	*SLC9A1*	616291
	HMSN6B	Optic atrophy Peripheral axonal neuropathy Myoclonus	*SLC25A46*	616505
	SCAR14	Intellectual disability	*SPTBN2*	615386
	SCAR12	Mental retardation Seizures Spasticity	*WWOX*	614322

Disease		Associated Clinical Features	Gene/locus	OMIM
ARCA	NADGP	Dystonia Athetosis Cognitive decline	*SQSTM1*	617145
	SCAR16	**Peripheral sensory neuropathy** **Cognitive impairments** **Pyramidal signs**	***STUB1***	**615768**
	SCAR11		*SYT14*	614229
	SCAN1	Sensorimotor neuropathy Hypo/areflexia Pes cavus	*TDP1*	607250
	SCAR23	Epilepsy Intellectual disability	*TDP2*	616949
	SCAR7		*TPP1*	609270
	COXPD3	Hypotonia Encephalomyopathy Cardiomyopathy	*TSFM*	610505
	COXPD29	Microcephaly Spasticity Epilepsy	*TXN2*	616811
	SCAR24	Cataracts	*UBA5*	617133
	SCAR4	Oculomotor abnormalities Pyramidal/extrapyramidal signs	*VPS13D*	607317
	CAMRQ1	Mental retardation Tremor	*VLDLR*	224050
	SCAR22	Intellectual disability Pyramidal signs	*VWA3B*	616948
	GAMOS1 (SCAR5)	Microcephaly Seizures Nephrotic syndrome	*WDR73*	251300
	SPAX2	Spasticity	*KIFIC*	611302
	SPAX3	Spasticity Hyperreflexia Urinary urgency Dystonia	*MARS2*	611390
	SPAX4	Spasticity Optic atrophy	*MTPAP*	613672
	SPAX5	Spasticity Oculomotor apraxia Dystonia Epilepsy	*AFG3L2*	614487
	SPG7	Spasticity Hyperreflexia	*SPG7*	607259

	Disease	Associated Clinical Features	Gene/locus	OMIM
X-linked	ASAT	Asymptomatic anemia	*ABCB7*	301310
	SCAX1	Hypotonia	*ATP2B3*	302500
	MICPCH	Intellectual disability Microcephaly	*CASK*	300749
	FXTAS	Cognitive decline Parkinsonism Tremor	*FMR1*	300623
	MRX60	Hypotonia Seizures Mental retardation Facial dysmorphism	*OPHN1*	300486
	MRXSCH	Mental retardation Microcephaly Hypotonia Epilepsy	*SLC9A6*	300243
	SCAX5	Neonatal hypotonia	Xq25-q27.1	300703
Mitochondrial	MERRF	Myoclonic epilepsy Deafness	*MTTK* *MTTL1* *MTTH* *MTTS1* *MTTS2* *MTTF*	545000
	NARP	Sensory neuropathy Retinitis pigmentosa	*MTATP6*	551500
	KSS	Retinopathy Cardiomyopathy	*MTTL1*	530000

I

Bioscience Reports (2017) **37** BSR20170251
DOI: 10.1042/BSR20170251

PORTLAND PRESS

Research Article

In vitro characterization of six *STUB1* variants in spinocerebellar ataxia 16 reveals altered structural properties for the encoded CHIP proteins

Yasaman Pakdaman[1,2], Monica Sanchez-Guixé[1], Rune Kleppe[3], Sigrid Erdal[1], Helene J. Bustad[4], Lise Bjrkhaug[5], Kristoffer Haugarvoll[6,7], Charalampos Tzoulis[6,7], Ketil Heimdal[8], Per M. Knappskog[1,9], Stefan Johansson[1,9] and Ingvild Aukrust[1,2]

[1]Center for Medical Genetics and Molecular Medicine, Haukeland University Hospital, Bergen, Norway; [2]Department of Clinical Science, University of Bergen, Bergen, Norway; [3]K.G. Jebsen Centre for Neuropsychiatric Disorders, Department of Biomedicine, University of Bergen, Bergen, Norway; [4]Department of Biomedicine, University of Bergen, Bergen, Norway; [5]Department of Biomedical Laboratory Sciences and Chemical Engineering, Western Norway University of Applied Sciences, Bergen, Norway; [6]Department of Neurology, Haukeland University Hospital, Bergen, Norway; [7]Department of Clinical Medicine, University of Bergen, Bergen, Norway; [8]Department of Medical Genetics, Oslo University Hospital, Oslo, Norway; [9]K.G. Jebsen Centre for Neuropsychiatric Disorders, Department of Clinical Science, University of Bergen, Bergen, Norway

Correspondence: Ingvild Aukrust (ingvild.aukrust@helse-bergen.no)

Spinocerebellar ataxia, autosomal recessive 16 (SCAR16) is caused by biallelic mutations in the STIP1 homology and U-box containing protein 1 (*STUB1*) gene encoding the ubiquitin E3 ligase and dimeric co-chaperone C-terminus of Hsc70-interacting protein (CHIP). It has been proposed that the disease mechanism is related to CHIP's impaired E3 ubiquitin ligase properties and/or interaction with its chaperones. However, there is limited knowledge on how these mutations affect the stability, folding, and protein structure of CHIP itself. To gain further insight, six previously reported pathogenic *STUB1* variants (E28K, N65S, K145Q, M211I, S236T, and T246M) were expressed as recombinant proteins and studied using limited proteolysis, size-exclusion chromatography (SEC), and circular dichroism (CD). Our results reveal that N65S shows increased CHIP dimerization, higher levels of α-helical content, and decreased degradation rate compared with wild-type (WT) CHIP. By contrast, T246M demonstrates a strong tendency for aggregation, a more flexible protein structure, decreased levels of α-helical structures, and increased degradation rate compared with WT CHIP. E28K, K145Q, M211I, and S236T also show defects on structural properties compared with WT CHIP, although less profound than what observed for N65S and T246M. In conclusion, our results illustrate that some *STUB1* mutations known to cause recessive SCAR16 have a profound impact on the protein structure, stability, and ability of CHIP to dimerize *in vitro*. These results add to the growing understanding on the mechanisms behind the disorder.

Introduction

The recessively inherited group of cerebellar ataxias (autosomal recessive cerebellar ataxia, ARCA) is commonly characterized by early onset and gradual worsening of gait, balance, and coordination over months and years. Friedreich ataxia (prevalence of 2–4/100,000) is known to be the most frequent type of ARCA, followed by ataxia telangiectasia (prevalence 1–2/100,000) and early onset cerebellar ataxia with retained tendon reflexes (prevalence 1/100,000) [1,2]. Many new ARCA genes have been identified recently due to the use of whole exome sequencing (WES) as routine in several diagnostics laboratories. Recently, it was shown that recessive mutations in *STUB1* can cause spinocerebellar ataxia, autosomal recessive 16 (SCAR16) in some families [3-10].

Received: 18 January 2017
Revised: 07 April 2017
Accepted: 10 April 2017

Accepted Manuscript Online: 10 April 2017
Version of Record published: 28 April 2017

Bioscience Reports (2017) **37** BSR20170251
DOI: 10.1042/BSR20170251

STUB1 encodes STUB1 (STIP1 homology and U-box containing protein 1), also known as C-terminus of Hsc70-interacting protein (CHIP), an evolutionary conserved protein of ∼35 kDa that is highly expressed as a dimeric co-chaperone in tissues that are active in terms of metabolism and protein turnover, such as brain, heart, and skeletal muscle. The protein was first identified as a tetratricopeptide repeat (TPR) domain-containing protein during a human cDNA library screening looking for proteins with a TPR domain possibly involved in stress regulation [11]. Further structural analysis revealed similarities between the C-terminus of CHIP (the U-box) and the E3 ligase component of the ubiquitin–proteasome pathway, suggesting an active role in ubiquitination of chaperone substrates for CHIP [12]. Thus, CHIP was discovered as the first ubiquitin ligase that directly associates with molecular chaperones. CHIP labels non-native proteins unable to be refolded by chaperones for proteasomal degradation [12-14].

The primary structure of CHIP has two main domains: an N-terminal TPR domain mediating the interaction of CHIP with Hsp70 and Hsp90 molecular chaperones; and a C-terminal U-box domain facilitating ubiquitination of chaperone substrates through the interaction with different E2 enzymes. These domains are separated by a central helical hairpin region (also termed the central coiled-coil (CC) domain), which influences the dimerization and stability of the whole protein [15].

To date, 19 pathogenic *STUB1* variants have been described associated with SCAR16 according to the Human Gene Mutation Database [16]. Studies reporting the structural/functional consequences of these variants are few and the protein folding and stability properties of CHIP variants have so far been poorly investigated. Six *STUB1* variants, i.e. E28K, N65S, K145Q, M211I, S236T, and T246M were selected for the present study. The overall aim was to characterize the structural properties of these CHIP mutants with special focus on protein structure, stability, and CHIP's ability to oligomerize *in vitro,* with the aim to discover new mechanisms for disease development of SCAR16. The six *STUB1* variants have been identified and reported as pathogenic in individuals with SCAR16 [3,5,7,10]; E28K and N65S were identified in two families with ARCA and cognitive impairment by our group [3]. T246M was first described by Shi et al. [9in a patient with ataxia and hypogonadotropic hypogonadism. This variant was included in the study due to phenotypic similarity with patients carrying the E28K and N65S mutations. Variants K145Q, M211I, and S236T were additionally selected to represent variants from CHIP protein domains reported to be crucial for CHIP dimerization or protein–protein interactions [5,7,10]. All these variants affect residues that are conserved across eukaryotic species. The positions of these variants within the CHIP protein structure as well as their position within the amino acid sequence alignment are shown in Figure 1.

Materials and methods

Plasmids and mutagenesis

Full-length cDNA encoding human CHIP was subcloned into the bacterial expression vector pETM-41 (EMBL) as previously described [3]. All *STUB1* variants were made using QuikChange XL Site-directed Mutagenesis Kit (Agilent Technologies). We verified the sequence of all constructs by Sanger sequencing.

Expression and purification of CHIP from *Escherichia coli*

The His-maltose-binding protein (MBP)-CHIP fusion proteins were expressed for 24 h at 25°C in the BL21-CodonPlus (DE3)-RP *E. coli* strain (Agilent Technologies). Cells were harvested by centrifugation at 4000×***g*** and lysed by sonication in 5 ml/g wet weight lysis buffer (50 mM $NaH_2PO_4 \cdot H_2O$, 300 mM NaCl, 10 mM imidazole, 20 mM 2-mercaptoethanol, 0.1% Tween-20, pH 8). The His-MBP-tagged proteins were purified using Ni-NTA agarose nickel resin (Qiagen), according to manufacturer's instruction. To generate CHIP, the His-MBP-tagged proteins were cleaved by Tobacco etch virus (TEV) protease (molar ratio 1:10) for 2 h at room temperature. In order to choose an appropriate buffer for protein storage and further experiments, TEV cleaved wild-type (WT) MBP-CHIP proteins were dissolved in three different buffer compositions and centrifuged for 19 h at 200000×***g*** (80000 rpm) at 4°C. All the pellets and supernatants were analyzed for CHIP protein content, using sodium dodecyl sulfate/polyacrylamide gel electrophoresis (SDS/PAGE) and followed by Coomassie Blue staining.

CHIP ubiquitination activity assay

In vitro ubiquitination activity assay was set up for both MBP-fusion and MBP-cleaved CHIP recombinant proteins. The reactions were prepared in a total volume of 20 μl, containing 2.5 μM (MBP)-CHIP (E3), 2.5 μM UbcH5c (E2) (Boston Biochem), 0.05 μM Ube1 (E1) (Boston Biochem), 250 μM ubiquitin (Boston Biochem), and 0.8 μM recombinant human His-HSPA8 (HSC71) (CHIP substrate) (Life Technologies AS, Thermo Fisher Scientific) in an ubiquitination buffer (50 mM Tris HCl, pH 7.5, 0.6 mM DTT, 2.5 mM Mg-ATP) and incubated at 37°C for 1 h. Protein samples were analyzed by SDS/PAGE and immunoblotting using either anti-CHIP (LS-C137950, LifeSpan

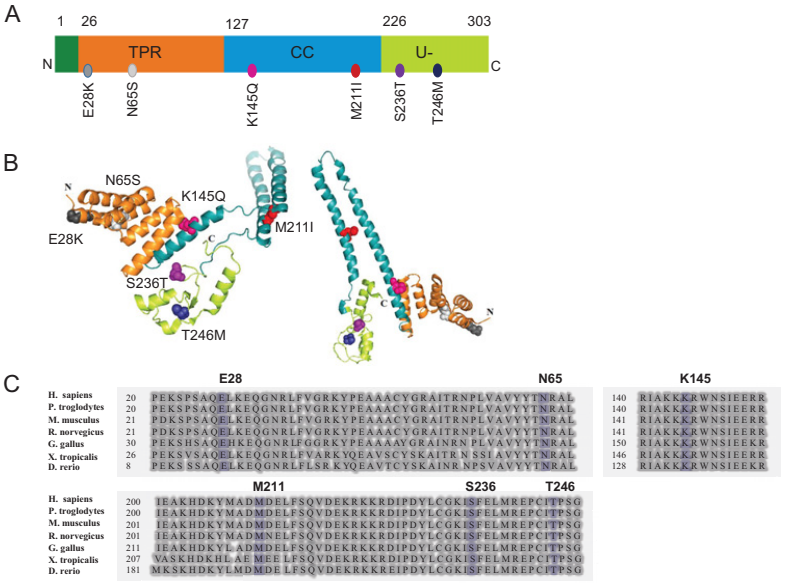

Figure 1. The position of the six selected variants in the CHIP protein

The position of selected variants is shown in (**A**) protein 1D structure and (**B**) 3D protein structure of the dimeric CHIP with colorful spheres. The 3D protein structure was created by using PyMOL software (https://www.pymol.org) [Protein Data Bank (PDB) code: 2C2L]. Minor modifications were performed in order to separate the two monomers of the dimer and to better visualize the location of each mutation as well as different protein domains. (**C**) Alignment of CHIP protein sequences from human (*H. sapiens*), chimpanzee (*P. troglodytes*), mouse (*M. musculus*), rat (*R. norvegicus*), chicken (*G. gallus*), frog (*X. tropicalis*), and zebra fish (*D. rerio*). Selected variants are shown in blue. The alignment was performed using the NCBI HomoloGene tool (https://www.ncbi.nlm.nih.gov/homologene).

Bioscience) or anti-Hsc70 (ADI-SPA-815-F, Enzo Life Sciences) to monitor CHIP self-ubiquitination or Hsc70 ubiquitination respectively.

Limited proteolysis assay

Trypsin was added to 30 μg of the MBP-cleaved CHIP protein at a CHIP to trypsin ratio of 1:600 (by mass) in a 100 μl reaction mixture (50 mM NaCl, 20 mM Hepes, and 2 mM DTT) and incubated at 25°C. The reactions were terminated at different time points (0, 5, 10, 20, and 30 min) by adding 18.5 μl of the reaction mixture to 5 μl NuPAGE LDS Sample Buffer (4×) (ThermoFisher Scientific), 1.4 μl NuPAGE Sample Reducing Agent (10×) (ThermoFisher Scientific), and 1 μl of the trypsin inhibitor (prepared at a trypsin to trypsin inhibitor mass ratio of 1:1.5). Samples were analyzed by SDS/PAGE followed by SYPRO Ruby staining and further quantified by Image Processing and Analysis in Java software (ImageJ, National Institutes of Health).

Size-exclusion chromatography

Different oligomeric states of the WT and mutant MBP-CHIP fusion proteins were studied by gel-filtration, using a Superdex 200 Increase 10/300 GL column (GE Healthcare) on the BioLogic DuoFlowTM Medium-Pressure Chromatography System (Bio-Rad Laboratories). The column was first equilibrated overnight with phosphate buffer (20 mM NaH_2P0_4, pH 7.4). One milligram of MBP-CHIP protein diluted in running buffer was prepared by centrifugation (13000×***g***, 10 min) and gel filtrated at a constant flow rate of 0.3 ml/min. Protein fractions were collected and analyzed using SDS/PAGE and Coomassie Blue staining.

Bioscience Reports (2017) **37** BSR20170251
DOI: 10.1042/BSR20170251

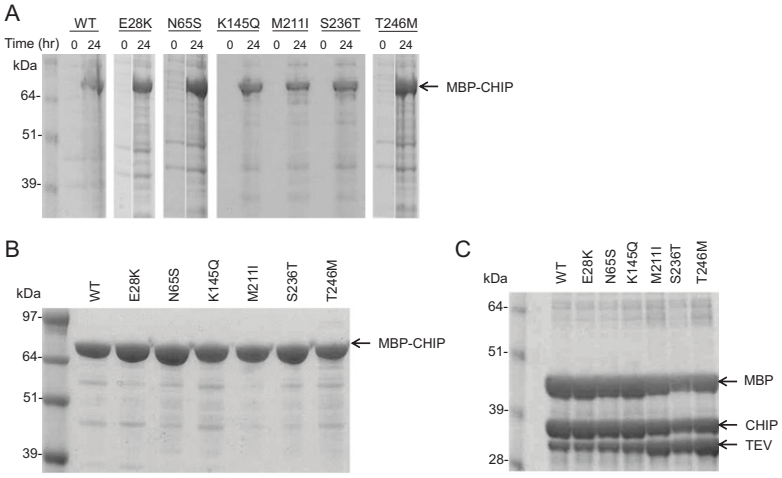

Figure 2. Expression and purification of WT and mutant forms of MBP-CHIP

(**A**) The expression of MBP-CHIP proteins of both WT and mutant forms at time 0 and 24 h after induction of protein expression by 0.5 mM IPTG in BL21 *E. coli* cells. (**B**) Purified WT and mutant forms of MBP-CHIP after Ni-NTA purification procedure. (**C**) WT MBP-CHIP fusion protein cleavage, using TEV protease to MBP-CHIP mass ratio of 1:10 and an incubation time of 2 h. All samples were analyzed by SDS/PAGE (10% gel) and Coomassie Blue staining.

Native polyacrylamide gel electrophoresis

Different conformational states of the WT and mutant CHIP proteins were studied by native gel electrophoresis and further analyzed by Coomassie Blue staining. Ten micrograms of MBP fusion protein (WT and mutants) was analyzed by NativePAGE^{TM} Bis-Tris gels (12%) (ThermoFisher Scientific) in Native PAGE^{TM} sample buffer using NativePAGE^{TM} Anode Buffer (1×) and light blue NativePAGE^{TM} Cathode Buffer (1×) as described by the manufacturer.

Circular dichroism spectroscopy

All the samples were prepared at a protein concentration of 6 μM in a buffer containing 10 mM potassium phosphate (pH 7.4) and 100 mM sodium fluoride. Protein concentrations were determined spectrophotometrically by using the theoretical extinction coefficient at A_{280} of 1.224 $M^{-1}cm^{-1}$ for WT-CHIP (and mutants) and 0.512 $M^{-1}cm^{-1}$ for MBP. CD spectra were recorded at 20°C in a Jasco J-810 spectropolarimeter equipped with a Peltier temperature control unit (Jasco Products). The far-UV measurements were recorded from 185 to 260 nm using a light path of 1 mm and the spectra obtained were the average of four scans at a scan rate of 50 nm/min. The final spectra were presented after buffer subtraction. Thermal denaturation profiles were obtained by recording the decrease in ellipticity at 222 nm as a function of temperature in the range 20–90°C with a scan rate of 40°C/h.

Results

Expression and purification of WT and mutant forms of CHIP

WT and mutant forms of MBP-fused CHIP were expressed in *E. coli*, and successful protein expression was verified for each mutant after IPTG induction as shown in Figure 2(A). Furthermore, fusion His-MBP-CHIP (WT and mutants) were purified by nickel resin (Figure 2B) and cleaved by TEV protease (Figure 2C). For minimal aggregation of CHIP recombinant protein, 100 mM HEPES (pH 8), 5 mM DTT, 100 mM NaCl, and 10% glycerol were selected as the storage buffer (Supplementary Figure S1).

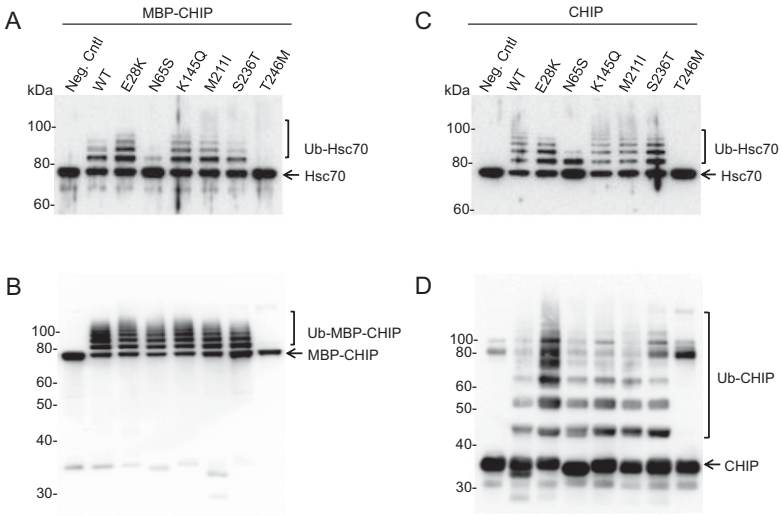

Figure 3. Ubiquitination activity of recombinant WT and mutant CHIP proteins

In vitro ubiquitination activity assay was performed using WT and mutant CHIP as ubiquitin ligases and Hsc70 recombinant protein as substrate. Hsc70-ubiquitination (**A** and **C**) and self-ubiquitination activities (**B** and **D**) were explored on MBP-CHIP fusion proteins (**A** and **B**) and MBP-cleaved CHIP proteins (**C** and **D**). The reaction was incubated for 1 h at 37°C and samples were analyzed for both Hsc70- and self-ubiquitination by SDS/PAGE and immunoblotting using antibodies against Hsc70 and CHIP respectively. As a negative control, the WT CHIP protein was used in a separate reaction without adding ubiquitin.

In vitro ubiquitination activity of WT and mutant forms of CHIP

CHIP participates in the ubiquitination of unfolded or misfolded substrates bound to chaperones via its U-box domain. In addition to the substrates, CHIP itself, and the heat shock protein chaperones are also known to be ubiquitinated by CHIP. To examine the enzymatic activity of the variants, ubiquitination assays were performed on recombinant CHIP both as MBP-fusion (Figure 3A and B) and as MBP-free (cleaved) proteins (Figure 3C and D). We investigated both the ability to ubiquitinate its substrate Hsc70 (Figure 3A and C) and its self-ubiquitination capacity (Figure 3B and D).

As seen from Figure 3(A) and (C), N65S and T246M displayed impaired Hsc70-ubiquitination activity for both MBP-fusion and MBP-free forms. Hsc70 seemed to be mono-ubiquitinated by the N65S mutant, while no Hsc70-ubiquitination was detected for T246M, confirming previous findings on these two variants [3,9]. Furthermore, T246M was unable to self-ubiquitinate both as MBP-fusion and cleaved proteins, while the N65S mutant showed similar level of self-ubiquitination as the WT (Figure 3B and D). The ubiquitination activities of the other mutants (E28K, K145Q, M211I, and S236T) were not overtly different from WT CHIP.

Protein stability analysis by limited trypsin proteolysis

In order to elucidate the protein structure and folding of the mutants, limited proteolysis assay was performed using trypsin digestion (Figure 4). Compared with WT, increased rate of trypsin degradation was demonstrated for all variants except N65S, with E28K and T246M being mostly affected. Interestingly, N65S presented a decreased trypsin-degradation rate compared with WT, indicating that the N65S mutation leads to a more compact and stably folded protein structure where the trypsin cleavage sites are most likely less accessible.

Oligomeric structures of MBP-CHIP fusion proteins analyzed by size-exclusion chromatography

The effects of mutations on the oligomeric structures of the MBP-CHIP proteins were studied by size-exclusion chromatography (SEC) (Figure 5). As expected, WT MBP-CHIP exists mainly in a dimeric form. Other high multimeric

Bioscience Reports (2017) **37** BSR20170251
DOI: 10.1042/BSR20170251

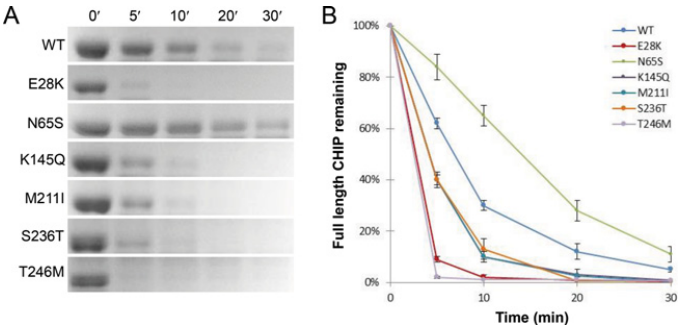

Figure 4. Limited proteolysis by trypsin of WT and mutant CHIP proteins

The proteolytic susceptibility of MBP-free CHIP proteins was explored for WT and mutants using trypsin for protein digestion. (**A**) Proteins were detected by SDS/PAGE and SYBRO Ruby staining after being subjected to trypsin proteolysis for various time periods (0–30 min). (**B**) Full-length proteins were quantified by ImageJ software, and the data for the average of three individual experiments were plotted against time. Each time point represents the mean of three readings conducted on three separate days ± SD (n=3).

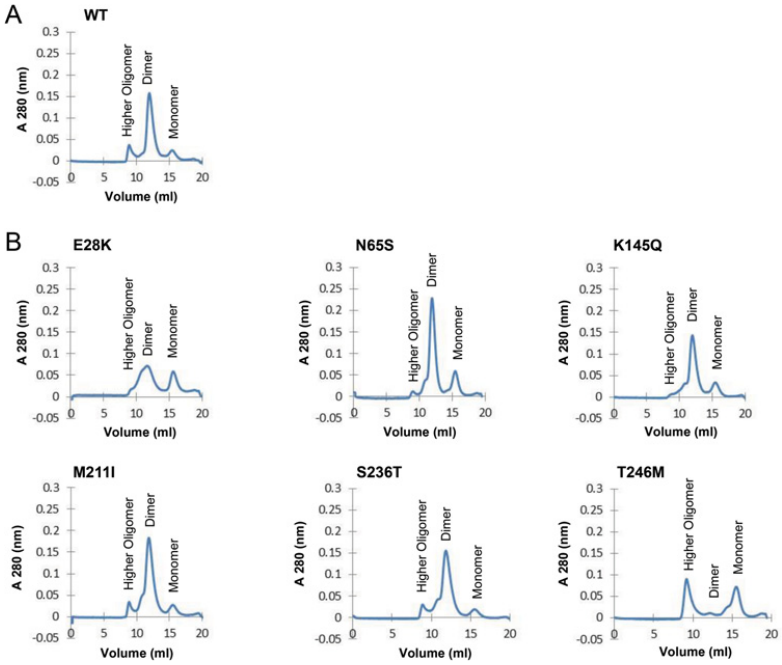

Figure 5. SEC of mutant recombinant MBP-CHIP fusion proteins

All the experiments were performed on 1 mg of MBP-CHIP at 0.3 ml/min at 4°C, using Superdex 200 10/100 GL columns and phosphate buffer (20 mM NaH_2PO_4, pH 7.4) as the running buffer, while monitoring protein absorbance at 280 nm. The elution profile of fractions corresponding to monomers, dimers, and higher oligomers are shown for the (**A**) WT CHIP and (**B**) mutants E28K, N65S, K145Q, M211I, S236T, and T246M.

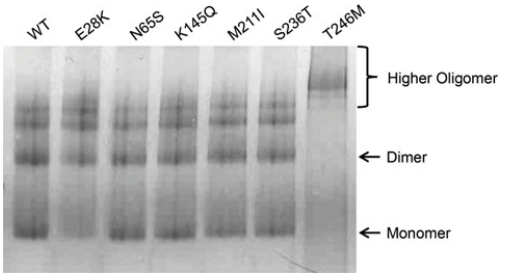

Figure 6. Oligomeric states of the WT and mutant MBP-CHIP by native gel electrophoresis

Ten micrograms of WT and mutant MBP fusion protein was tested for migration on a 12% native-PAGE gel. Protein bands were visualized following Coomassie Blue staining.

forms and monomeric WT MBP-CHIP could also be detected by SEC, although these forms were of low abundance (Figure 5A).

In the chromatogram of E28K, the peak representing dimeric CHIP was less pronounced compared with WT CHIP with relatively more monomers and possibly tetramers (Figure 5B). In contrast, for the N65S mutant, the results indicate large amounts of dimers and less high-oligomeric forms compared with WT. The chromatograms for K145Q, M211I, and S236T were similar to WT. Finally, gel-filtration of the T246M mutant showed high levels of large oligomeric structures as well as monomers, with very little dimeric CHIP. Altogether, these data suggest that the oligomeric structures of MBP-CHIP fusion protein are most prominently affected by mutations E28K and T246M, demonstrated by reduced dimeric peaks (E28K and T246M) and higher oligomer peaks (T246M).

Oligomeric states of MBP-CHIP fusion proteins analyzed using native polyacrylamide gel electrophoresis

Native polyacrylamide gel electrophoresis (native-PAGE) allows for a high-resolution analysis of the oligomeric state and molecular mass of native protein structure by using Coomassie G-250 as a charge-shift molecule. Separation of five major protein bands was observed for all the samples except for T246M (Figure 6). T246M migrated as a higher-order oligomer form, suggesting formation of aggregates for this mutant. The E28K mutant exhibited lower amounts of monomers (reduced by 67%), as seen by a faint monomer band in addition to lower amounts of dimers (reduced by 28%), compared with the WT, indicating a small shift toward the lower-order in the dimer–oligomer equilibrium for this mutant. Overall, these results suggest that while the higher-order oligomers serve as the major conformational state of T246M, the other mutants displayed almost the same oligomeric patterns as WT MBP-CHIP with small deviations observed for the E28K variant.

Secondary structure content of MBP-CHIP fusion proteins measured by circular dichroism spectroscopy

Crystallographic analysis of mouse CHIP indicates high degrees of α-helical structure due to the presence of two domains consisting mainly of α-helices (TPR and CC domains) [17]. Results from the far-UV circular dichroism (CD) spectra of both WT and mutant MBP fusion proteins demonstrated two minima at 208 and 222 nm, which is typical of proteins with a high helical content (Figure 7A). The difference in ellipticity of CD signals ([]) observed for the mutants indicates changes of the conformational properties of these proteins relative to WT. Minor changes were observed for E28K, K145Q, M211I, and S236T, whereas a large loss of α-helicity was noticed for T246M. In contrast, N65S was identified as the only mutant with increased α-helical content compared with the WT.

Thermal unfolding of MBP-CHIP fusion proteins as measured by circular dichroism

The effect of mutations on the thermal stability of MBP-CHIP protein was examined by investigating molar ellipticity () at 222 nm as a function of temperature (Figure 7B). The mid-point of each of the three transitions (mid-point of the thermal denaturation, T_m) for denaturation is given in Table 1 and was determined from the first derivatives of the transition curve. Transition temperatures in the range of ∼41–45°C, ∼55–57°C, and ∼62–74°C were observed for

Bioscience Reports (2017) **37** BSR20170251
DOI: 10.1042/BSR20170251

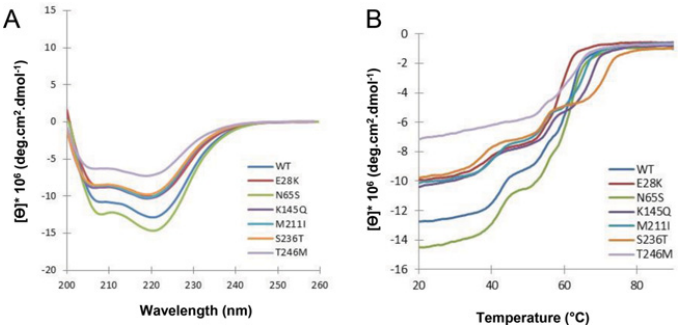

Figure 7. Secondary structure content and thermal unfolding profiles of WT and mutant CHIP proteins

(**A**) Far-UV CD spectra were recorded for 6 μM WT and mutant MBP-CHIP proteins in the range of 200–260 nm at 20°C. (**B**) Thermal unfolding curves were obtained for WT and mutant MBP-CHIP proteins by monitoring CD signal at 222 nm from 20 to 90°C. All the spectra presented in this figure are background corrected and smoothed.

Table 1 Mid-point of transitions for thermal unfolding of MBP-CHIP proteins

T_m	WT	E28K	N65S	K145Q	M211I	S236T	T246M
T_m (1)	44.2	42.4	44.5	42.7	43.9	41.2	–
T_m (2)	55.8	55	56.2	57	56.2	56.2	55.4
T_m (3)	64.5	62.4	65.1	69.5	67.7	73.8	66.8

The transitions temperatures (°C) were determined from the first derivative of the thermal unfolding curves using the Spectra Manager software (Jasco products).

denaturation of all the protein samples, except for T246M with only two transitions at ∼55 and 67°C (Figure 7B, light purple line and Table 1). This mutant also demonstrated a decrease in ellipticity, indicating loss of secondary structure. The loss in ellipticity, in addition to a more gradual unfolding with an apparent loss of the first transition seen for WT and all other mutants, indicates an unstable protein structure more prone to aggregation. The other mutants presented unfolding profiles with similar shapes as compared with the WT curve, although with smaller changes in the transition temperatures. For comparison, the thermal denaturation of MBP protein alone monitored by CD (Supplementary Figure S2) exhibited one T_m value of 56°C. This transition temperature corresponds well with the second transition observed for the MBP-fusion protein samples (Table 1). Therefore, it is most likely that the first (∼41–45°C) and third transitions (∼62–74°C) of the thermal denaturation curves of MBP-CHIP proteins are associated with unfolding of the CHIP protein itself and not MBP. We can only speculate that the first transition represents denaturation of the dimeric CHIP, while the third transition represents unfolding of the monomeric CHIP. Comparing the T_m of ∼44°C (first transition) seen for WT MBP-CHIP, all of the mutants showed lower first transitions T_m values than WT (Table 1), indicating decreased thermal stability of dimeric structures for the mutants. Hence, S236T with the first transition T_m of ∼41°C was regarded as the least stable protein in the dimeric conformation (Figure 7B, orange line and Table 1). Moreover, the absence of first transition on the thermal denaturation curve of T246M (Figure 7B, light purple line) suggested a very small amount of dimeric structures for this protein. The apparent T_m of CHIP mutants varied more in the third transition (possible monomeric phase) than the first transition (possible dimeric phase), as can be seen by the melting transitions ranging from ∼62 to 74°C in the third transition compared with ranging from 41 to 45°C in the first transition (Table 1).

Discussion

The present study provides additional insight concerning the effect of *STUB1* mutations in the development of ARCA disease through examining the activity and structural properties of the encoded CHIP protein mutants. Our results illustrate that some *STUB1* mutations known to cause recessive SCAR16 can affect the protein structure and stability in addition to the ability of CHIP to dimerize *in vitro*. This provides an alternative mechanism to the previously

suggested direct effects on CHIP's E3 ubiquitin ligase properties and interaction with its chaperones [3]. We speculate that at least some *STUB1* mutations mediate disease by affecting the CHIP E3 ubiquitin ligase interactions and function through modification of its oligomeric states and structural stability. As a result, the protein quality control system fails to eliminate damaged proteins properly which, in turn, cause toxicity and cell death.

The effects of different *STUB1* mutations on the E3 ubiquitin ligase activity of CHIP

Reduced levels of Hsc70-ubiquitination activity were observed for N65S located in the TPR domain. This mutation affects an asparagine residue that was previously reported to be involved in CHIP substrate binding [18]. However, another mutation in the same domain (E28K) resulted in similar ubiquitination activity as the WT for both Hsc70 substrate- and auto-ubiquitination, indicating that the substrate binding of CHIP was not affected by this mutation. Complete loss of ubiquitination activity was observed for CHIP-T246M for both Hsc70 substrate and CHIP itself. The T246M substitution (located at the U-box domain of CHIP) can affect the interaction of CHIP with the ubiquitin–proteasome pathway components and result in abolished ubiquitination activity of the CHIP protein as also suggested by Shi et al. [9]. These findings are in complete accordance with previous results obtained from the ubiquitination activity analysis of these three mutations [3,9].

The ubiquitination activity of the three variants K145Q, M211I, and S236T has to our knowledge not been investigated before, and our results revealed that they have WT-like ubiquitination activities *in vitro* (Figure 3). Interestingly, M211I and S236T are not found in the Exome Aggregation Consortium (ExAC) and K145Q only in heterozygous carriers (Minor allele frequency = 0.07%). All three variants affect highly conserved amino acid residues (Figure 1C) and all were reported to co-segregate with the disease [4,7,10]. Altogether, this indicates that these missense variants are pathogenic, but do not affect the ubiquitination activity *in vitro*. Furthermore, it was reported that CHIP protein levels are reduced in HEK293 cells transfected with M211I [4], supporting a loss-of-function mechanism. These three mutations, together with E28K, have been found in ARCA patients in a compound heterozygous form together with either a non-sense or a frameshift *STUB1* mutation [3,5,7,10]. The premature stop codon in the second allele probably leads to the truncation of the protein and/or to nonsense-mediated RNA decay.

Oligomerization studies discovered high aggregation propensity for T246M

SEC showed that T246M forms aggregates, pointing to a conformational change in the structure of this mutant (Figure 5), and further confirmed by native-PAGE (Figure 6) and in corroboration with others [19]. The necessity of dimerization for activity of CHIP was indicated by a study on CHIP from *Homo sapiens* (hCHIP), where a deletion mutant lacking the central CC domain, important for CHIP dimerization, was shown to have no E3 ligase activity [15]. Another study analyzing the crystal structure of Prp19 U-box suggested dimerization as a common architecture for the U-box and RING-finger families of E3 ubiquitin ligases, which play an essential role in the stability and functionality of these enzymes [20]. Thus, the complete loss of function observed in the *in vitro* ubiquitination activity assay for the T246M mutant might be caused by both impaired ubiquitin ligase activity (as a result of impaired interaction with ubiquitination enzymes) and formation of oligomeric protein structures. On the contrary, increased amount of dimeric structures was observed for N65S with a dimer peak higher than that of the WT (Figure 5B). However, since the mutation is not located in the CC domain of CHIP, which is important for dimerization, the mutation might indirectly lead to general conformational changes that promote CHIP dimerization.

Mutants T246M and N65S displayed remarkable differences in secondary structure content

The α-helical content of WT CHIP obtained from its far-UV CD spectroscopy spectrum corresponds well with the previously reported crystallographic data (Figure 7A)[17]. Reduced levels of ellipticity were, however, observed in the spectra from the majority of mutants, suggesting decreased levels of α-helical structure content in these mutants compared with WT. The largest loss of α-helicity was shown for the T246M mutant, which can be explained by its tendency to aggregate as discussed above. On the contrary, the N65S mutation generated a CHIP structure with an increased secondary structure content of α-helices, and corroborated the SEC findings for this variant (Figure 5B).

It is important to consider limitations associated with the use of MBP fusion proteins while monitoring structural properties. The remarkable ability of MBP to increase the solubility of fusion partners has made it a commonly used affinity tag for protein purification. Unfortunately, we were not able to purify CHIP from MBP despite several attempts using both amylose and nickel affinity chromatography, and SEC (data not shown). The latter could probably be

Bioscience Reports (2017) **37** BSR20170251
DOI: 10.1042/BSR20170251

explained by the similar molecular weights of CHIP and MBP of 35 and 43 kDa respectively. Therefore, we cannot be certain whether the overall protein folding and assembly may be different for MBP-CHIP fusion proteins compared with purified MBP-free CHIP. It is, therefore, possible that our assay gives a conservative estimate of the mutational effects on misfolding and aggregation due to the potential chaperone assisting properties of MBP [21]. However, as the CD results of WT CHIP are very comparable with two previous CD studies on purified MBP-free CHIP [15,22], it is probable that the MBP does not have substantial effects on the results in our assay.

In addition, since our main focus was to investigate differences in protein structure/folding of WT CHIP compared with CHIP mutants, rather than the folding of WT CHIP per se, we believe our structural analyses of MBP fused to CHIP are relevant.

N65S, the only mutant with increased structural stability against limited proteolysis

Limited proteolysis of a globular protein occurs mostly at flexible loops, and regular secondary structures such as helices are not subjected to cleavage (segmental mobility). Thus, the decreased susceptibility identified for CHIP-N65S against limited proteolysis is expected to be associated with a structure that contains a larger number of α-helices compared with the WT, which is in corroboration with the far-UV CD spectra of this mutant (Figures 4 and 7). The induced stability and proteolytic resistance in the structure of N65S may also be a consequence of more dimeric states discovered during gel-filtration analysis of this mutant (Figure 5B). In addition, a protein's susceptibility to proteolysis can be functionally linked to its energy landscape that is encoded within the amino acid sequence [23]. With this view, proteolytic susceptibility of folded proteins requires access to high-energy cleavable sites, making a compactly folded protein a poor substrate for proteolytic digestion. Therefore, decreased susceptibility of N65S can be the result of acquiring a more compact structure compared with the WT and the other mutants.

Mutants K145Q, M211I, and S236T displayed approximately the same degree of proteolytic digestion, being lower than that of T246M yet higher compared with the WT. This suggests that the former proteins achieve a somewhat looser, flexible structure, which makes them more susceptible toward proteolysis. This is in agreement with the results from far-UV CD where these mutants all showed similar loss of ellipticity compared with the WT at equal protein concentrations, indicating a loss in secondary structure. An additional decrease in α-helical content in the structure of K145Q, M211I, and S236T mutants could explain their reduced susceptibility against limited proteolysis. A loss in ellipticity was also observed for E28K; however, this mutant presented high level of susceptibility toward limited proteolysis similar to that of T246M. An explanation might be the high amount of trimeric/tetrameric structures identified for this protein during gel-filtration analysis that could indicate that the high proteolytic susceptibility of E28K is due to the unfolded/flexible structures of the protein molecule that appear during the formation of lower-order oligomers [24].

Circular dichroism revealed new insights into the conformational dynamics and thermal stability of CHIP protein mutants

Denaturation of small globular proteins generally follows a two-state mechanism involving a single unfolding transition (T_m), and two forms of fully native (N) and unfolded (U) proteins. However, many proteins have recently been observed to stabilize intermediates between the N and U states, and therefore show more than one transition during their unfolding profile [25,26]. This behavior is usually found in multi-domain/multimeric proteins where different domains/meres unfold independently and at different temperatures. Analysis of data obtained from such curves is often more complicated than that of a single-stage unfolding pattern. In the case of MBP-CHIP, the three transitions detected during thermal denaturation of the WT protein are assumed to be associated with unfolding of (in order) dimeric CHIP, MBP, and monomeric CHIP (Figure 7B). Dimeric CHIP is stabilized by both inter- (between the monomers) and intramolecular (within the monomers) forces. Therefore, it is possible that the disruption of intermolecular interactions during the first transition temperature (∼44°C) of MBP-CHIP proteins generates both dissociated MBPs and monomeric CHIPs. Subsequently, increased temperature results in unfolding of each MBP and CHIP monomers through disruption of interactions within the proteins (intramolecular interactions). By examining the thermal denaturation of 'MBP-only' (Supplementary Figure S2), and based on other CD studies done on the unfolding transition of this protein [21,27], the second transition of MBP-CHIP (∼56°C) is interpreted to arise from MBP alone. Therefore, CHIP itself (monomer) is expected to unfold at ∼64°C corresponding to the last transition temperature.

All investigated mutants apart from T246M presented thermal unfolding curves similar to WT, indicating that the whole conformation and dynamics of the protein were not largely affected by the mutations. Rather, differences are

more pronounced between the dimeric and monomeric unfolding transition temperatures that determine the thermal stability of mutant protein structures. In the dimeric state, N65S has similar stability as WT, but higher than other mutants (T_m of ∼44°C). The higher degree of dimerization observed during SEC analysis of this mutant can possibly explain this observation. Moreover, N65S was the only mutant with an increased level of α-helicity and stability against limited proteolysis. Taken together, these findings indicate a stabilizing effect for N65S mutation, resulting in a more compact CHIP protein structure.

To summarize our data, we can conclude that the ubiquitination activity of CHIP was impaired under the effect of mutations N65S and T246M while the other mutants showed intact activities. Increased amounts of dimeric structures, as well as higher levels of secondary structures, were discovered for N65S. In contrast, the T246M mutation generated a flexible protein structure with decreased α-helicity and a high tendency for aggregation. Decreased secondary structure content and proteolytic stability was observed for K145Q, M211I, and S236T. Overall, these results provide first *in vitro* evidence regarding the protein structural and folding properties, as well as new additions on the ubiquitination activity of *STUB1* mutations. Future studies should focus on the *in cellulo* characterization of mutations, using appropriate cell lines and animal models. Since all the mutants were associated with altered stability *in vitro*, it is likely that this will lead to reduced cellular levels of these variants, as was seen for E28K, N65S, and M211I previously [3,4]. Therefore, further investigations are required in order to find out how misfolding of CHIP itself can lead to the development of SCAR16 *in vivo*.

Acknowledgments

We wish to thank Jorunn Bringsli and Guri E. Matre for their technical assistance.

Accession numbers

STUB1 cDNA: GeneBank accession no. **NM_005861.3**

Competing interests

The authors declare that there are no competing interests associated with the manuscript.

Author contribution

Y.P. performed all the experiments except for *STUB1* cDNA subcloning and mutant plasmid generation of variants E28K, N65S, and T246M, which were performed by M.S.-G. and S.E. R.K. assisted in all the SEC performance and analysis. H.J.B. contributed to CD data analysis. Y.P., I.A., S.J., P.M.K., M.S.-G., S.E., L.B., K.H., C.T., and K.H. planned the experiments and analyzed the data. Y.P. and I.A. wrote the paper with further contributions from all authors.

Funding

This work was supported by Helse Vest [grant number 911810].

Abbreviations

ARCA, autosomal recessive cerebellar ataxia; CC, coiled-coil; CD, circular dichroism; CHIP, C-terminus of Hsc70-interacting protein; ExAC, Exome Aggregation Consortium; Hsc, Heat shock cognate; Hsp, Heat shock protein; MBP, maltose-binding protein; PDB, Protein Data Bank; SCAR, Spinocerebellar ataxia, autosomal recessive 16; SCAR16, spinocerebellar ataxia 16; SDS/PAGE, sodium dodecyl sulfate/polyacrylamide gel electrophoresis; SEC, size-exclusion chromatography; STUB1, STIP1 homology and U-box containing protein 1; TEV, Tobacco etch virus; T_m, mid-point of the thermal denaturation; TPR, tetratricopeptide repeat; WES, whole exome sequencing; WT, wild-type.

References

1 Palau, F. and Espinós, C. (2006) Autosomal recessive cerebellar ataxias. *Orphanet J. Rare Diseases* **1**, 47
2 Anheim, M., Tranchant, C. and Koenig, M. (2012) The autosomal recessive cerebellar ataxias. *N. Engl. J. Med.* **366**, 636–646
3 Heimdal, K., Sanchez-Guixé, M., Aukrust, I., Bollerslev, J., Bruland, O., Jablonski, G.E. et al. (2014) STUB1 mutations in autosomal recessive ataxias–evidence for mutation-specific clinical heterogeneity. *Orphanet J. Rare Diseases* **9**, 146
4 Bettencourt, C., de Yébenes, J.G., López-Sendón, J.L., Shomroni, O., Zhang, X., Qian, S.-B. et al. (2015) Clinical and neuropathological features of spastic ataxia in a spanish family with novel compound heterozygous mutations in STUB1. *The Cerebellum* **14**, 378
5 Casarejos, M.J., Perucho, J., López-Sendón, J.L., de Yébenes, J.G., Bettencourt, C., Gómez, A. et al. (2014) Trehalose improves human fibroblast deficits in a new CHIP-mutation related ataxia. *PLoS ONE* **9**, e106931
6 Cordoba, M., Rodriguez-Quiroga, S., Gatto, E.M., Alurralde, A. and Kauffman, M.A. (2014) Ataxia plus myoclonus in a 23-year-old patient due to STUB1 mutations. *Neurology* **83**, 287–288

Bioscience Reports (2017) **37** BSR20170251
DOI: 10.1042/BSR20170251

7 Depondt, C., Donatello, S., Simonis, N., Rai, M., Van Heurck, R., Abramowicz, M. et al. (2014) Autosomal recessive cerebellar ataxia of adult onset due to STUB1 mutations. *Neurology* **82**, 1749–1750
8 Ronnebaum, S.M., Patterson, C. and Schisler, J.C. (2014) Emerging evidence of coding mutations in the ubiquitin–proteasome system associated with cerebellar ataxias. *Human Genome Variation* **1**, 14018
9 Shi, C.-H., Schisler, J.C., Rubel, C.E., Tan, S., Song, B., McDonough, H. et al. (2014) Ataxia and hypogonadism caused by the loss of ubiquitin ligase activity of the U box protein CHIP. *Hum. Mol. Genet.* **23**, 1013–1024
10 Shi, Y., Wang, J., Li, J.-D., Ren, H., Guan, W., He, M. et al. (2013) Identification of CHIP as a novel causative gene for autosomal recessive cerebellar ataxia. *PLoS ONE* **8**, e81884
11 Ballinger, C.A., Connell, P., Wu, Y., Hu, Z., Thompson, L.J., Yin, L.-Y. et al. (1999) Identification of CHIP, a novel tetratricopeptide repeat-containing protein that interacts with heat shock proteins and negatively regulates chaperone functions. *Mol. Cell. Biol.* **19**, 4535–4545
12 Höhfeld, J., Cyr, D.M. and Patterson, C. (2001) From the cradle to the grave: molecular chaperones that may choose between folding and degradation. *EMBO Rep.* **2**, 885–890
13 Cyr, D.M., Höhfeld, J. and Patterson, C. (2002) Protein quality control: U-box-containing E3 ubiquitin ligases join the fold. *Trends Biochem. Sci.* **27**, 368–375
14 Murata, S., Minami, Y., Minami, M., Chiba, T. and Tanaka, K. (2001) CHIP is a chaperone-dependent E3 ligase that ubiquitylates unfolded protein. *EMBO Rep.* **2**, 1133–1138
15 Nikolay, R., Wiederkehr, T., Rist, W., Kramer, G., Mayer, M.P. and Bukau, B. (2004) Dimerization of the human E3 ligase CHIP via a coiled-coil domain is essential for its activity. *J. Biol. Chem.* **279**, 2673–2678
16 Stenson, P.D., Ball, E.V., Mort, M., Phillips, A.D., Shiel, J.A., Thomas, N.S. et al. (2003) Human Gene Mutation Database (HGMD): 2003 update. *Hum. Mutat.* **21**, 577–581
17 Zhang, M., Windheim, M., Roe, S.M., Peggie, M., Cohen, P., Prodromou, C. et al. (2005) Chaperoned ubiquitylation—crystal structures of the CHIP U box E3 ubiquitin ligase and a CHIP-Ubc13-Uev1a complex. *Mol. Cell.* **20**, 525–538
18 Wang, L., Liu, Y.-T., Hao, R., Chen, L., Chang, Z., Wang, H.-R. et al. (2011) Molecular mechanism of the negative regulation of Smad1/5 protein by carboxyl terminus of Hsc70-interacting protein (CHIP). *J. Biol. Chem.* **286**, 15883–15894
19 Rubel, C., Soss, S., McDonough, H., Chazin, W., Patterson, C. and Schisler, J. (2015) The unfolding tail of CHIP mutation in gordon holmes syndrome. *FASEB J.* **29**, no.1, supplement LB420
20 Vander Kooi, C.W., Ohi, M.D., Rosenberg, J.A., Oldham, M.L., Newcomer, M.E., Gould, K.L. et al. (2006) The Prp19 U-box crystal structure suggests a common dimeric architecture for a class of oligomeric E3 ubiquitin ligases. *Biochemistry* **45**, 121–130
21 Chakraborty, D., Rodgers, K.K., Conley, S.M. and Naash, M.I. (2013) Structural characterization of the second intra-discal loop of the photoreceptor tetraspanin RDS. *FEBS J.* **280**, 127–138
22 Graf, C., Stankiewicz, M., Nikolay, R. and Mayer, M.P. (2010) Insights into the conformational dynamics of the E3 ubiquitin ligase CHIP in complex with chaperones and E2 enzymes. *Biochemistry* **49**, 2121–2129
23 Park, C., Zhou, S., Gilmore, J. and Marqusee, S. (2007) Energetics-based protein profiling on a proteomic scale: identification of proteins resistant to proteolysis. *J. Mol. Biol.* **368**, 1426–1437
24 Fontana, A., de Laureto, P.P., Spolaore, B., Frare, E., Picotti, P. and Zambonin, M. (2004) Probing protein structure by limited proteolysis. *Acta Biochim. Polonica-English Ed.* **51**, 299–322
25 Mayne, L. and Englander, S.W. (2000) Two-state vs. multistate protein unfolding studied by optical melting and hydrogen exchange. *Protein Sci.* **9**, 1873–1877
26 Englander, S.W. (2000) Protein folding intermediates and pathways studied by hydrogen exchange. *Annu. Rev. Biophys. Biomol. Struct.* **29**, 213–238
27 Ganesh, C., Shah, A.N., Swaminathan, C., Surolia, A. and Varadarajan, R. (1997) Thermodynamic characterization of the reversible, two-state unfolding of maltose binding protein, a large two-domain protein. *Biochemistry* **36**, 5020–5028

SUPPLEMENTARY FIGURES

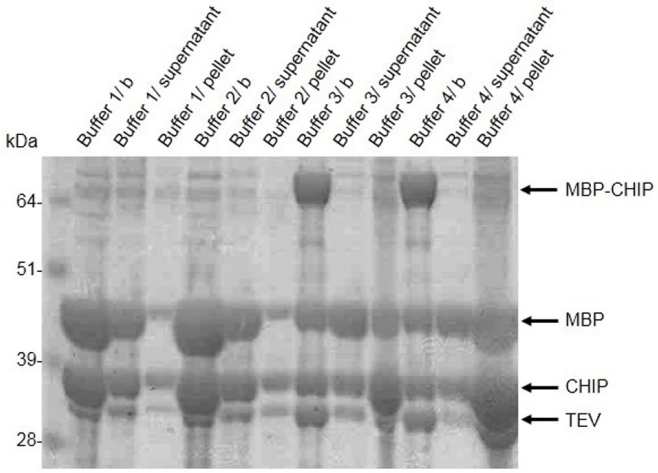

Figure S1. Aggregation analysis of the TEV cleaved WT MBP-CHIP protein

Aggregation analysis was performed before (b) and after 19 hours ultracentrifugation of protein at 200,000 x g (80000 rpm) at 4°C, using four different buffer compositions: (1) 100 mM Hepes pH 8, 5 mM DTT, 100 mM NaCl, 10% Glycerol, (2) 20 mM Tris HCl pH 7.4, 200 mM EDTA, 1 mM Sodium azide, 1 mM DTT, (3) 50 mM NaH_2PO_4, 5 mM DTT, (4) 20 mM NaH_2PO_4 pH 7.4

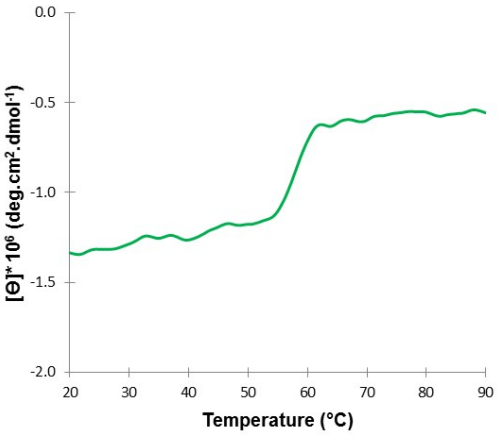

Figure S2. Thermal denaturation profile for MBP

The thermal unfolding curve was obtained by monitoring CD signal at 222 nm from 20 to 90°C. The spectrum presented in this figure is background-corrected and smoothed.

Errata

Page 21, line 14: “replaced by” is corrected to “replace”.

Page 29, line 11: “ribosome” is corrected to “proteasome”.

Page 54, line 10: “a-synuclein” is corrected to “α-synuclein”.

Paper III, page 19, line 12: “6H” is corrected to “6I”.

Paper III, page 19, line 16: “6I” is corrected to “6H”.

Paper III, page 20, line 16: The reference number is updated to “21”.

Paper III, page 20, line 19: “a-synuclein” is corrected to “α-synuclein”.

Paper III, page 32, line 16: “H” is corrected to “I”.

Paper III, page 32, line 16: “I” is corrected to “H”.

Paper III, page 33, line 9: “A-G” is corrected to “A-C and E-G”.

Graphic design: Communication Division, UiB / Print: Skipnes Kommunikasjon AS

uib.no

ISBN: 9788230848654 (print)
9788230865057 (PDF)